NTNU – Trondheim
Norwegian University of
Science and Technology

Approaches for assessment of weld fatigue and verification of the effective notch stress approach

Øyvind Sæbø Fagnastøl

Subsea Technology
Submission date: June 2014
Supervisor: Bernt Johan Leira, IMT

Norwegian University of Science and Technology
Department of Marine Technology

NTNU
Norwegian University of Science and Technology
Department of Marine Technology

Master Thesis, Spring 2014

for

Master Student Øyvind Sæbø Fagnastøl

Approaches for Assessment of Weld Fatigue and Verification of the Effective Notch Stress Approach

Metoder for Estimering av Utmattings-skade i Sveiser og Verifikasjon av Effektiv Kjervspennings-metodikk

It is generally advised to avoid using fillet welds in the joints where fatigue failure has large consequences. The main reason is less reliable NDE results compared to full penetration joints. However, fillet welds are used or desired in some offshore designs due to geometry and fabrication of the structure. In such cases, fatigue cracks can be initiated and grow not only from weld toe to the base material but also from the weld root through the fillet weld or into the section under weld.

There are three well-known methodologies when using stress based or S-N curves in fatigue analysis of welded connections; nominal stress, hot-spot stress, and notch stress. In most of offshore standards and recommended practices, S-N curves are provided for the first two methods due to their relatively quick applications in the industry.

To assess fatigue life of weld root, it is necessary to calculate an effective stress in the weld throat. The effective stress then needs to be accompanied by a proper S-N curve to estimate fatigue life. This requires a fine 3-D finite element model to be built in order to calculate stresses at the weld root and compare it with the notch stresses and hot-spot stresses at the weld toe. However, using detailed finite element (FE) model and using notch stress methodology is not efficient in the offshore industry since there might be a high number of such joints in a large structure.

The aim of the study is accordingly to provide a basis for efficient and relatively simplified fatigue methodology of fillet welded joints. The following topics are to be addressed as part of the work:

1. Further verification work in relation to the notch stress approach for different dimensions of cruciform joints is to be performed.

2. Sample joints with different geometries are selected in cooperation with AkerSolutions in order to represent some generic fillet welded joints. 3D fine FE modeling of the joints is performed according to the results obtained from pre-project work and step 1.

3. Fatigue life estimation is performed for the toe and root of welds according to the related S-N curves and comparison is made between the results for the different welds.

4. Curve fitting of the results is carried out. If possible, a simple approach for fatigue analysis (design/design modification) of fillet welded joints is outlined based on the resulting curves.

Recommendations for design/design modification of fillet welds for increase of fatigue resistance should also be aimed at.

The work scope may prove to be larger than initially anticipated. Subject to approval from the supervisor, topics may be deleted from the list above or reduced in extent. In the thesis the candidate shall present his personal contribution to the resolution of problems within the scope of the thesis work. Theories and conclusions should be based on mathematical derivations and/or logic reasoning identifying the various steps in the deduction.

The candidate should utilise the existing possibilities for obtaining relevant literature.

The thesis should be organised in a rational manner to give a clear exposition of results, assessments, and conclusions. The text should be brief and to the point, with a clear language. Telegraphic language should be avoided.

The thesis shall contain the following elements: A text defining the scope, preface, list of contents, summary, main body of thesis, conclusions with recommendations for further work, list of symbols and acronyms, references and (optional) appendices. All figures, tables and equations shall be numbered.

The supervisor may require that the candidate, in an early stage of the work, presents a written plan for the completion of the work. The plan should include a budget for the use of computer and laboratory resources which will be charged to the department. Overruns shall be reported to the supervisor.

The original contribution of the candidate and material taken from other sources shall be clearly defined. Work from other sources shall be properly referenced using an acknowledged referencing system.

The thesis shall be submitted in electronic version:

- Signed by the candidate
- The text defining the scope included
- Drawings and/or computer prints which cannot be bound should be organised in a separate folder.

Supervisor: Professor Bernt J. Leira Supervisor in Aker Solutions: Majid Anvari

Deadline: June 10th 2014

Trondheim, January 16th, 2014

Bernt J. Leira

NTNU
Norwegian University of Science and Technology
Department of Marine Technology

Abstract

Fatigue of welded structures is commonly assessed in three ways. These are the nominal stress-, the structural hot spot- and the effective notch stress approach. As the applicability of the approaches differs, these differences have been discussed. The effective notch stress approach has been validated for a cruciform fillet welded and fully penetration welded joint, according to DNV (2012). The same fillet welded joint was further investigated for varying weld sizes. The results show, that for a weld size half the length of the validation model, fatigue life was estimated to be 140% longer than that of the nominal approach. Further investigations revealed that there is a nonlinear relation between effective notch stress and weld sizes, while comparison of the notch stress and nominal stress approaches indicate that a linear relation is to be expected. Two explanations have been discussed. Firstly, the size of the notch may be dependent on the weld size, caused by loading mode alternations of the notch. And secondly, the linear relation found may be caused by simplifications made for the nominal stress approach. Equations describing the relation between the two approaches have been proposed. Based on the established methodology for the cruciform joint, a second joint provided by Aker Solutions has been assessed for weld root fatigue. This joint is a knee plate located in a horizontal brace of a drilling vessel. The knee plate was analysed by means of a local finite element model subjected to a variable loading, which was defined from provided stress range exceedances diagrams for one boundary. For simplicity, the opposite boundary of the brace was fixed. All simplifications made, for both model and boundaries, have been discussed and concluded to be acceptable and conservative, based on comparison to weld toe fatigue. Weld root fatigue life was assessed by means of Miner summation, and compared to weld toe fatigue. Based on the proposed equations and the linear relation found between the nominal- and the notch stress S-N curves, a weld size providing a longer fatigue life at the weld root, rather than that at the toe, was proposed.

NTNU
Norwegian University of Science and Technology
Department of Marine Technology

Sammendrag

Utmatting av sveiste konstruksjoner vurderes ofte ved hjelp av tre forskjellige metoder: Den nominelle spenningsmetoden, den effektive strukturelle hot-spot spenningsmetoden og den effektive kjervspennings-metoden. Anvendelsesområdene for metodene er ulike, og disse forskjellene har blitt diskutert. Den effektive kjervspennings-metoden er blitt validert for et platekors, sveist med både kilsveis og fullstendig gjennombrent sveis, i henhold til anbefalinger fra DNV (2012). Sveiserotens utmattingslevetid for den samme kilsveiste konstruksjonen ble videre undersøkt for varierende sveisestørrelser. Resultatene viser at for et sveisemål som er halvparten så stort som i det valideringsmodellen, blir utmattingslevetiden beregnet til å være 140% lengre enn hva som blir anslått ved bruk av den nominelle spenningsmetoden. Ytterligere undersøkelser viser at det er et ikke-lineært forhold mellom effektiv kjervspenning og sveisestørrelser, mens en sammenligning med den nominelle metoden viser at man kan forvente en lineær sammenheng. To mulige årsaker til dette har blitt diskutert. For det første kan størrelsen av kjerv være avhengig av sveisestørrelsen, som en følge av endret lastmodus ved endring av sveisestørrelse. For det andre kan det lineære forholdet som ble funnet være forårsaket av forenklinger innad i den nominelle spenningsmetoden. Ligninger som beskriver forholdet mellom de to metodene er blitt foreslått. Basert på den etablerte metodikken for platekorset, ble én ytterligere modell, gitt av Aker Solutions, analysert for utmatting ved sveiseroten. Denne konstruksjonen er en kneplate fra et borefartøys horisontalstag. Kneplaten ble analysert ved hjelp av en lokal elementmodell som ble undersøkt for variabel belastning, definert av spenningsoverskridelsesdiagrammer gitt av Aker Solutions, for én grenseflate i modellen. For enkelhets skyld ble den andre motstående grenseflaten fastlåst. Alle forenklinger, for både modell og grenseflater, har blitt diskutert, og basert på sammenligninger med utmattingslevetid for sveisetå ble det konkludert med at disse var akseptable og konservative. Utmattingslevetid for sveiseroten ble vurdert ved hjelp av Miner-summasjon, og sammenlignet med utmattingslevetid for sveisetåen. Med bakgrunn i de foreslåtte ligningene, og det lineære forholdet basert på den nominelle metoden, foreslås det en sveisestørrelse som gir lengre utmattingslevetid ved roten, enn ved tåen av sveisen.

NTNU
Norwegian University of Science and Technology
Department of Marine Technology

Acknowledgement

This master's thesis is a part of a 2-year Master of Science program at the Norwegian University of Science and Technology, department of Marine Technology. The thesis has been developed in cooperation with Aker Solutions MMO -Asset Integrity Management, in continuation of a previous master's thesis by Djan Eirik Djavit and Erik Strande, also in made in cooperation with Aker Solutions.

I would like to express my gratitude to my supervisor, Professor Bernt J. Leira for guidance with the thesis, and for defining the project task. I would also like to thank my co-supervisor Majid Anvari, Ph.D. at Aker Solutions for guidance, literature propositions and outlining of the project task. Also thanks to Professor Stig Berge for guidance with interpretation of regulations, and his eager to share his knowledge of fatigue assessments and former work on the topic.

I would also like to thank Erik Strande for his help during finite element analyses, Arve Flesche for providing input data to analyses, and Roger Rong for his help with providing a work station capable of performing the demanding analyses, all of them at Aker Solutions.

Special thanks to Julie L.L. Torbjørnsen for all her help and for coming with me to Trondheim. Finally I would like to thank my fellow students at the office, and former HIB'ers, for all the good memories.

Øyvind Sæbø Fagnastøl

Trondheim, June 7th 2014

Table of content

Table of figures

List of tables

Abreviations

Base- & Brace model	The brace model consists of one quarter of the brace models cross section, which is used in analysis of the fillet welded knee plate.
BV1 & BV2	Models of the brace outer plate, representing a simplified brace plate and the exact brace plate.
DNV	Det Norske Veritas.
Elec	Elements along a quarter circumference.
FEA	Finite Element Analysis.
IIW	International Institute of Welding.
Root 1, 2 & 3	Defined positions for the fictitious weld root notch.
SCF	Stress concentration factor.
Target values	Values for stress, fatigue life or stress concentration factor that have been established based on the nominal stress approach.
Toe 1 & 2	Defined positions for the fictitious weld toe notch.

Nomenclature

A	Area [m^2].
a	Crack length [m].
$\bar{a}$	Tabulated parameter for design SN-curves.
C	Material constant.
d	Depth [m].
D	Miner sum
E	Elasticity modulus for steel.
F	Force [N].
F_f	Form factor dependent of crack geometry and loading.
I	Moment of inertia [m^4]
K	Stress intensity factor [$MPam^{1/2}$].
ΔK	Stress intensity factor based on stress range [$MPam^{1/2}$].
k	Tabulated parameter for design SN-curves. Determines magnitude of thickness effect.
M	Moment [Nm].
m	Tabulated value for design SN-curves. Determines the slope of the curve.
N	Number of cycles to failure.
n	Number of cycles for one stress block, used for Miner summation.
n'	Vector defining the center of each stress block, used for Miner summation.
S	Stress [MPa].
s	Microsupport factor.
t	Thickness of member.
t_{ref}	Reference thickness, thickness of the tested member.
T	Time [years].
α	Factor used for the hotspot approach when stress is more parallel to the weld.
ρ	Real notch radius [m].
ρ^*	Microsupport length[m].
ρ_f	Fictitious notch radius [m].
σ	Stress [MPa].
$\Delta\sigma$	Stress range [MPa].
σ_b	Bending stress [MPa].
$\Delta\sigma_{cor}$	Target effective notch stress expressed with the effective notch stress for a weld size *a* [MPa].
σ_m	Membrane stress [MPa].
σ_{max}	Maximum stress [MPa].
σ_{nom}	Nominal stress [MPa].
τ	Shear stress [MPa].

1 Introduction

1.1 Background

Fatigue failure of welded joints is an old and well-known issue (Schijve, 2012), and has been seen to develop due to cracks forming and growing under repeated or fluctuating loading (Maddox 1991). Fatigue cracks are found to initiate in structures, even though the applied stress is less than the ultimate strength of the structure. This is due to stress concentrations at-, and close to discontinuities in the structures. A simple way to illustrate this is to look at a holed plate subjected to a tensile membrane stress, as seen in Figure 1.

a) b)

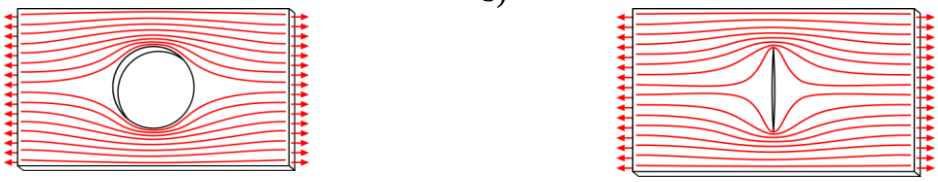

Figure 1 – Illustration of stress concentrating close to discontinuities: a) holed plate (Hole force lines, 2013), b) Notched plate (Crack force lines, 2013)

The distribution of stress over the cross section at the hole is not evenly distributed, and it is seen that stress tends to concentrate closest to the edge of the hole as shown in Figure 2. The conclusion is that local changes in section causes disturbances in the flow of stress, and thus stress concentrations occur (Maddox, 1991).

A typical place for stress concentrations to occur is at the transition between weld and plate, known as the weld toe, and also at the weld root as shown in Figure 3 (Maddox, 1991).

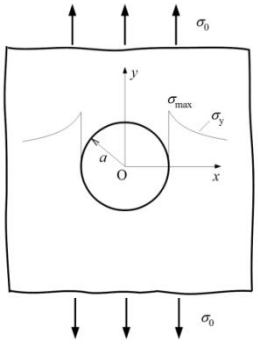

Figure 2 - Stress distribution in a holed plate over the cross section of the hole's position (Stress concentration by a hole, 2013).

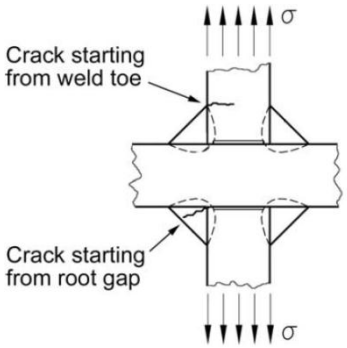

Figure 3 – Possible failure modes for a transversely loaded fillet weld (Fricke & Doerk, 2006)

The stress concentration at the weld toe is in general the critical area, but for some structures stress concentrations at the weld root can be more severe than that of the weld toe. Both of the cases may lead to a fatigue crack and ultimately failure of the structure.

There are several methods for assessing fatigue strength and service life of welded structures using local approaches. These approaches are based on structural stresses, notch stress and fracture mechanics, and they all have different applicability (Radaj, 1996)

The nominal stress approach is performed by comparing well tested specimens with the detail in question. Each test specimen is associated to a SN-curve according to direction of loading, weld geometry and the technological properties of the weld.

The hot spot stress method is a local approach for fatigue assessment of the weld toe, performed by a finite element analysis (FEA). The method began developing in the 1960s, and saw breakthroughs in the 1970s. The method is today well described by DNV (2012) and the international institute of welding (Hobbacher, 2009a).

The most recent approach for fatigue assessments in welded structures is the effective notch stress method, which also is a method performed using FEA (Schijve, 2012). The method has recently been included in fatigue recommendations issued by DNV (2012) and IIW (Hobbacher, 2009a). This approach can be used to assess fatigue at the weld root as well as the weld toe.

A former study, performed by Strande and Djavit (2013), showed that a larger weld size resulted in higher fatigue life for the effective notch stress approach. This study is in a continuation of these results.

1.2 Objectives

The objective of this study is to introduce the effective notch stress approach, and to compare it with other available approaches for fatigue assessments, such as the effective hot spot- and nominal stress approach. Applicability of the methods will be summarized and discussed. A fillet welded and fully penetration welded cruciform joint will be analyzed using the effective notch stress approach, and validated by comparing the results with the nominal stress approach, according to recommended practice (DNV, 2012). A mesh convergence study will be performed and discussed together with other parameters found to influence the results of the analyses. The effective notch stress approaches will be investigated for varying weld sizes, and performed for a welded detail provided by Aker Solutions.

1.3 Limitations

This study will not describe the basics of FEA. A basic knowledge of finite elements is thus assumed.

2 Approaches for assessment of weld fatigue

2.1 Stress concentration in welded structures

For a simple structure with a uniform cross sectional area subjected to a tensile load, nominal stress is defined as given in equation (1). As formerly shown, stress concentrations are due to changes in section. A way of describing the magnitude of these concentrations is by introducing a stress concentration factor (SCF) according to equation (2), as given by DNV (2012). A SCF is thus the relation between nominal stress and the stress concentration.

$$\sigma = \frac{F}{A} \quad (1)$$

$$SCF = \frac{\sigma_{max}}{\sigma_{nom}} \quad (2)$$

Producing a smoother transition between plate and weld toe will give a lower stress concentration (Berge, 2006). This is however difficult to achieve by welding under normal conditions. There are however weld improvement methods that can be applied post welding. Several improvement methods have been listed by Berge (2006), including amongst others:

- Peening methods: Introducing plastic deformation at the weld by impacting the weld with a specially intended tool. Reduces residual stresses that arise during welding.
- Post-weld heat treatment: Heating the weld and maintaining a high temperature over time, followed by slowly cooling down the weld. Reduces residual stresses in the weld.
- Grinding of the weld toe by burr or disc grinding, and weld toe re-melting techniques: Improves the weld toe geometry such that stress concentrations at the toe are reduced.

Although all these methods have demonstrated improved fatigue strength for the weld toe, they are uncertain as they rely on quality of workmanship, environment and other factors (Berge, 2006). They are therefore not considered in general design of welds, but rather used as a way of improving welds that are under dimensioned, or for weld repairs.

The weld toe is in general the most likely site for fatigue cracking, but for partially penetrated welded joints under transverse loading, such as a fillet welded cruciform joint as shown in Figure 3, stress concentration will also occur at the root of the weld (Maddox, 1991). The stress concentration at the root depends on joint geometry and extent of weld penetration, and can be more severe than that of the weld toe. A fatigue crack may then propagate from the root across the weld throat, which is difficult to detect by non-destructive testing (DNV, 2012). Seeing that a root defect is harder to detect than a toe defect, DNV (2012) recommends the use of a design such that weld toe failure is more likely than a root failure.

2.2 Fatigue life

Fatigue life is commonly expressed with S-N curves, also known as Wöhler curves, which have been determined for several types of welded joint details typically found in structures (DNV 2012, Hobbacher, 2009a). In order to determine the S-N curve for one detail, several duplicate test specimens for this detail have to be tested (Leira, Syvertsen, Amdahl, & Larsen, 2011). Each test is normally performed by subjecting the specimen to an alternating load with constant mean stress and stress amplitude. By repeating the test for different stress amplitudes the number of cycles to failure and stress amplitude can be plotted in a scatter diagram with a logarithmic scale.

The design curves issued by IIW and DNV are based on these failure curves. DNV (2012) determines the design curve as the mean value of fatigue life minus two standard deviation curves, which is associated to a 97.7% probability of survival. DNV's design curves are shown in Figure 4.

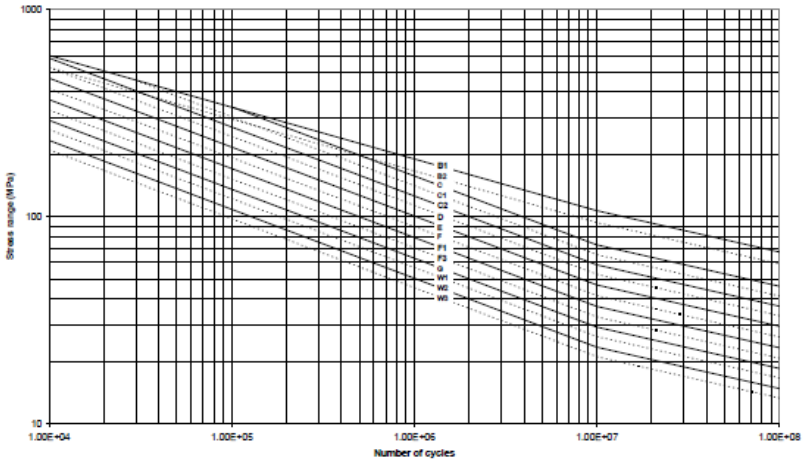

Figure 4 –Design curves issued by DNV (2012)

DNV (2012) defines the basic design S-N curves according to equation (3). When designing a detail with greater thickness than that of the test specimen's, one has to account for a thickness effect. This can be achieved by utilizing equation (4).

$$\log N = \log \bar{a} - m \log \Delta\sigma \quad (3)$$

$$\log N = \log \bar{a} - m \log \left(\Delta\sigma \left(\frac{t}{t_{ref}} \right)^{k} \right) \quad (4)$$

Here N is the predicted number of cycles to failure for a stress range $\Delta\sigma$. The values $\log \bar{a}$, m and k are tabulated for each design curve, and the choice of design curve is made depending mainly on method of fatigue assessment, environmental corrosive conditions and for the nominal approach also the detail class. The reference thickness (t_{ref}), which is the thickness of the tested specimen, is 32mm for tubular joints and 25mm for all other welded joints.

2.3 Assessment of residual life by fracture mechanics

Fracture mechanics is used to describe how defects and cracks affect materials and structures (Berge, 2006). It has been found that the stress and strain field around a crack can be uniquely defined by a stress intensity factor that in general can be expressed as shown in equation (5), for mode 1 loading in Figure 5.

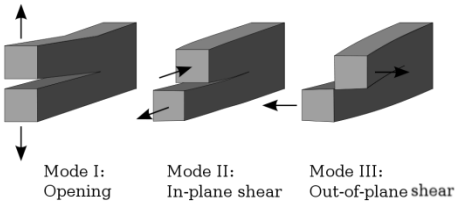

Figure 5 -Loading modes (Berge, 2006)

$$K = S\sqrt{\pi a}F_f \qquad (5)$$

For the stress intensity factor K, S is the nominal stress, a is the crack length, and F_f is a form factor that depends on crack length, crack geometry and loading configuration. Form factors for several cases are tabulated and/or presented in graphs in BS 7910 (BSI, 2005).

Fatigue history can be separated into three stages as shown in Figure 6. The first stage, crack initiation, is at a micro level, caused by variations between the crystalized grains at the surface of the metal (Berge, 2006). Theory for stage 1 crack initiation has not been well established. The second stage of crack growth starts when the crack has grown, and changed orientation and shape into the mode 1 loading configuration, as shown in Figure 5. For welded joints, this stage is dominating due to initial defects like slag intrusions, lack of fusion between steel and weld, and other weld defects. The third stage is the failure stage, where the crack growth rate accelerates rapidly.

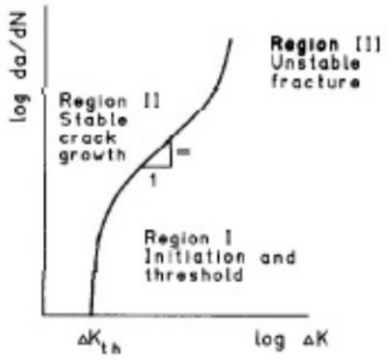

Figure 6 - Crack growth curve. Fatigue crack growth rate (da/dN) as a function of stress intensity range ΔK (Næss, 1985)

For the second stage the crack growth rate is stable, as shown in Figure 6 as region II, and the crack growth curve may be approximated by the Paris-Erdogan crack growth relation as shown in equation (6), also called *the Paris-law* for short (as cited in Berge, 2006).

$$\frac{da}{dn} = C(\Delta K)^m \qquad (6)$$

For the Paris-law, C and m are material constants that can be found for instance in BS 7910 (BSI, 2005). K is the stress intensity factor which can be found according to equation (5), where the stress is inserted as stress amplitude ΔS.

Assuming fatigue crack growth according to the Paris law, the number of cycles may be calculated as an integral as shown in equation (7), where equation (6) have been rearranged and ΔK is inserted as equation (5).

$$N = \int_{a_i}^{a_f} \frac{da}{C(\Delta K)^m} = \int_{a_i}^{a_f} \frac{da}{C\left(\Delta S\sqrt{\pi a}F_f\right)^m}$$

$$= \frac{1}{C\left(\Delta S\sqrt{\pi}\right)^m} \int_{a_i}^{a_f} \frac{da}{(\sqrt{a}F_f)^m} \qquad (7)$$

Where a_i and a_f are the initial and the final crack length at failure, respectively. In order to solve the integral, the form function which is dependent on crack length must be determined. Assuming that the initial crack growth is slow, and that most of the fatigue life is during the

growth of the first millimeters of the crack, the form function may be presumed constant (Berge, 2006). The integral may then be solved as shown in equation (8).

$$N = \frac{1}{C\left(\Delta S\sqrt{\pi}F_f\right)^m}\int_{a_i}^{a_f} a^{-\frac{m}{2}} = \frac{1}{C(\Delta S\sqrt{\pi}F_f)^m}\frac{a_f^{1-\frac{m}{2}} - a_i^{1-\frac{m}{2}}}{1-\frac{m}{2}} \quad (8)$$

By evaluating equation (8), it can be found that the initial crack length have major influence on fatigue life, while the assumed size of the failure crack length has minor influence (Berge, 2006).

As the initial defects are difficult to determine, crack growth rates are primarily in region I of Figure 6 and such small cracks are outside the validity range of linear-elastic fracture mechanics, it is not practical to use fracture mechanics for calculation of design life (Berge, 2006). Fracture mechanics may be used as a conservative estimate for design life, but is more useful for calculation of residual life, inspection- planning and reliability assessment. In order to calculate residual life it must therefore be possible to determine the crack size in a reliable way.

2.4 Influence of weld geometry on weld fatigue

For cruciform joints, it has been found that fatigue strength can be increased by improving the geometry of the weld, such that fatigue strength at the root is increased to a higher strength than that of the toe.

This has been implemented for fillet welds in general, in recommendations given by DNV (2012).

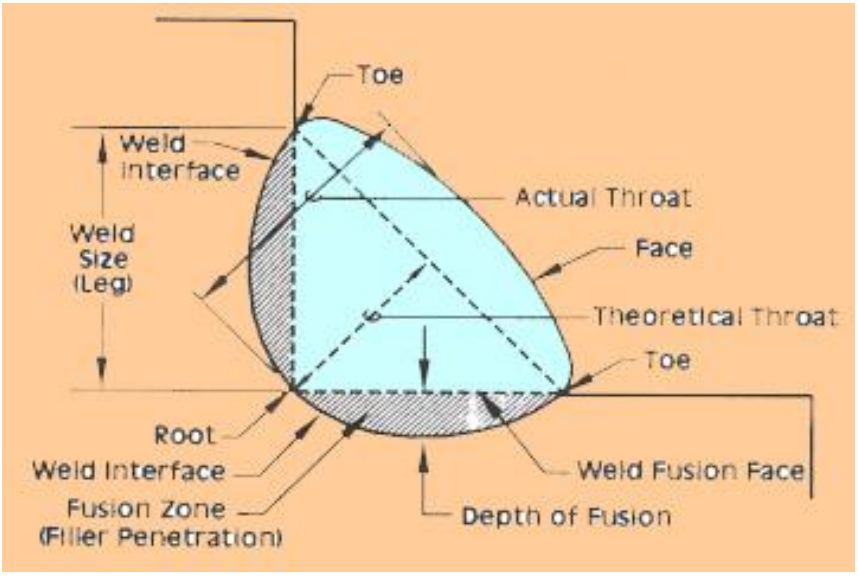

Figure 7 - Fillet weld properties (Weld Diagram, 2013)

Weld leg size

It has been found that for fillet welded cruciform joints, increased fatigue strength at the weld root can be achieved by increasing the leg length of the weld (Petershagen, 1975). By increasing the weld legs sufficiently, the joint will fail at the toe rather than the root, as the weld toe is not affected by the increased weld leg size.

Weld penetration

For fillet welds, the root of the weld can behave crack-like, thus the fatigue life consist only of the second and third stage of fatigue life, respectively region II and III in Figure 6. This will lead to a decrease of fatigue life (Maddox, 1991).

By increasing the degree of weld penetration, Ouchida and Nishioka (as cited in Petershagen, 1975) found that the weld leg size needed to avoid fatigue failure at the root is reduced. The fatigue strength at the weld toe is not significantly affected by the increased penetration.

The degree of welding penetration depends on the welding method, and deeper penetration can be obtained by automatic welding methods (Petershagen, 1975)

Recommended practice

In order to avoid weld root fatigue failure from occurring prior to a fatigue failure at the toe, DNV (2012) have issued recommendations on the design of fillet welds. These recommendations are based on the parameters defined in Figure 8, where level of penetration is defined as the edge length $2a_i$, and the weld leg size and plate thickness is given as h and t_p, respectively.

Leg size relative to the plate thickness and weld penetration length relative to plate thickness, can then be compared in Figure 9 in order to determine the most likely fatigue failure mode.

It is noted that for cruciform joints, an additional requirement of the edge distance $2a_i \geq 10mm$, is required in order to determine that weld toe fatigue is the most likely fatigue failure mode.

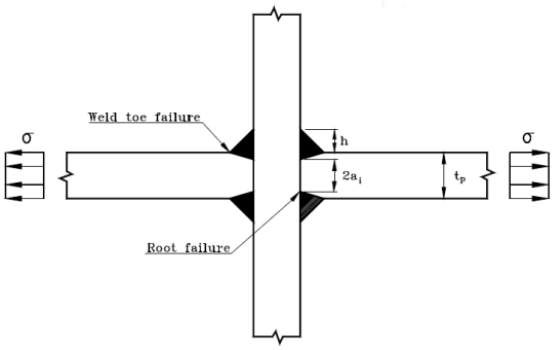

Figure 8 - Weld parameters used to evaluate failure mode (DNV, 2012)

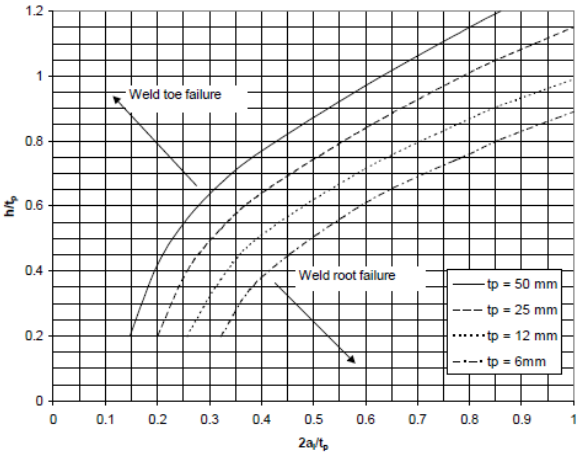

Figure 9 - Graph for evaluating failure mode for partial and fillet penetration welds (DNV, 2012)

2.5 Fatigue analysis using the nominal stress approach

2.5.1 General

Nominal stress is defined as the average stress in a welded joint (Hobbacher, 2009b). Assessing fatigue life using the nominal stress approach is achieved by comparing the detail at hand with detail classes of well tested typical joints, associated to standard S-N curves (Fricke, 2003). Both DNV (2012) and IIW (Hobbacher, 2009a) have issued a set of S-N curves, with an associated set of fatigue classes for typical joint details.

Detail dimensions, welding methods, and other parameters will however vary, and these variations are not covered by the detail classes (Hobbacher, 2009b). In order to use the nominal stress approach, there must therefore be a comparable well tested joint. Another issue is that stresses in the section considered may vary due to macro-geometrical notch effects close to the weld, such as large cut-outs and other sources for unequal stress distributions. This makes it difficult to determine the nominal stress, and determination is thus left to the engineering assessment of the designer. It is however common to take the averaged stress, a distance 1 or 1.5 times the thickness away from the weld toe.
Another uncertainty is that a FEA calculates the geometric stress concentrations, and not the effective stress concentrations, which is relevant for fatigue (Hobbacher, 2009b). The former is however always greater than the latter, resulting in overestimated stress, but yet conservative design.

2.5.2 The nominal stress approach for a cruciform joint

According to DNV (2012), when plate thickness of the load carrying member is less than 20mm, fatigue assessments at both weld root and toe are to be evaluated for the following joints: Partial penetration tee-butt-, effective full penetration in tee-butt- and a cruciform fillet welded joint as shown in Figure 10.

For fatigue assessment at the root of the weld, the nominal stress to be evaluated is the weld stress. Fatigue assessment of the weld toe is evaluated using the nominal plate stress.

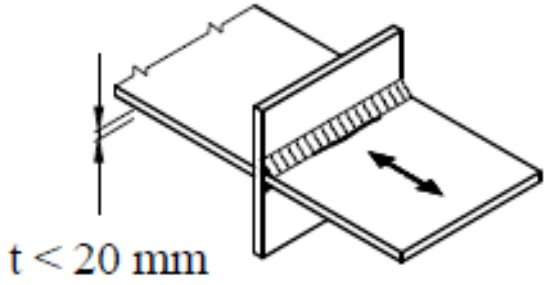

Figure 10 - Construction detail: Cruciform joint (DNV, 2012).

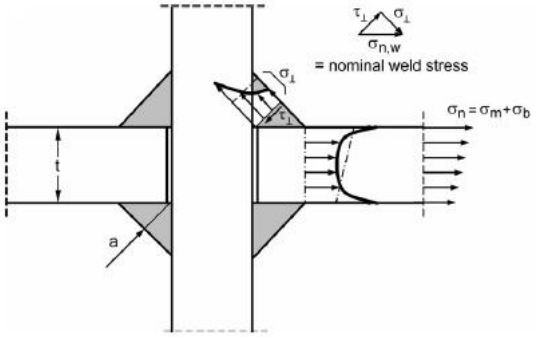

Figure 11 - Nominal stress in a fillet welded cruciform joint (Fricke, 2013).

Weld stress for a cruciform joint

As seen in Figure 11, all stresses can be assumed to be transferred through the fillet weld itself. A special weld stress, based on averaged stress components in the weld throat, is commonly applied according to equation (9) (Fricke, 2013).

$$\sigma_{nom,w} = \sqrt{\sigma_{\perp}^2 + \tau_{\perp}^2} \quad (9)$$

Here $\sigma_{\perp}^2$ and $\tau_{\perp}^2$ are defined in Figure 11, as the stress normal to the throat section and shear stress in the weld throat section, respectively.

The nominal stress can be determined by equilibrium conditions for simple cases, or for complex cases, by use of FEA using the forces or stresses in the weld (Fricke, 2013).

Considering the cruciform joint in Figure 11, subjected to a simple nominal stress composed of a membrane stress component σ_m and a bending stress component σ_b. The nominal stress can be determined by comparing the stress through the weld area, to the stress through the plate area (Fricke, 2013). The membrane stress contribution is found by comparing the axial force in the plate to the axial force in the weld. Similarly, the bending moment in the plate can be compared to the bending moment in the weld.

The bending moment in the plate and weld can be obtained according to equation (10) and (11), respectively.

$$M_{plate} = \frac{\sigma_{b,p} I_x}{y_0} = \frac{\sigma_{b,p} \frac{t^3 d}{12}}{\frac{t}{2}} = \frac{\sigma_{b,p} t^2 d}{6} \quad (10)$$

$$M_{weld} = F\frac{t}{2} = \sigma_{b,w} A \frac{t}{2} = \sigma_{b,w} a \frac{td}{2} \quad (11)$$

$\sigma_{b,p}$	-	*Plate bending stress*	t	-	*Plate thickness*
$\sigma_{b,w}$	-	*Weld bending stress*	a	-	*Weld throat*
F	-	*Force corresponding to moment in weld*	A	-	*Area of which the stress is acting*

The depth d, of the joint is taken as a unit length, which for the case of the detail in Figure 10 is equal for weld and plate. For the plate moment, the weld stress is assumed to act on the minimum weld throat area which is the weld's throat size multiplied with the depth. The membrane stress and bending stress contributions can then be found by equilibrium according to equations (12) and (13), respectively.

$$F_{plate} = 2F_{weld} \rightarrow td\sigma_{m,p} = 2ad\sigma_{m,w} \rightarrow \sigma_{m,w} = \sigma_{m,p} \frac{t}{2a} \quad (12)$$

$$M_{plate} = 2M_{weld} \rightarrow \sigma_{b,p} \frac{t^2 d}{6} = 2(\sigma_{b,w} ad \frac{t}{2}) \rightarrow \sigma_{b,w} = \sigma_{b,p} \frac{t}{6a} \quad (13)$$

The nominal weld stress is then obtained as shown in equation (14), by adding the stress contributions (Fricke, 2013)

$$\sigma_{n,w} = \sigma_{m,w} + \sigma_{b,w} = \sigma_{m,p} \frac{t}{2a} + \sigma_{b,p} \frac{t}{6a} \quad (14)$$

It is mentioned that for details subjected to multi-axial loading, the weld stress may be calculated according to DNV (2012), by using equation (15).

$$\Delta\sigma_w = \sqrt{\Delta\sigma_{\perp}^2 + \Delta\tau_{\perp}^2 + 0.2\Delta\tau_{\parallel}^2} \quad (15)$$

Here, the averaged shear stress parallel to the weld $\tau_{\parallel}$ has been accounted for, as shown in Figure 12.

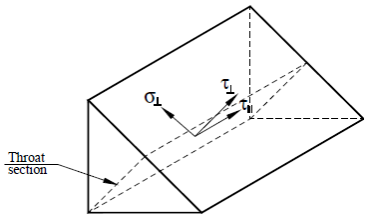

Figure 12 - Stress components used for weld stress calculations subjected to multiaxial loading (DNV, 2012).

Assessing fatigue life

Analyzing fatigue at the weld root, DNV (2012) recommend comparing the nominal weld stress with the "W3" SN-curve. The weld toe is assessed by comparing the nominal plate stress with the *G* SN-curve. In Figure 13, it can be seen that compared to stress amplitude, the weld root SN-curve (W3-curve) yields shorter fatigue life than the weld toe SN-curve (G-curve). It is noted, that the G-curve is used when the most probable failure mode, toe or root, has not been determined.

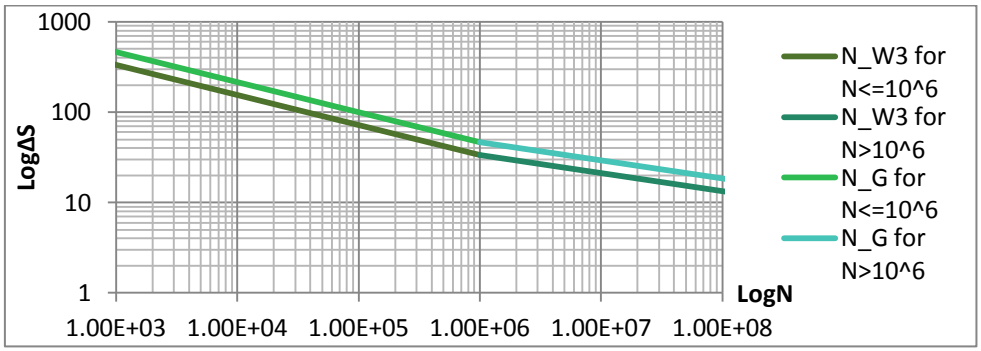

Figure 13 –The W3- and G Design SN curves.

2.6 The structural hot spot approach

2.6.1 General

The term *hot spot* is used as an area of geometric inhomogeneity, typically subjected to fatigue crack initiation (Radaj, Sonsino, & Fricke, 2009). For plate structures, typical hot spots are shown in Figure 14. The hot spot stress approach saw a great breakthrough in the 1970s, when it was discovered that the local stresses should be extracted at a distance from the hot spot, depending on plate thickness (Fricke & Kahl, 2005). Later, investigations were summarized and structural stress at the hot spot was defined by Radaj (1990) as the surface

stress, which can be derived. The structural stress is dependent on the shape, dimensions and the way the components are arranged, in addition to the level of loading and type of loading (Radaj et al., 2009).

The stress distribution through the thickness is usually non-linear in a welded plate (Hobbacher, 2009b). The stress can then be separated into three parts: Membrane, shell bending and non-linear peak stress as shown in Figure 15.

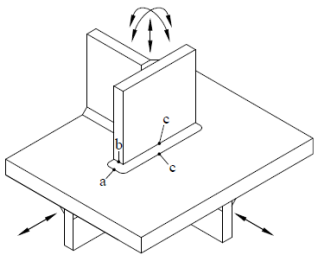

Figure 14 - Hot spots at weld toes for plate structures (DNV, 2012).

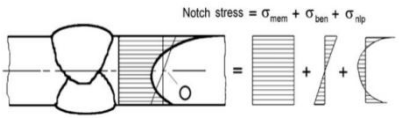

Figure 15 - Non-linear stress separated into membrane, shell bending and non-linear peak stress (Hobbacher, 2009b).

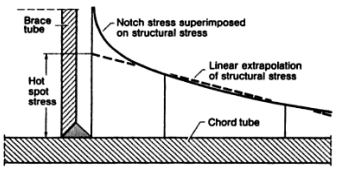

Figure 16 - Linearization of surface stress (Radaj, Dieter, Sonsino, & Fricke, 2006).

The structural stress, also known as geometrical stress, includes all the notch effects of the detail except for the non-linear part caused by the weld profile (Hobbacher, 2009b), which is generally ignored in a FEA (Radaj et al., 2009). This non-linear part is instead accounted for by the applied S-N curve (DNV, 2012). The structural hot spot stress at the weld toe, is found by linearly extrapolating the surface stresses at defined distances away from the weld toe (Radaj et al., 2009), as shown in Figure 16. These distances are determined differently by the regulation societies and agencies, but the concept is the same.

The structural hot spot stress approach requires fine meshing, and therefore one may obtain a geometric stress concentration factor (SCF), according to equation (16), by introducing a local shell-, or solid sub model subjected to a unit load (DNV, 2012). By doing this, stresses at the hot spot may easily be calculated for any unit load applied to the sub model.

$$SCF = \frac{\sigma_{hotspot}}{\sigma_{nom}} \quad (16)$$

2.6.2 The structural hot spot approach according to DNV

DNV (2012) has recommended two methods, A and B, for derivation of hot spot stress. Both methods are applicable for both shell and solid FEA, by extracting principal stresses. For shell elements, the weld is not modeled, and the hot spot stress is obtained at the plate-plate intersection. For solid models the weld is included and the hot spot stress is obtained at the

weld toe, as shown in Figure 17. In the following, hot spots considered in the FEA refer to these locations.

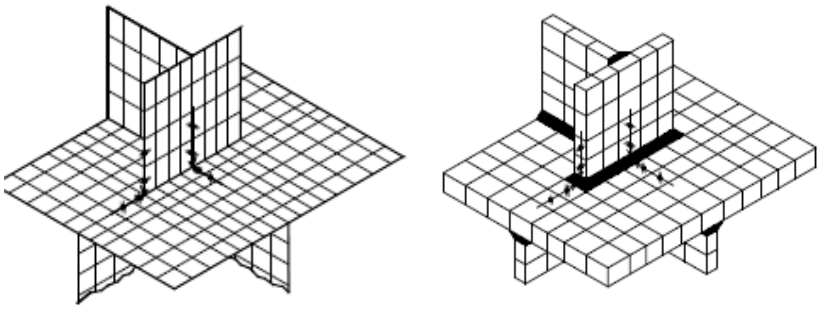

Figure 17 –Shell- and solid element model of a welded structure (DNV, 2012)

Method A uses linear extrapolation to the hot spot, from the surface stresses at $\frac{t}{2}$ and $\frac{3t}{2}$ from the hot spot, where t is the thickness of the plate on which the weld toe is located. Using method B, the stress at a distance $\frac{t}{2}$ from the hot spot is evaluated. The effective hot spot stress for the two methods can then be calculated according to formulas given in DNV's RP-C203 (2012).

For shell elements, DNV recommends using 8-noded elements, particularly for cases with steep stress gradient, or 4-noded elements with improved in-plane bending modes. Extracting stresses at $\frac{t}{2}$ and $\frac{3t}{2}$ is convenient when using rectangular 8-noded plate or shell elements, as stresses may be extracted at the mid side gauss points, for an element size equal to the thickness of the plate. The plate thickness is hence the preferred mesh size.

When meshing a three dimensional model, the mesh size for the first two or three elements should be equal to the thickness of the plate for both length and width, however, the width should never exceed the thickness of the attachment (including weld legs) at the hot spot. For hot spots termed *c* in Figure 14, the latter applies in regard to the thickness of the web plate behind the attachment.

If using 20-noded solid elements, one element in the thickness direction is sufficient, and applying reduced integration with two Gauss points in the thickness direction allows for determining membrane and bending components of the stress. Using 8-noded elements, a minimum of four elements in the thickness direction is recommended. When using solid elements, stresses must first be extrapolated from the Gaussian points to the surface, then interpolated to the points at the required distance from the hotspot, before being applied according to method A or B, see Figure 18.

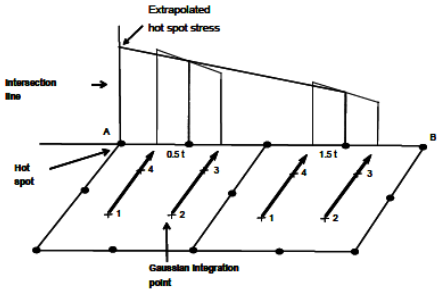

Figure 18 –Obtaining hot spot stress with solid elements by method A (DNV, 2012).

In order to account for the direction of the principal stresses as shown in Figure 19, the effective hot spot stress can be calculated according to equation (17) and (18) for method A and B, respectively. Here $\Delta\sigma_{\perp}$, $\Delta\sigma_{\parallel}$ and $\Delta\tau_{\parallel}$ are respectively stresses normal to the weld, -parallel to the weld, and shear stresses at the plane of the weld toe. The alpha factor is used when principal stress is more parallel to the weld, as shown in Figure 19, and depends on detail class (DNV, 2012).

$$\sigma_{Eff} = max\begin{Bmatrix}\sqrt{\Delta\sigma_{\perp}^2 + 0.81\Delta\tau_{\parallel}^2} \\ \alpha|\Delta\sigma_1| \\ \alpha|\Delta\sigma_2|\end{Bmatrix} \quad \alpha = \begin{cases}0.90\ for\ class\ C2\ detail \\ 0.80\ for\ class\ C1\ detail \\ 0.72\ for\ class\ C\ detail\end{cases} \qquad (17)$$

$$\sigma_{Eff} = max\begin{Bmatrix}1.12\sqrt{(\sigma_{\perp})^2 + 0.81\Delta\tau_{\parallel}^2} \\ 1.12\alpha|\Delta\sigma_1| \\ 1.12\alpha|\Delta\sigma_2|\end{Bmatrix} \qquad (18)$$

Where $\Delta\sigma_1$ and $\Delta\sigma_2$ are the principal stress, calculated according to equation (19) and (20), respectively.

$$\Delta\sigma_1 = \frac{\Delta\sigma_{\perp} + \Delta\sigma_{\parallel}}{2} + \frac{1}{2}\sqrt{((\Delta\sigma_{\perp} - \Delta\sigma_{\parallel})^2 + 4\Delta\tau_{\parallel}{}^2} \qquad (19)$$

$$\Delta\sigma_2 = \frac{\Delta\sigma_{\perp} + \Delta\sigma_{\parallel}}{2} + \frac{1}{2}\sqrt{((\Delta\sigma_{\perp} - \Delta\sigma_{\parallel})^2 + 4\Delta\tau_{\parallel}{}^2} \qquad (20)$$

a) b)

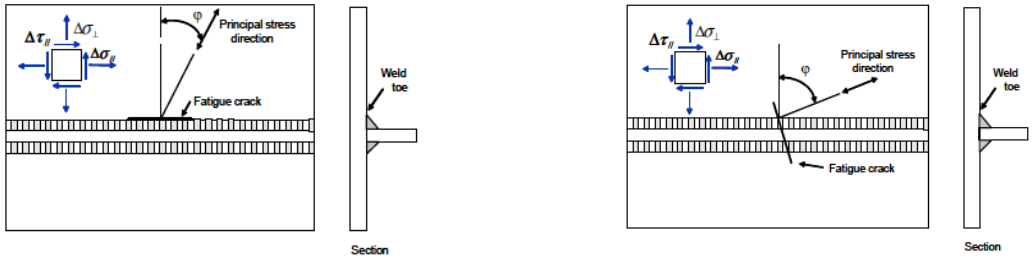

Figure 19 - Local stresses at welded structure with a) fatigue crack along weld toe for a principal stress normal to the weld and b) when principal stress direction is more parallel to weld toe (DNV, 2012)

For hot spots at plates subjected to significant plate bending, DNV recommends reducing the bending stress component by 40%, according to equation (21), for calculations of the effective hot spot stress.

$$\Delta\sigma_{e,hot\ spot} = \Delta\sigma_{m,hot\ spot} + 0.60\Delta\sigma_{b,hot\ spot} \quad (21)$$

Where $\Delta\sigma_{e,hot\ spot}$, is the effective hot spot stress, $\Delta\sigma_{m,hot\ spot}$ is the membrane- and $\Delta\sigma_{b,hot\ spot}$ is the bending stress component at the hot spot.

Assessment of fatigue strength is in general done by comparing the effective hot spot stress with the D-curve. However, for simple cruciform joints, T-joints in plated structures or simple butt welds welded from one side, DNV (2012) recommends using the nominal SN-curve for the relevant detail.

2.7 The effective notch stress approach

The effective notch stress method is a linear elastic approach for assessing fatigue life in welded structures by modeling the weld toe or root, with a reference radius ρ_f. This reference radius accounts for irregularities in the weld, as well as non-linear behavior (Sonsino et al. 2012).

Due to a high stress concentration factor for respectively, a sharp or pointed notch in linear elastic conditions, extremely high or infinitely high stresses will occur (Radaj, Lazzarin, & Berto, 2013). In reality, these notched parts have a considerable failure strength, which indicates that there must be an effect that counteracts the high stress build up. Heinz Neuber (as cited in Radaj et al., 2013) found that this microstructural support effect can be described by averaging the maximum notch stresses in a small material volume at the notch root, and that this average stress can be described by the maximum stress in a similar notch with a larger fictitious radius, as shown in Figure 20. The size of this fictitious notch radii can be found using equation (22).

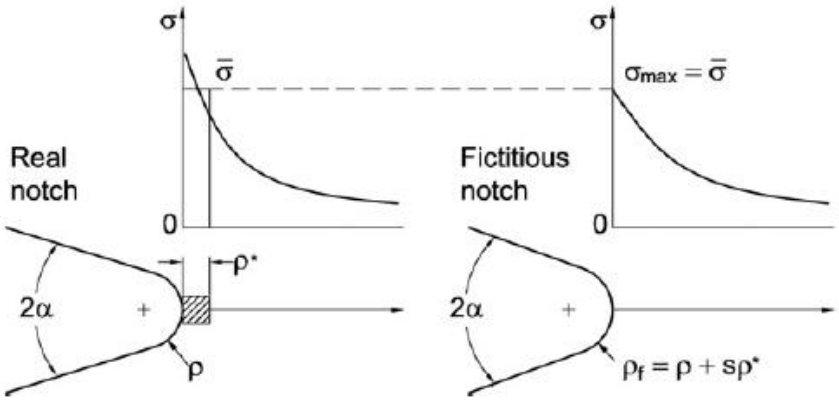

Figure 20 - Obtaining the average stress in the real notch by maximum stress in a notch with a larger fictitious radius (Radaj et al., 2013)

$$\rho_f = \rho + s\rho^* \qquad \begin{matrix} \rho_f - Fictitious\ notch\ radius \\ \rho - Real\ notch\ radius \\ s - microsupport\ factor \\ \rho^* - microsupport\ length \end{matrix} \qquad (22)$$

Due to irregularities of welded joints at the weld toe and root, normal determination of notch stress cannot be applied (Hobbacher, 2009b). However it has been shown that the irregular notch may be replaced by an effective notch with the radius ρ_f, equal to 1mm. This has been done by considering the worst case scenario: The notch is sharp, that is, with no real radius ($\rho = 0$). For welded steel structures the microsupport length and microsupport factor has been conservatively estimated to $\rho^* \approx 0.4$mm and $s \approx 2.5$ (Radaj, 1990). These factors are today recommended by DNV (2012) and IIW (Hobbacher, 2009a), in application of the notch stress approach for plates with thicknesses $t \geq 5mm$. For thinner plates it is mentioned that a fictitious radii $\rho = 0.05$ is commonly used (Sonsino et al., 2012), this will not be further addressed as such thicknesses are less common in ships and offshore structures.

Lately it has been stated by Radaj et al. (2013) that the description of ρ^* and s is a too rough estimate, and that the microsupport factor should be chosen according to loading modes as shown in Figure 5. An improved microsupport factor was found to be $s = 2.0$ for mixed loading modes 1 and 2, and $s = 1.0$ for loading mode 3. This results in fictitious notch radiuses of 0.8mm and 0.4mm, respectively. The introduction of a loading mode dependent microsupport factor may however cause difficulties, as it may prove challenging to determine the loading mode for the detail at hand.

The effective notch stress method is by DNV (2012) and IIW (Hobbacher, 2009a) considered inapplicable for joints where considerable stress components are parallel to the weld. The IIW also limits the method to naturally formed welds, i.e. without weld improvements.

In a FEA, the notch may be modeled such that the cross section of the weld has a blunt circular notch at the weld toe, and a keyhole at the weld root, which is shown in Figure 21. DNV do not give details on how the notch is to be positioned, although it can be interpreted

from figures given by DNV (2012) and IIW (2009a), that the notch is modeled such that the notch surface is touching the geometric root of the weld, and that the notch center is at the same plane as the continuous plate's surface. This is also shown in Figure 23 and Figure 22d. The IIW describes the positioning of the notch as the following:

"The effective notch radius is introduced such that the tip of the radius coincides with the root of the real notch" (Hobbacher, 2009a, p.34).

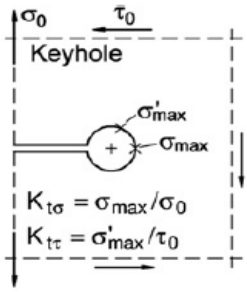

Figure 21 - Illustration of keyhole geometry (Radaj et al., 2013).

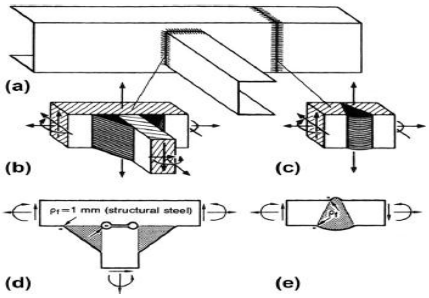

Figure 22- a) Part with welded joints, b), c) close-up of welded joints with internal forces, d), e) modeling of keyhole at the weld root and toe (Radaj et al., 2013)

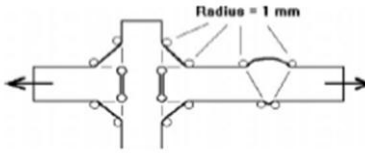

Figure 23 – Modeling of the fictitious notch root at fillet- and but welded joints (Hobacher,

In a research paper by Fricke (2013), modeling of the notch for lap joints and cover plates shown in Figure 24 is performed in a different way, and described as the following:

"The keyhole notch has been placed such that the minimum distance between the rounded notch and the weld surface is exactly the throat thickness" (Fricke, 2013, p.781).

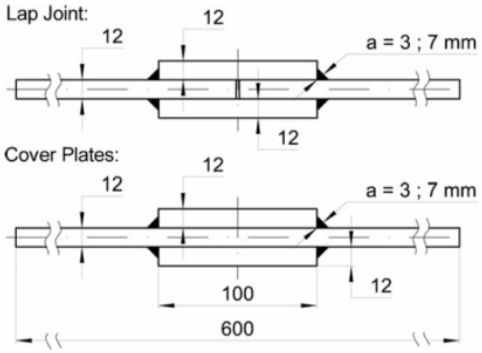

Figure 24 - Lap joints and cover plates (Fricke, 2013)

For simple models one may estimate a stress concentration factor (SCF) by dividing the fictitious notch stress by the nominal stress, in the same manner as equation (2) was utilized for the hot spot method.

Due to the implementation of the relatively small notch radius compared to the structure, mesh density has to be even lower in order to sufficiently represent the notch. Thus, computational time is high in comparison with the hot spot method. DNV (2012) recommends the use of minimum 4 elements along a quarter of the notch circle circumference, if using quadratic elements. For a fictitious notch with 1mm radii, this corresponds to a mesh size of approximately 0.4mm at the notch surface.

In addition to assessing the gap at the weld toe, this method also gives the opportunity of assessing a possibly present weld root gap as well as weld toe angle, leg lengths and undercut (Hobbacher, 2009b). The assessment of fatigue life may then be executed according to IIW, by comparison with the FAT225 SN-curve for steel welded joints, and FAT 72 for aluminum (Hobbacher, 2009a), or according to DNV by comparing with SN-curves given by the parameters in Table 1 for welded steel joints. It is noted that the notch stress is assumed to account for the thickness affect, and is thus not included in the SN-curve.

Table 1 - The effective notch stress S-N curves (DNV, 2012).

Notch stress SN-curves		
Environment	$\log \bar{a}$	$\log \bar{a}$
Air	$N \leq 10^7$ cycles $m_1 = 3.0$	$N > 10^7$ cycles $m_2 = 5.0$
	13.358	17.596
Seawater with cathodic protection	$N \leq 10^6$ cycles $m_1 = 3.0$	$N > 10^6$ cycles $m_2 = 5.0$
	12.958	17.596
Seawater with free corrosion	For all N $\log \bar{a} = 12.880$ and $m_1 = 3.0$	

DNV (2012) has described a validation procedure for the effective notch stress analysis methodology. The procedure involves comparing results obtained from the effective notch stress approach to the nominal stress approach, for a cruciform joint. A SCF target value at the root of a fillet welded cruciform joint is given as 6.25. Based on interpretation, it is assumed that an unfortunate typing mistake has been made by writing *root* rather than *toe*. If this is the case, the SCF target value at the *toe* of a full penetration welded cruciform joint is given as 3.17. The value, and hence the former assumption should however be verified.

2.8 Comparison of the approaches for assessment of fatigue life

The nominal stress approach is a rather simple and quick way of assessing fatigue, both at the weld toe and at the weld root. However, the method is not always applicable due to the limited types of detail classes, and that for some cases nominal stress cannot be defined (Bruder, Störzel, Baumgartner, & Hanselka, 2012).

When the nominal stress approach is not applicable, the effective hot spot and -notch stress approach are good alternatives. Both methods account for the structural geometry surrounding

the weld. Only the notch stress approach considers the weld shape, enabling fatigue assessments at the root of the weld as well as the toe. That being said, the effective notch stress approach requires a solid FEA model, and thus computational time is dramatically increased. A summary of the approaches are given in Table 2.

Table 2 - Comparison of the design fatigue life approaches.

Nominal stress approach	**Structural hot spot approach**	**Effective notch stress approach**
Nominal stress must be defined.	Well described procedure (DNV and IIW)	Recently included in recommendations by DNV and IIW.
Requires a comparable detail class.	Requires quite fine meshing, and thus sub-modeling may be required.	Requires very fine mesh, thus computational time is high and a sub-model is required for most cases.
Simple to apply if nominal stress and detail class can be found.	Applicable for FEA using either shell or solid elements.	Applicable only for solid elements with the weld modeled.
Describes fatigue at both weld toe and weld root.	Fatigue assessment at weld toe only.	Describes fatigue at both weld toe and weld root.
SN-curve is defined for each case dependent on detail class.	Generalized SN-curve (D-curve). Except for simple cruciform joints, T-joints in plated structures or simple butt welds welded from one side	Generalized SN-curve.

2.9 Cumulative damage

Fatigue design of welded structures is based on constant amplitude stress, and as marine structures are subjected to stochastic variable amplitude loading, a way of assessing the damage inflicted during a time history is needed. A load history is commonly represented by an exceedances diagram of stress ranges, as shown in Figure 25a, where stress range has been plotted for number of exceedances based on different types of load histories (Næss, 1985).

a) b)

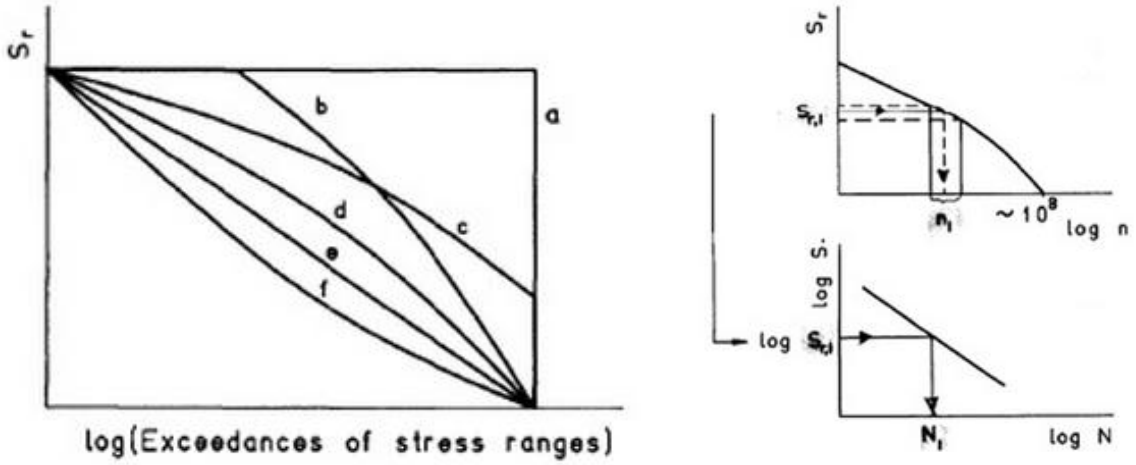

Figure 25 - a) Exceedances diagram of stress ranges and b) the miner summation procedure for one stress block (Næss, 1985).

A common method of assessing the cumulative damage is by Miner summation (Næss, 1985). The procedure is carried out by dividing the stress exceedances diagram into stress blocks as shown in Figure 25b, based on the assumption that the damage inflicted per load cycle is constant in each block. Then, for each stress block, a stress range $S_{r,i}$ and a number of cycles n_i may be defined. By further calculating the design life N_i, for each stress range based on the SN-curve for the relevant detail, the damage sum is defined according to equation (23).

$$D = \sum_i \frac{n_i}{N_i} \quad (23)$$

If the damage sum is equal to or larger than one, the detail is expected to fail within the time of the load history (Næss, 1985). Further, as the damage sum is equal to one for fracture within the time history of the spectrum, the fatigue life (years) may be obtained from equation (24), where T_0 denotes the total time interval of the spectrum in years, and T_f represents the fatigue life of the detail.

$$T_f = \frac{T_0}{D} \quad (24)$$

3 Methodology

3.1 Validating the effective notch stress approach

DNV (2012) has given recommendations for validation of the effective notch stress methodology. The model given for assessment of weld root fatigue is the fillet welded cruciform joint shown in Figure 26. As the weld is considered a pure fillet weld, which is corresponding to a value of 1 at the x-axis of Figure 9, the failure mode for the fillet welded joint is clearly expected to be root failure.

In order to verify the positioning of the fictitious notch at the weld toe, a model consisting only of this notch was made. This is equivalent to a full penetration welded joint as shown in Figure 27, with the same dimensions as for the fillet welded joint. Fatigue assessment was thus compared using the nominal stress approach, applying the F-curve (DNV, 2012).

The effective notch stress analysis was performed using the FEA software Abaqus. When the positioning of the notch had been concluded, a third model was made where the fictitious notch at both the weld toe and root were included, in order to represent the weld toe of the fillet welded joint. This model will be referred to as the *combined* model. For the combined model, fatigue assessments using the nominal stress approach were performed using the F3-curve for the weld toe and the W3-curve for the root (DNV, 2012).

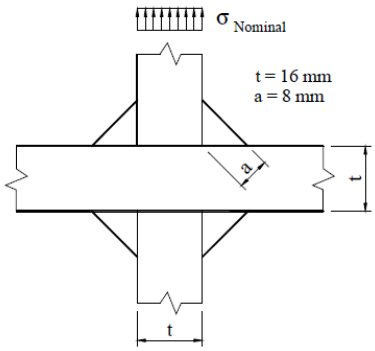

Figure 26 – Fillet welded cruciform joint for evaluation of weld root fatigue (DNV, 2012)

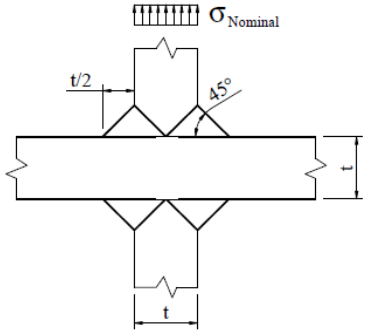

Figure 27 - Full penetration welded cruciform joint for evaluation of weld root fatigue (DNV, 2012)

Target values for the effective notch stress approach were obtained by comparing to fatigue assessments based on the nominal stress approach. Deviation from these target values were calculated by equation (25)

$$Deviation = \frac{measured\ value - target}{target} \quad (25)$$

When the results from the FEA were found to be satisfying compared to the target values, fatigue life was calculated based on the notch stress fatigue curve, and compared with fatigue

life obtained from the nominal stress approach. Fatigue life deviation from the nominal approach was calculated in the same manner as for stress deviation.

3.1.1 Establishing target stress values

Target values for the effective notch stress approach were determined based on the nominal stress approach, and compared to the expected SCF's given by DNV. This was done in order to get an insight in the calculations, and also to sort out and verify that the assumption of the formerly mentioned typing mistake was justified. The target values were obtained by demanding the fatigue life for the nominal- and notch stress approach to be equal. An illustration of the process is shown in Figure 28, where the arrows represent application of SN-curves according to approach, the nominal stress- and the effective notch stress approach.

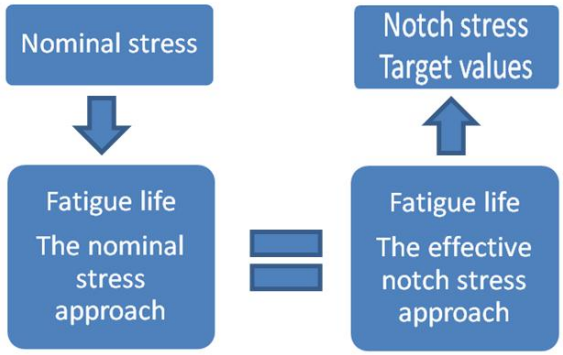

Figure 28 - Procedure for obtaining target notch stress values, where arrows represents appliance of SN-curve.

By entering the design curve parameters for both methods into equation (3) and solving for $\Delta\sigma_{notch}$, an expression for the target value is obtained as shown in equation (26). The SN curve parameters can be recognized as nom and $notch$, for respectively the nominal- and the effective notch stress SN-curves. By further rearranging the parameters, a target notch stress value may be obtained using equation (27).

$$\Delta\sigma_{notch,target} = 10^{\frac{m_{nom}\log(\Delta\sigma_{nom})+\log(\bar{a}_{notch})-\log(\bar{a}_{nom})}{m_{notch}}} \quad (26)$$

$$\Delta\sigma_{notch,target} = (\Delta\sigma_{nom})^{\frac{m_{nom}}{m_{notch}}} \left(\frac{\bar{a}_{notch}}{\bar{a}_{nom}}\right)^{\frac{1}{m_{notch}}} \quad (27)$$

The parameters used for the nominal stress approach are according to the design curves and stress parameters given in Table 3, as stated by (DNV, 2012).

Table 3 - Design curves and stress according to the nominal approach.

Investigation point	Design curve	Stress range
Root of fillet weld	W3	Weld stress
Toe of fillet weld	F3	Nominal stress
Toe of fully penetrated weld	F	Nominal Stress

As can be seen from the table, fatigue life assessments for the weld root is performed by taking the weld stress as the stress range, according to equation (14), where the nominal bending stress component was set to zero.

3.1.2 **Modelling**

In the FEA all dimensions were kept constant, except for the fictitious notches which' positions were to be found. The weld root notch was modelled with a keyhole, with a height of 0.1mm, and all notches were given a radius of 1mm.

As the positioning of the fictitious notch at the weld toe only was found illustrated in figures, such as Figure 23, two positioning alternatives were considered. These are shown Figure 29, and hereafter referred to as *toe 1* and *toe 2*. Toe 1 is based on interpretation of figures seen in the literature. It was also considered that positioning of the notch at the weld toe should be similar to the definitions given for the root. Thus, toe 2 was defined on the basis of the two formerly cited definitions from Hobbacher (2009a) and Fricke (2013).

a) b)

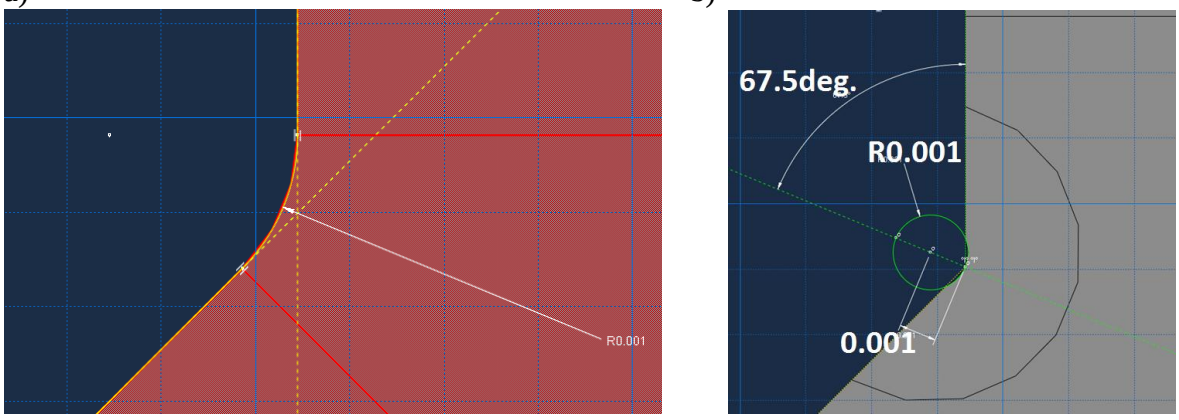

Figure 29 - Fictitious notch at weld toe: a) "toe 1" and b) "toe 2".

Similarly, the positioning of the fictitious notch at the root of the weld had to be determined. Three positions were defined as shown in Figure 30, which will be referred to as root 1 through 3. Root 1 and root 3 both correspond to Hobbacher's definition of the root position, but only root 1 correspond to Fricke's definition, which was applied in an analysis for cover plates and lap joints. As early results were somewhat lower than expected, root 2 was introduced in order to determine the sensitivity of the root placement.

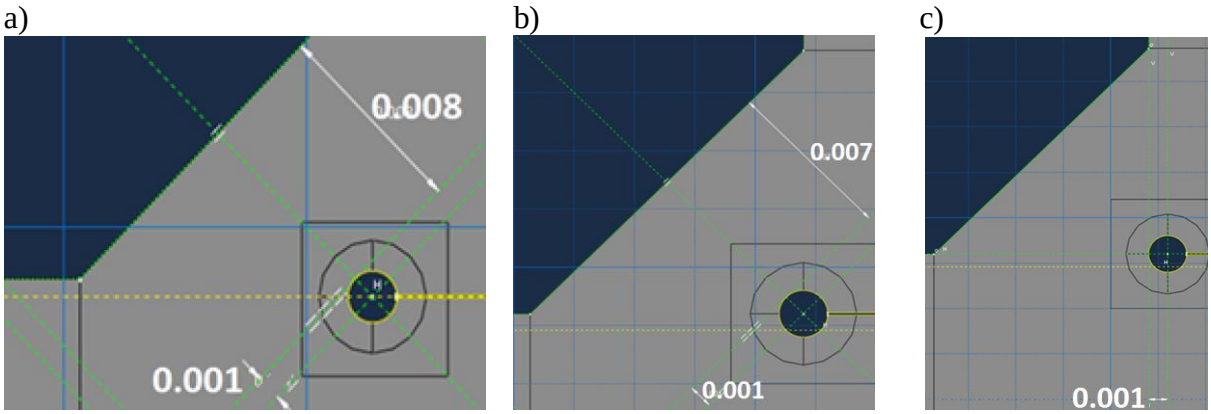

Figure 30 - Modelled fictitious notch at the weld root. a) *root 1*, b) *root2,* c) *root 3*.

3.1.3 Loads, boundary conditions and material properties

For the FEA, steel with elasticity modulus $E = 210GPa$ was used. The material was given linear elastic material properties, that is, yield stress was not defined.

The nominal stress was introduced as a negative pressure on the upper surface of the load carrying plate, as seen in Figure 31.

For boundary conditions, the lower surface was fixed in all translational directions. All rotations were kept free.

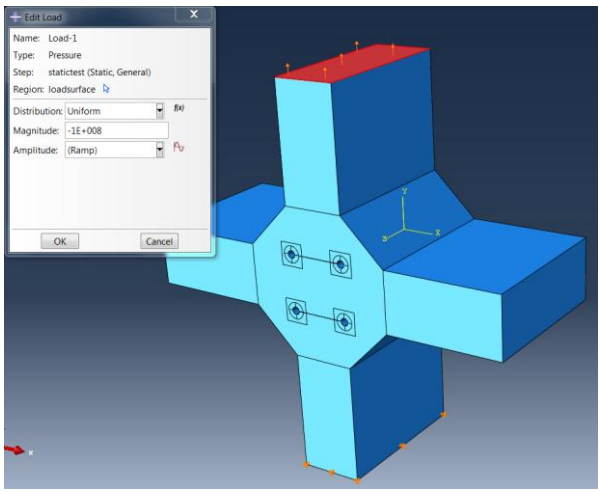

Figure 31 - Load and boundary conditions assigned to the model.

3.1.4 **Meshing**

The model was meshed using 20-noded quadrilateral elements, without reduced integration, that is the Abaqus' C3D20 element. Different meshing techniques were used in order to have smooth transitions from the very fine mesh surrounding the notch, to the coarser mesh used in less significant areas. In general, this was done by dividing the part into partitions, which is shown in Figure 32. Partitioning the model made it possible to define a desired number of elements along the edges of each partition, known as mesh seeding. Mesh seeding was performed by assigning mesh seeds for the inner fine mesh first, and expanding towards the coarser mesh.

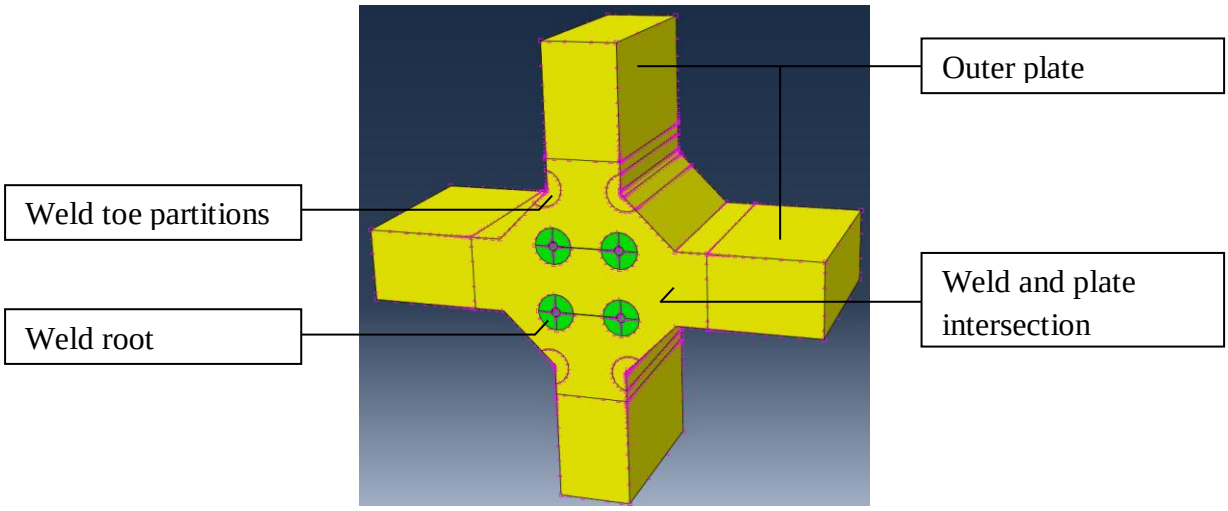

Figure 32 - Partitoning and seeding of the model.

Partitions were also assigned different mesh controls, which altered the mapping of the mesh. Three types of mesh controls were used:

- Structured mesh
- Medial axis
- Advancing front

Establishing good transitions was found to be an especially time consuming task for solid models, as transitions for hexagonal elements can only be altered in one plane at a time.

A mesh convergence study was performed for the most promising weld root and toe positions, by adjusting the number of elements per quarter circumference at the notches.

Weld root

The weld root mesh was seeded by assigning seeds both radially and circumferentially. It was found that in order to have the best transition from the weld root notch, the cross section of the weld root partition had to be further partitioned into 4 equal parts, as shown in Figure 33. This gave the opportunity of meshing these partitions with a structured mesh. The radius of

the partition was initially chosen as 2.2mm, but later redefined to 4mm, which extends over approximately half the weld size. The radial seeds were given a bias ratio, resulting in a decreased element size towards the notch surface. This gave the elements a low aspect ratio, as the circumferential length varies linearly in the radial direction.

a) b)

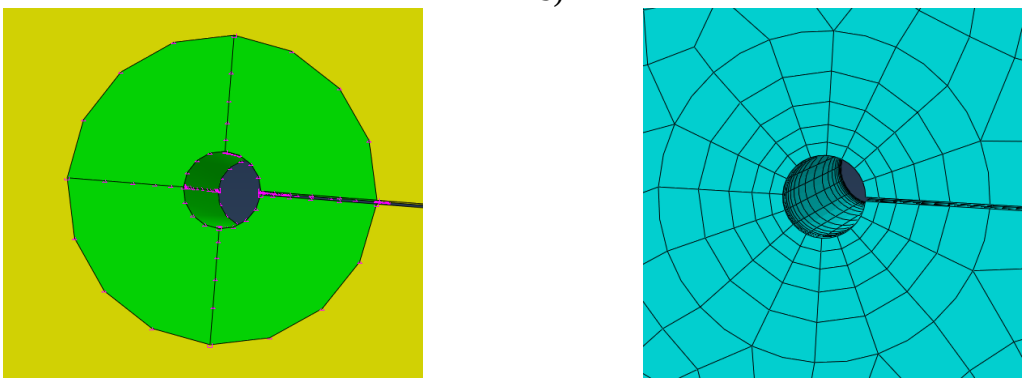

Figure 33 - Mesh at the weld root partition: a) partition surrounding the root, b) mesh obtained

Weld toe

The weld toe mesh was performed in the same way as for the weld root, with the partition radius defined with the same center as the weld toe notch. However, structured mesh gave small element angles, and it was thus decided to use the medial axis mesh control, which gave the most uniform mesh. Both of these techniques are illustrated in Figure 34.

It was also observed, that when using 4 elements along the quarter circumference, stress was more concentrated between the nodes. It was therefore decided to use 5 elements, which gave the opportunity of extracting these higher stresses at the nodes.

The outer edge of the weld toe partition was in general seeded with a number of elements 2.5 times the number of elements at the notch surface.

a) b)

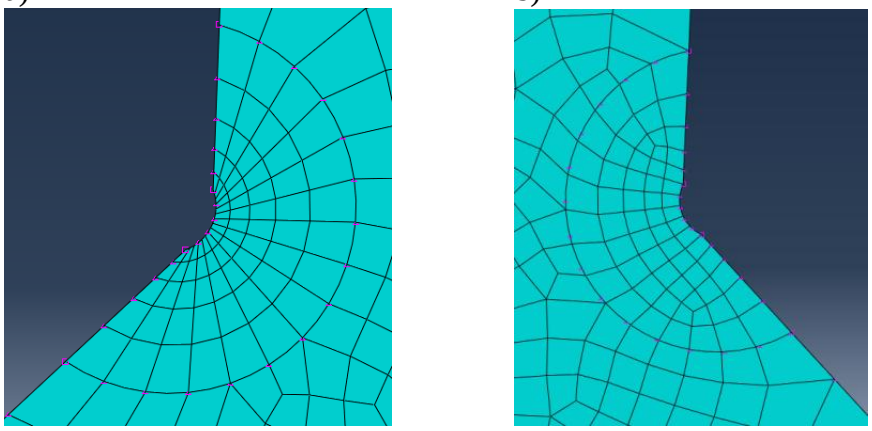

Figure 34 - Mesh at the weld toe partition: a) using structured mesh, b) using medial axis control.

Globally

In the weld and plate interaction area, advancing front controlled mesh was applied with a mesh seed of 1.7mm, which was seen to provide a smooth transition. Meshing with this controller gave the opportunity of meshing these complicated partitions with the most possible uniform mesh.

In the depth direction of the model, the weld and plate interaction area were given a double biased seed. This was done in order to have a finer mesh at the locations found to give the highest stress concentrations. Similarly a double biased seed was also introduced over the plate thickness, resulting in a finer mesh closest to the weld toe.

In order to minimize the number of elements, and thus the computational time, the plates were divided into four partitions at a distance 4mm from the weld toe. This formed the outer plate partitions, which were permitted the use of an advancing front controlled mesh. This gave the opportunity of having a coarser mesh towards the plate ends, as shown in Figure 35, by reducing the number of elements in the depth and longitudinal plate direction, towards the plate outer ends.

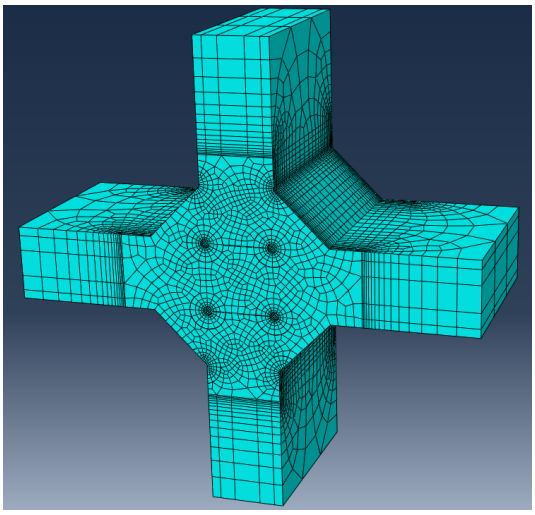

Figure 35 - Mesh for the fillet welded joint including both root 1 and toe 2 notches.

3.1.5 Extracting stresses

The results of the analysis were first visually inspected, in order to determine any possible mechanisms. The nodes containing the highest stresses were observed to follow a line in the depth direction. A path was thus created though these nodes in the un-deformed model, such that the highest stresses in the notch could be obtained at the path-node intersections. Maximum principal stress along this path was plotted as a function of length, and the maximum value of this stress was taken as the effective notch stress. The path is plotted on the deformed model in Figure 36.

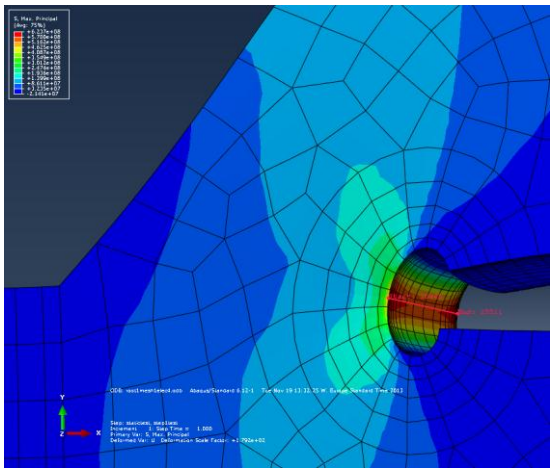

Figure 36 - Extracting stresses along a path.

3.1.6 Comparing the results

SCF's for both the weld toe and -root were obtained using equation (2), and compared to the target values by use of equation (25). Design life was assessed for both approaches, using their respective design curve parameters, according to equation (3). Similarly to the SCF's, design life for the two approaches were compared using equation (25).

3.2 Parametric weld size study

In order to check the effects on the effective notch stress for varying weld sizes, the verification model was analyzed for 4 additional weld sizes. All calculations were done according to the validated methodology, and all dimensions and mesh attributes were kept as similar to the verification model as possible, although some minor alterations were required.

In the analyses, the weld root partitions were scaled according to change in weld size. There was however an exception for the model containing a 4mm weld size, where the notch partitions were observed to become too small, forcing a decrease in the maximum number of elements in the radial direction to become less than three elements. This was redeemed by creating the notch partitions with the same radial size as the model with 6mm weld size.

As the results were found to deviate from the target values, two types of attempts were made in order to find the parameters influencing this discrepancy. The first attempt investigated a relation between the fictitious notch size and the weld size. The second attempt investigated a relation between the target stress values and the obtained effective notch stress, by implementing weld size as a variable. The attempts will further be addressed to as the notch size- and the notch stress correction studies.

3.2.1 Notch size study

An effort was made to find an ideal fictitious notch radius, capable of representing the target stresses. The procedure is shown in Figure 37, and further explained.

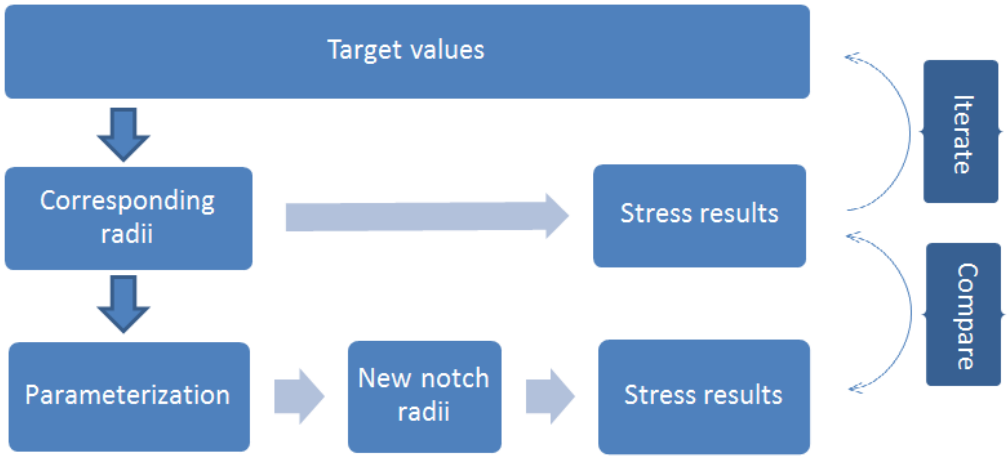

Figure 37 – Procedure of notch size parameter study.

The ideal fictitious notch radii was found by making an educated guess as to what notch radii would correspond to the desired stress value, followed by extrapolation of the values obtained. This was done in an iterative manner, until a satisfyingly low deviation was achieved.

In order to find parameters giving a relation between weld size and notch radiuses, these values were plotted in a graph and fitted with linear and second order polynomials, which is shown in Figure 61.

Verification of the parameters' precision was found by computing new notch radiuses for the weld sizes. By further comparing the stress results obtained from these parameterized notch sizes with the iterated stress results, the precision of the parameters were quantified.

3.2.2 Notch stress correction study

In order to investigate any relation between the target values and the obtained effective notch stresses, notch stress relative to the target stress was plotted for the defined weld sizes in Figure 63. Linear and second order polynomials were then fitted to the plots, giving parameters to describe the relation, as shown for the second order polynomial in equation (28).

$$\frac{\Delta\sigma_{notch}}{\Delta\sigma_{target}} = ax^2 + bx + c \qquad (28)$$

By solving the equation for $\Delta\sigma_{target}$, a corrected effective notch stress is obtained from the fitted parameters, and equation (29) is established. The corrected notch stress is thus a correction of the obtained FEA results, assuming that the nominal approach is the more precise approach. More importantly, it describes the relation between the two approaches.

$$\Delta\sigma''_{cor} = \frac{\Delta\sigma_{notch}}{ax^2+bx+c} \qquad (29)$$

The parameters were verified by calculating corrected notch stress for all weld sizes, and comparing the corrected notch stress with the target values obtained from the nominal approach.

3.2.3 Determining weld size by extrapolating notch stress

For an effective notch stress analysis, it might be useful to assess fatigue life for either an increase or a decrease of weld size, without running several analyses. From equation (27), used for finding target notch stresses, it can be found that for a constant membrane stress and

constant plate thickness, effective notch stress may be extrapolated. By inserting the weld stress (14), into the target notch stress equation (27), and further assuming same slopes for the SN-curves, target notch stress can be defined from equation (30).

$$\sigma_{notch,target} = \frac{1}{a}\left(\sigma_{m,p}\frac{t}{2} + \sigma_{m,p}\frac{t}{2}\right)\left(\frac{\bar{a}_{notch}}{\bar{a}_{nom}}\right)^{\frac{1}{m_{notch}}} \quad (30)$$

From this equation, it is clearly seen that for varying weld sizes, the other parameters can be assumed constant, and thus only determine the slope of the linear relation.

For an effective notch stress analysis with a weld size a_0 and an obtained effective notch stress
$\sigma_{notch,0}$, the effective notch stress $\sigma_{notch,i}$, for a weld size a_i may be determined by equation (31). The precision of the extrapolation is however affected by the relation between target notch stress and actual effective notch stress. That is, the extrapolation implies an assumption of the effective notch stress to be linearly varying for weld sizes.

$$\sigma_{notch,i} = \sigma_{notch,0}\frac{a_0}{a_i} \quad (31)$$

3.3 Fillet welded knee plate

The second joint, provided by Aker Solutions, is an extension of a brace gusset plate. This extension is in the form of a knee plate, welded against the brace and a ring stiffener as shown in Figure 38 a and –b, respectively. All drawings for the required geometry are given in Appendix I.

a)

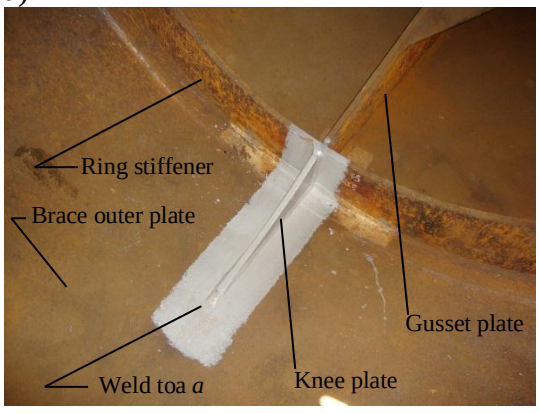

b)

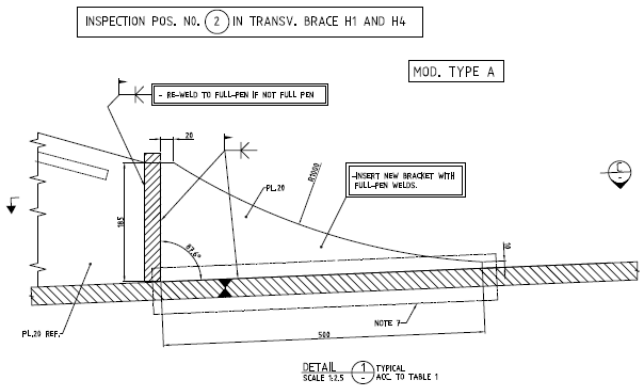

Figure 38 – a) picture of the knee plate located inside brace H1 and b) drawing of the knee plate with dimensions as used in analysis.

Fatigue life of the welded knee plate has been assessed by Aker Solutions for weld toe *a* shown in Figure 38a, that is the weld toe in the thickness direction of the knee plate. The fatigue life was assessed for variable amplitude loading using Miner summation and the effective hot spot method B for shell elements. In addition to assessing the cumulative damage, an SCF for the weld toe had been found, by subjecting a local model to a unit load of 1MN in the brace axial direction. These results were used for verification of the solid FEA model.

In order to assess weld root fatigue of the fillet welded knee plate, a solid FEA was made, based on the validated methodology established for the cruciform joint. As both modelling and FEA calculations of solids are time consuming processes, the model was limited to consist of the part indicated in Figure 39 only.

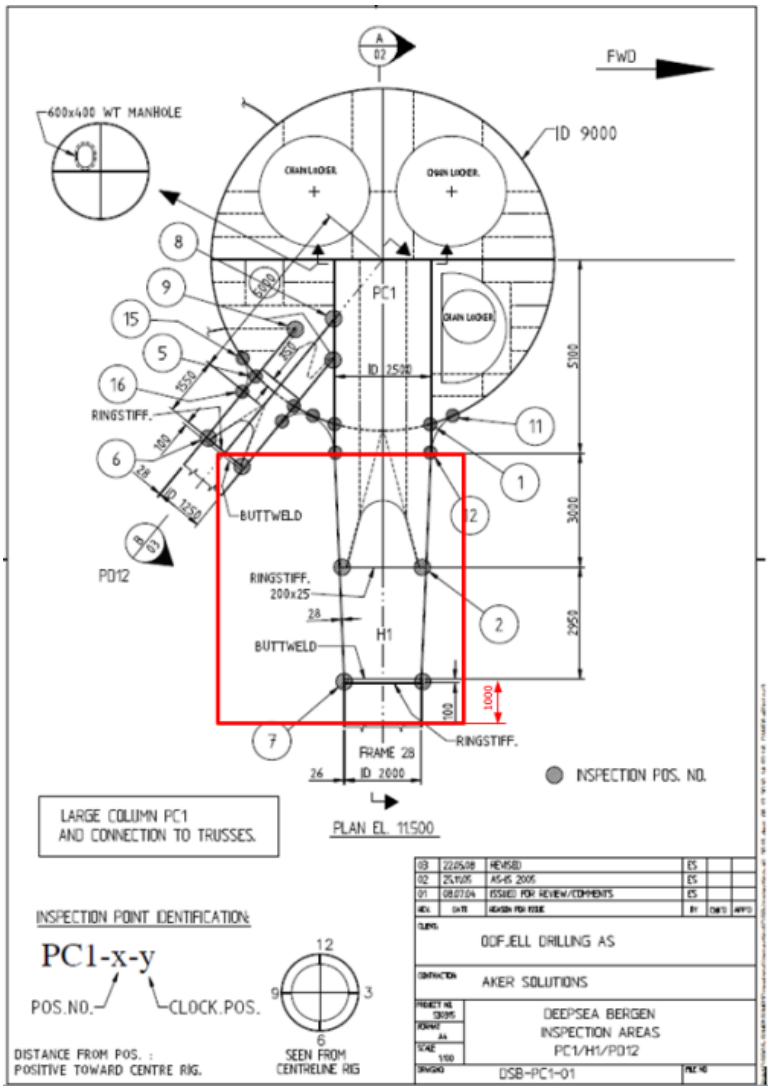

Figure 39 - Model used for fatigue analysis, indicated on inspection drawing of column PC1 and brace H1.

This part, which further will be referred to as the brace model, consists of the brace from the knee plates, intersecting the brace and column, and 1m past the second brace-ring stiffener. This allowed for a symmetrical cross section about both the horizontal- and vertical axis of the brace. A mesh of one fourth of the model was therefore sufficient, as mirroring attributes to either represent or create the entire model could be defined. The quarter model will further be referred to as the base model.

As the loading conditions provided by Aker solutions were non-symmetrical, mirrored boundary conditions could not be applied. It was therefore seen necessary to create a mesh for the entire part. This was achieved by assembling four base models and merging the nodes at the intersecting boundaries. Some simplifications were however necessary. Methodology differing from the validated methodology is further addressed.

3.3.1 Model simplifications

When modelling solids in Abaqus, the tools available are somewhat limited considering the complicated geometries needed to represent a fictitious weld root notch. The complex geometries resulted in difficulties when meshing the part, which were not seen solvable by further partitioning.

Simplification of knee plate

An attempt was made to model the knee plate with an outer surface having the same curvature as the brace. This also leads to having a curved weld, which means that the weld root notch also must follow this curvature. Creating such a notch was found to be quite cumbersome, and it was thus decided to create a part used for the cut-out, as shown in Figure 40b. Both approaches were found to be time consuming and resulted in partitions that could only be meshed using tetrahedron elements. This was seen to be caused due to a conflict between the notch root and the outer surface geometry of the knee plate.

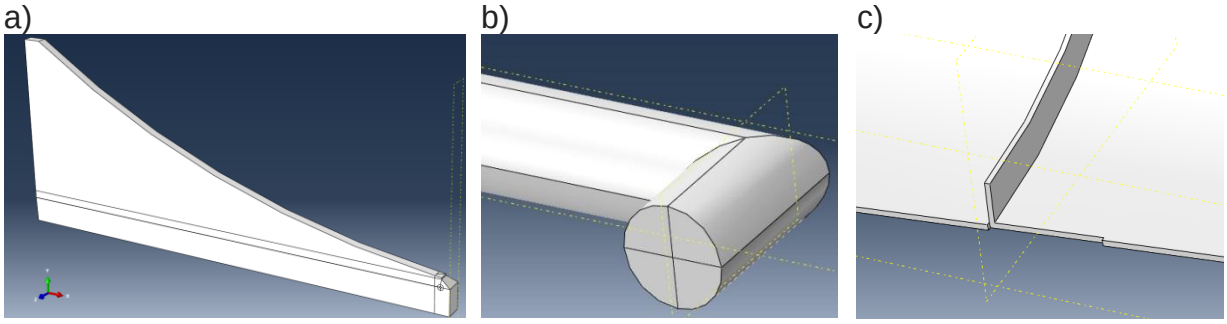

Figure 40 - a) The knee plate, b) the part intended for cutting out a weld root notch and c.) the cut-out for the knee plate

Due to the complications of having a curved surface surrounding the knee plate, parts of the brace was made flat along the entire length of the brace. This was done by creating a 1/8 -

cross section of the brace, and further make a cut out of 25mm for the knee plate as shown in Figure 40c. This gave the opportunity of creating a simplified knee plate without any curved surfaces, except for what is shown in Figure 40a. The resulting model is shown in Figure 41 where the simplified surfaces have been highlighted. This simplification was later verified by comparing two models without stiffening, the first, a perfectly circular brace and the second, containing the simplification used in the base model.

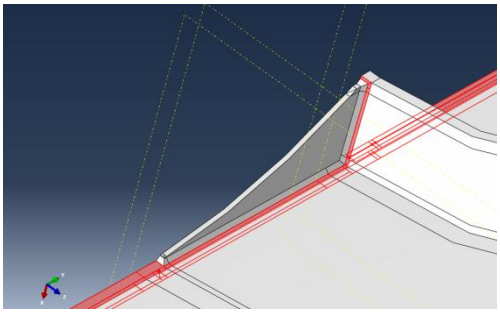

Figure 41 – Half the base model where the highlighted surfaces have been simplified by making them flat.

Knee plate ending

The weld and knee plate is from Figure 38a seen to be ground flush. The notch stress approach is however limited to natural formed welds and the FEA-model was therefore modelled as such. Although the model was intended to be made according to Figure 42a, this would result in a pointed knee plate end, forcing the elements in this area to be triangular. A triangular mesh was seen to give bad element shapes, due to the partitioning needed for the notch root. The weld was therefore modelled as shown in Figure 42b, in order to allow for hexagonal elements. The dimensions of the knee plate were as specified in the drawings, and the weld size and weld leg lengths were respectively 6mm and approximately 8.5mm.

a)

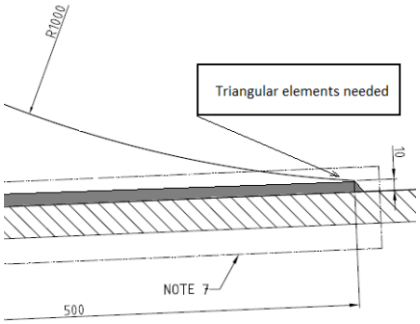

b)

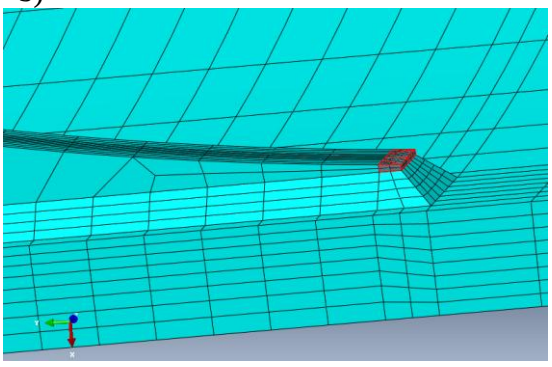

Figure 42 – Illustration of the simplification needed where a) illustrates the pointed knee plate and b) The simplified model, where the highlighted geometry allows for hex elements.

Other simplifications

The intersection between the gusset plate and the ring stiffener was moved 1mm towards the brace outer plate. This was necessary to avoid conflicts between gusset- and knee plate mesh.

3.3.2 **Meshing**

A mesh was first assigned to the base model, which was further copied and assembled to the full brace. During meshing of the base model, tie constraints were automatically created, due to incompatible interfaces between partitions close to the notch root partition. The tie constraints were however seen to only be applied at the edges of the incompatible faces. Tie constraints for the entire surface were thus created manually for all the incompatible faces in the knee plate.

The base model

The mesh was applied to the base model according to the methodology used in the verification model. However, due to the complex structure of the knee plate, some element angles were somewhat lower in parts of the model, as indicated in Figure 43. The low element angles at the gusset plate were found to be a result of the fine and relatively complex mesh at the knee plate. Efforts made to create a coarser mesh towards the end of the gusset plate were seen to affect the knee plate mesh. Finding a solution to this was found to be very time consuming, and therefore not further explored. The low element angles at the right hand ring stiffener have not been further explored, as focus has been on optimizing element shapes at the knee plate. At the knee plate, some elements were seen to have element angles as low as 27 degrees.

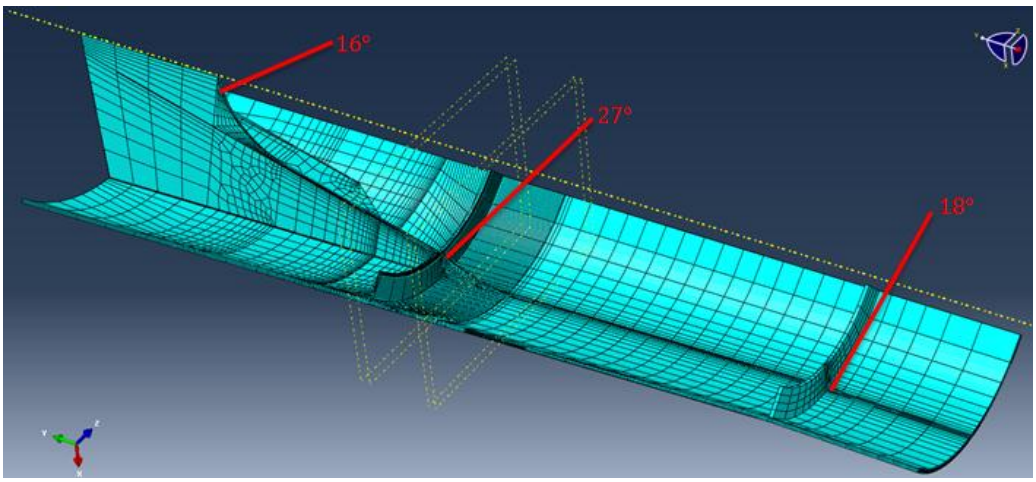

Figure 43 – Overview of the lowest element angles and their locations.

Although several attempts were made at avoiding element warnings, some warnings had to be accepted. The quarter model consists of 60022 quadrilateral elements, of which analyses warnings were reported for 5968 elements. These warnings are mainly due to the high aspect ratio in the gusset plate and brace outer plate. Figure 44 gives an overview of the areas containing elements subjected to analysis warnings.

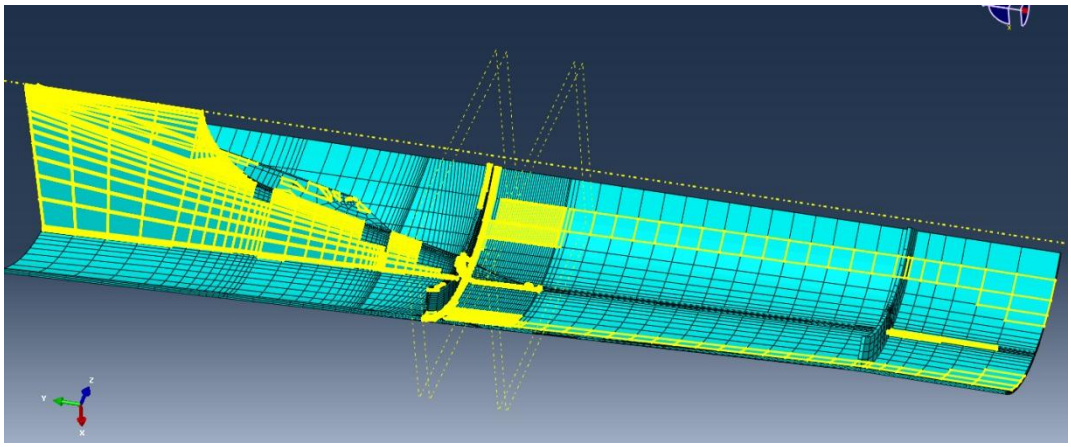

Figure 44 - Analysis warnings highligted in the base model.

At the corner point where the knee plate, brace and ring stiffener intersect, the root partition is also seen to contain element warnings, as shown in Figure 45a. These elements were early seen to have the lowest angles in the root partition. Although efforts were made to improve element angles, an improvement strategy was not found. It was also seen that some elements close to the root partition also contained element warnings, as illustrated in Figure 45 b.

a) b)

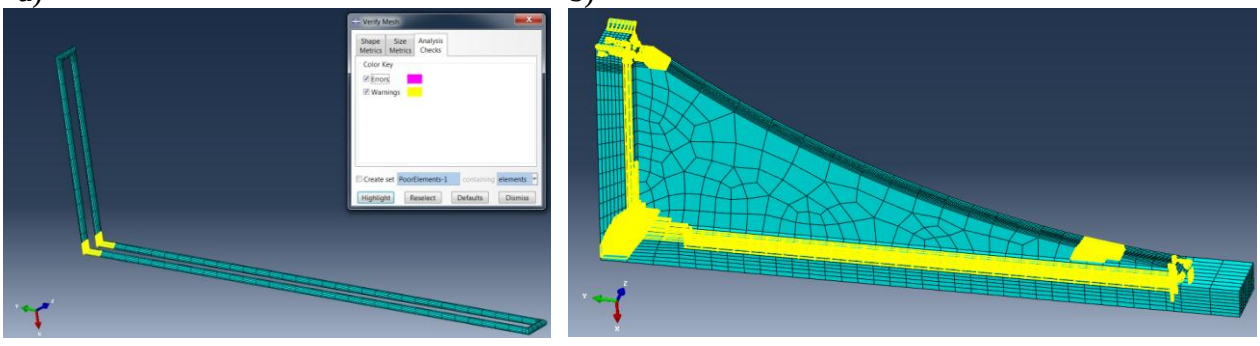

Figure 45 – Analysis warnings at a) the weld root partition, and b) the knee plate

The final base model was divided into a total of 329 regions, which were made by 230 operations of different kinds, in order to mesh the part satisfactorily. Despite the element warnings, no mechanisms were visually observed in the resulting analyses.

Assembling the brace model

The brace model was assembled by four copies of the base model. Nodes at the boundaries, intersecting the four base models, were then merged to form a complete mesh of the brace shown in Figure 46. Only when a complete element representation of the brace was defined, tie constraints, loads and boundary conditions could be dealt with.

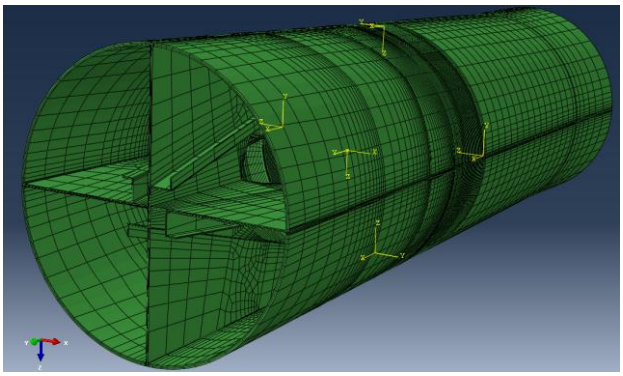

Figure 46 - The assembled element representation of the brace.

Tie constraints

When meshing two partitions that share a common face, all the nodes at this face must be shared between the elements at both sides of the face. It was seen that when Abaqus was unable to merge the nodes across a common face, it prompts the user whether to use tie constraints to redeem the problem. Although it was made an effort to avoid tie constraints, it was found to be unavoidable at the faces shown in Figure 47a. Tie constraints were however limited to partitions surrounding the root partitions, and not the actual root partitions, as shown in Figure 47. In figures b and c, the partitions from both sides of the incompatible faces have been illustrated, which if compatible, should have been a reflection of each other.

a) b) c)

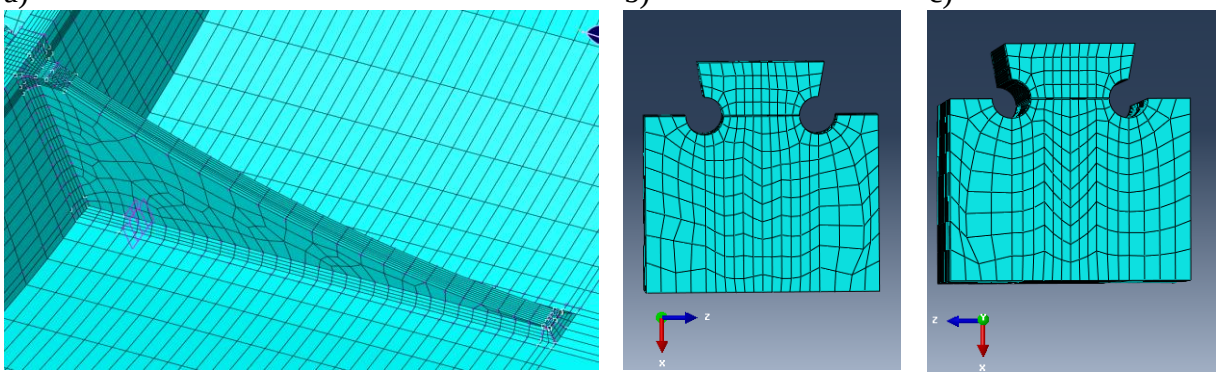

Figure 47 – a) Knee plate with tie constraints and surfaces subjected to these constraints at b) closest to the ring stiffener, c) furthest from the ring stiffener

Later visual checks of the analyses results showed that the tie constraints, which were automatically applied by Abaqus, were only tying the nodes at the edges of the partiton faces, as shown in Figure 48a. This was resolved by manually applying tie constraints to all element surfaces at the incompatible faces. The resulting element behaviour is illustrated in Figure 48b

a) b)

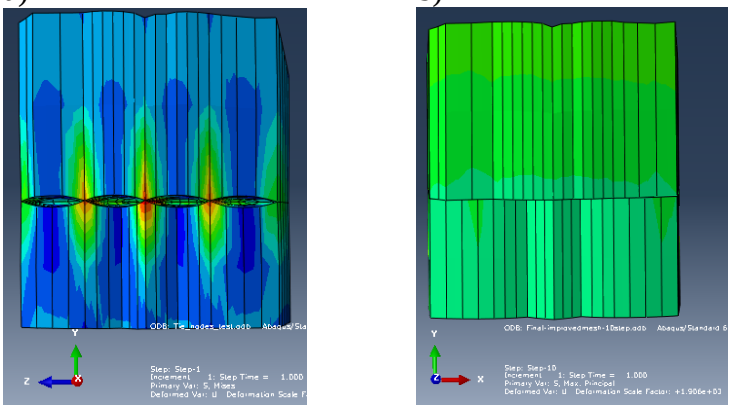

Figure 48 - Elements on both sides of the incompatible faces with a) automated tie constraints and b) manually applied tie constraints at element surfaces

3.3.3 Loads and boundary conditions

Boundary conditions

As the stiffness of the brace and column intersection was unknown and obtaining the stiffness would require a larger courser model, the boundary conditions were simplified. The simplification was performed by considering the column to be stiff, and thus all element surfaces were fixed at the column side of the brace model, according to Figure 39.

Unit load

In order to obtain a SCF for the weld toe, the brace model was first subjected to a unit load. This was done by subjecting the brace model to a negative pressure corresponding to 1 MN over the cross section of the brace. Thus, the unit load was applied in the same manner as for the validation model, with the same magnitude as applied by Aker Solutions' unit loaded FEA.

Loading according to Miner summation

In order to compare assessed fatigue life with the results obtained by Aker Solutions, the loading had to be defined in a similar manner. A data set containing stress range exceedances diagrams from a global FEA model was thus provided by Aker Solutions. The data set consist of 97600 rows and 6 columns, hence only the first rows are included in appendix B as an

example. The data contains 61 stress ranges for 8 Gauss points, at 8 elements. That is two elements containing 8 nodes each, at brace clock positions 3-, 6-, 9- and 12o'clock. An overview of the provided data is given in Figure 49, where a stress range exceedances diagram has been defined for 15 stress blocks. The data also account for wave directions from 0 to 360 degrees with 15 degrees step interval, as well as a combination of all directions. The latter is used in the further analyses.

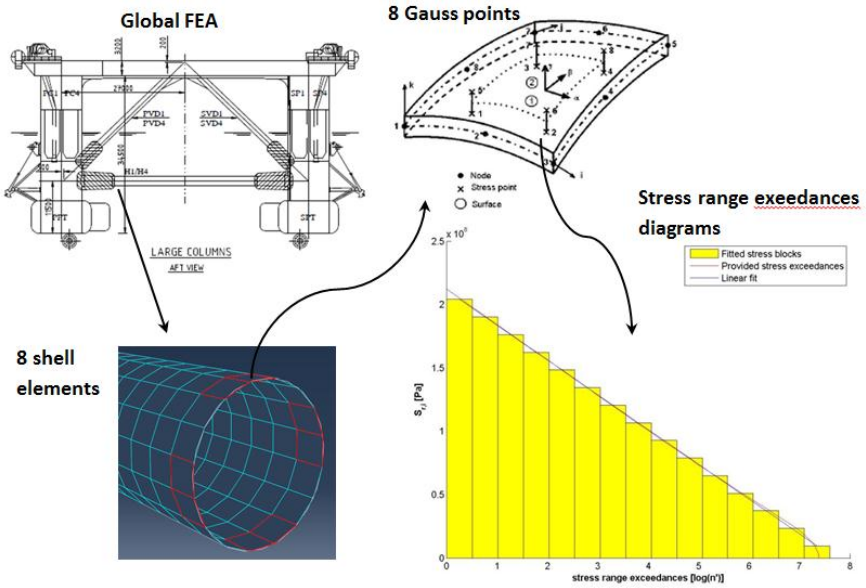

Figure 49 - Overview of the provided data for one Gauss point, resulting in one sress range exceedances diagram.

As the data provided was quite extensive, it was decided to create a Matlab script. The resulting script given in Appendix C, reads and processes the provided data, as well as generates Abaqus input commands.

In order to recreate the stress fields provided from the global model, expressions for the stress range exceedances diagrams were established for every Gauss point. As the diagrams were seen to be approximately linear, the Matlab script fits each diagram with a linear fitted equation. This equation was further used to obtain stress ranges $S_{r,i}$, corresponding to predefined number of cycles' n'_i which were defined in a vector n'. The n'-vector was defined as a logarithmic evenly distributed vector, representing the centre of each stress block, and containing i number of desired analyses steps. A plot containing stress range exceedances, the linear fitted curve, as well as the fitted stress blocks is shown in Figure 50. The width of each block represents the number of cycles n_i for each stress block, which later was used for calculating the damage sum, and thus not to be confused with the n'-vector. The corresponding stress ranges were further averaged for each clock position, resulting in i mean stress ranges $\bar{S}_{r,i}$, for each clock position.

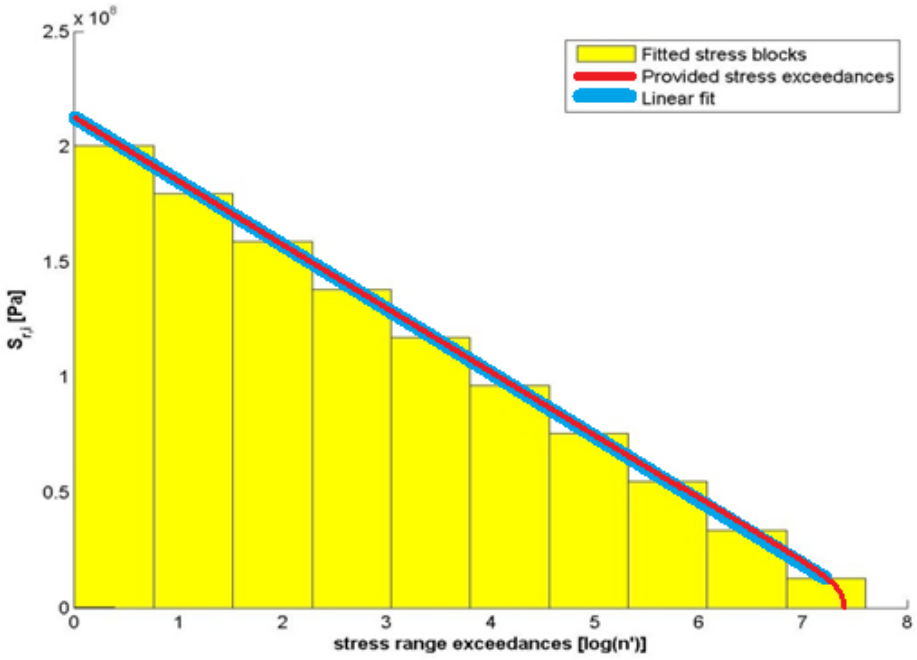

Figure 50 - Provided stress range exceedances diagram for one Gauss point, the linear fitted curve and the stress blocks used for the fit.

Further, Abaqus input commands were exported into a text file, which could be copied directly into the Abaqus' *kernel command line interface*. The input commands, which are given in Appendix D, create mapped analytical stress fields for every analysis step, based on the averaged stress at the four clock positions. Field mapping and a resulting field is shown in Figure 51, where the average stress is assumed to be located at the middle of the brace thickness. The input commands also create the number of analysis steps needed, and a load for each step, which is defined as a pressure of unity. The analytical fields are then assigned to the loads, and as Abaqus automatically propagate loads used in previous steps, these loads are disabled.

a) b)

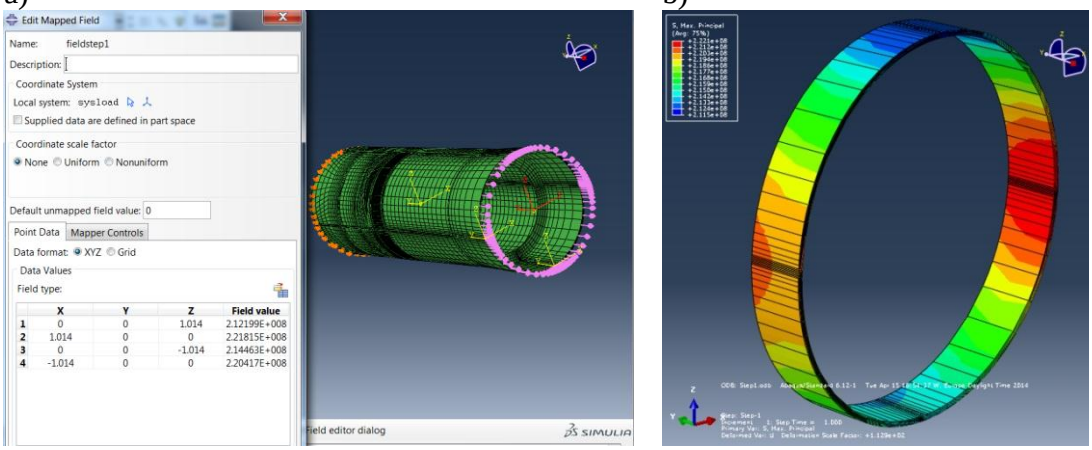

Figure 51 - a) Creating mapped field, and b) Resulting stress field.

3.3.4 Obtaining the effective notch stresses

Upon completion of the analyses, 4 weld root paths were defined at the 12o'clock position, which was the clock position seen to have the highest stress concentrations. The weld toes and roots along these paths, will for simplicity further be addressed to as a, b, c and d, as shown in Figure 52.

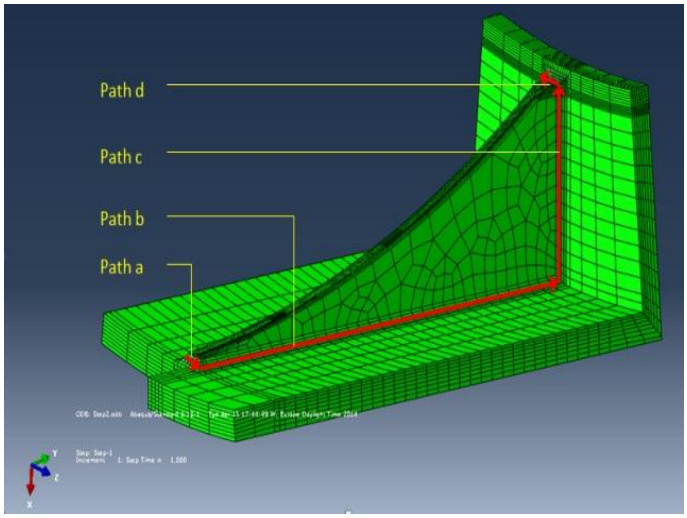

Figure 52 - Weld root paths including direction of stress extraction.

3.3.5 Obtaining the effective hot spot stresses

Hot spot stresses were evaluated for every clock position, for the weld at the end of the knee plate, corresponding to path a in Figure 53. Principal stresses were needed to calculate the effective hot spot stress. By plotting the maximum principal stresses' directions in Abaqus, it was seen that they were acting normal to the weld toe at the read out points, as seen in Figure 53a.

a) b)

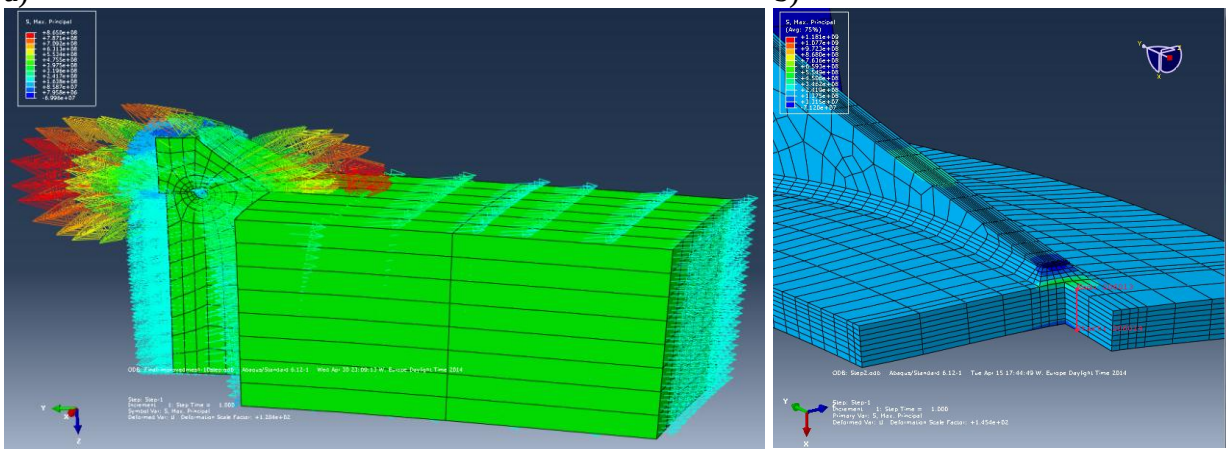

Figure 53 - Hot spot stresses with principal directions shown in a), extracted along the path shown in b)

As Abaqus extrapolates stresses from the Gauss points to the nodes, and the maximum stresses in the path shown in Figure 53b were observed to be at the same surface as the weld toe, maximum principal stress from this path was taken as the read-out stress for the effective hot spot approach.

The read-out stress was then inserted directly into equation (18), for calculation of the effective hot spot stress according to method B. As principal stresses were seen to act normal to the weld, the alpha factor was taken as 1. The brace was not seen to be significantly affected by bending, and a reduction of the bending stress component by 40% could not be utilized.

3.3.6 Cumulative damage

Cumulative damage was calculated based on the Miner summation procedure, using both the effective notch stress and the effective hot spot stress, for weld roots and weld toe, respectively. This was done in order to compare the damage sum with results obtained from Aker Solutions' fatigue assessments. The damage sum was found utilizing equation (21), where n_i was calculated based on the n'-vector. N_i was taken as the design life according to equation (4) and (3) for the effective hot spot stress and effective notch stress respectively, calculated using their respective stresses obtained for each analysis step i.

3.3.7 Verification of the simplified brace plate

As the base model was simplified along the entire length of the brace, by flattening the brace at a small cross sectional area, it was decided to investigate the affects this had on the FEA results. This was done by making two simplified models of the brace, excluding all stiffeners. The first model was made similar to the full model, hereby denoted Brace validation model 1 (BV1) . Hence BV1 was made as four quarters of the brace, with a flat partition corresponding to the full model, as shown in Figure 54 a. The second model shown in Figure 54 b, was made as a full 360 degree cone/cylinder. This model will be referred to as brace validation model 2 (BV2). The two models were applied the same boundary conditions as the full model, and a negative uniform pressure of 1MPa as loading.

a) b)

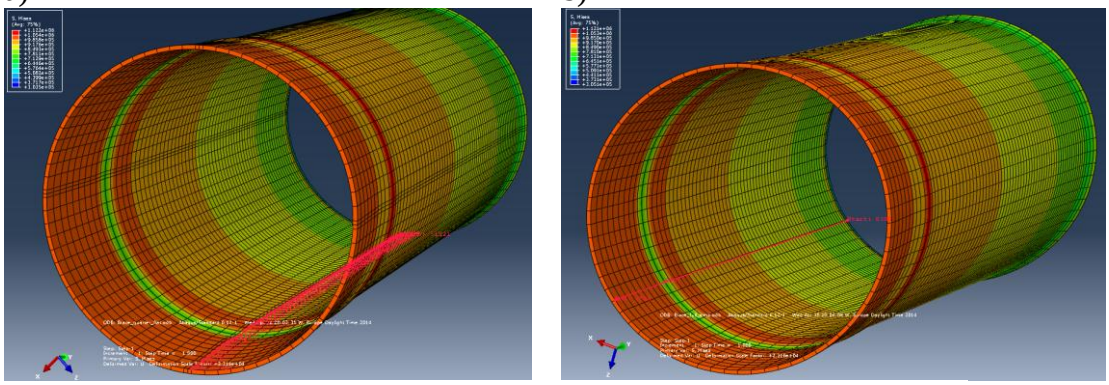

Figure 54 – Boundary conditions applied at a) BV1 and b) BV2, with two out of three paths used for stress extractions.

Stresses in BV1 were extracted along paths at both the edge, as shown in Figure 54 a, and at the centre of the flattened partition. For BV2, a random path was selected, as stress does not vary in the cross sections of this model. If the simplifications were justified, the difference between the results from the two models was expected to be minimal.

3.4 Comparing the results

Stress concentrations

As Aker Solutions provided an SCF for weld toe *a*, an SCF for the same weld toe in the brace model was found based on an analysis of this model subjected to a unit load. The results were further compared to Aker Solutions' results in order to verify the brace model, and to verify that loading was correctly defined.

Cumulative damage

The loading, which was based on results from Aker Solutions' global model, is only applied on the cross section at one side of the brace model. The boundary on the other side of the brace model, towards the column, was fixed based on the assumption that the column was stiff. An evaluation of the boundary conditions was thus performed by comparing the cumulative damage obtained using the effective hot spot stress, to the fatigue life assessed by Aker Solutions.

Summary of compared values

An overview of the results that are compared and what they are compared to is shown in Table 4.

Table 4 - Overview of which results that are compared and what they are compared to.

Why it is compared	What is compared	What it is compared to
Verify the target notch stress SCF's given by DNV for the validation model.	Target SCF values calculated using the nominal approach for a cruciform joint.	Target SCF values given by DNV.
Validate the effective notch stress methodology.	SCF's found from FEA of the cruciform joint, for weld root and – toe.	Target SCF's given by DNV and calculated by the nominal approach.
Investigate the nominal, and the effective notch stress approach for varying weld sizes.	Effective notch stress at the weld root of the cruciform joint for varying weld sizes.	Target notch stress values, established from the nominal approach.
Validate simplifications of the brace outer plate.	The simplified brace model, BV1.	The BV2 model.
Validate loading and modelling of the brace model.	SCF results from brace model.	Aker solutions SCF results.
Validate boundary conditions of the brace model.	Fatigue life of weld toe *a*, found by the effective hot spot approach and Miner summation.	Aker solutions fatigue life results from a global model.
Propose a weld size that results in a greater fatigue life at the weld root than that of the weld toe, for the knee plate.	Weld root fatigue for the brace model, obtained by extrapolated effective notch stress.	Weld toe fatigue results from both the brace model and Aker Solutions.

4 Results

4.1 Cruciform joint –validation according to DNV

4.1.1 Target notch stress values

Using equation (27), a target SCF at the weld toe of the full penetration welded cruciform joint was found to be approximately 3.17. For a fillet welded cruciform joint with the same dimensions, a SCF for the weld toe and -root were found to be approximately 4.02 and 6.25 respectively. This is shown in Table 5, and illustrated for the weld root of the fillet welded joint in Figure 55, by comparing the fatigue design curves in air for the nominal approach to the notch stress design curve. As can be seen in the figure, the fatigue life obtained from a stress amplitude using the nominal stress approach (lower SN-curve), corresponds to the same fatigue life for the notch stress approach (upper SN-curve) with a higher stress amplitude.

Table 5 - Target value for effective notch stress.

	Nominal approach		Notch stress approach	
	N	Δσ	N	Δσ
Weld root fillet	9.333E+04	100	9.340E+04	625.00
Weld toe full pen	7.161E+05	100	7.160E+05	316.98
Weld toe fillet	3.516E+05	100	3.516E+05	401.78

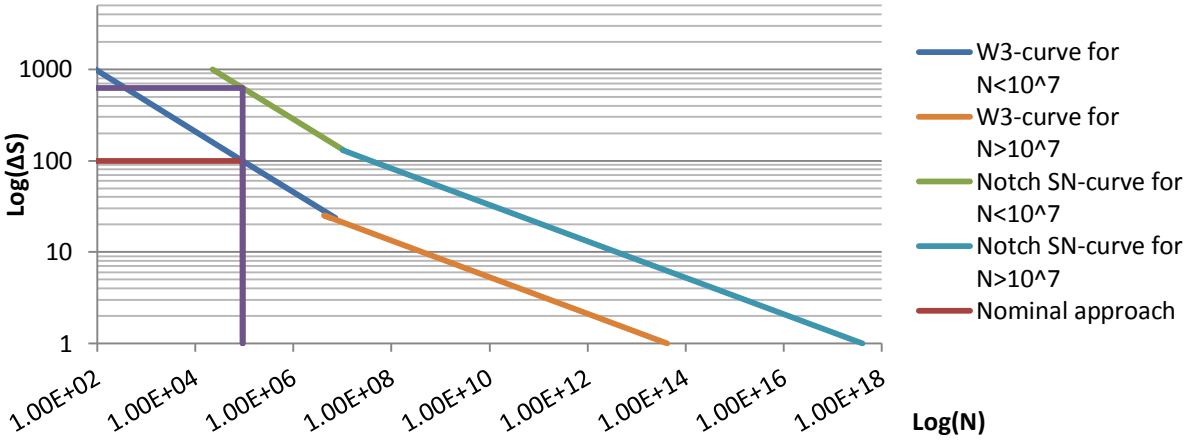

Figure 55 - Comparing design curves for the effective notch stress and nominal stress approach for the weld root.

Comparing the SCF's obtained with the ones given by DNV (2012), it can be seen that for the weld root they are identical. The SCF obtained for the weld toe of the full penetration welded joint justifies the assumption that a typing mistake has been done in DNV (2012), and that the weld toe SCF of the fully penetration welded joint is 3.17.

The SCF obtained at the weld toe of the fillet welded joint is however different from the SCF of 3.57 given by DNV. By further inspection, it was found that the same SCF was obtained by using the F1-curve parameters, although it is stated by DNV that the F3-curve has been used. The result using the F1 design curve parameters is given in Table 6.

Table 6 - Target value for the effective notch stress, obtained using the F1 curve.

	Nominal approach		Notch stress approach	
	N	Δσ	N	Δσ
Weld toe (fillet weld)	5.000E+05	100.00	5.000E+05	357.28

4.1.2 Effective notch stress

The stresses obtained from the defined paths are shown in Figure 56 and Figure 57, for respectively root 1 and toe 2 configurations. It is seen that for the weld root notch, stress seems to concentrate a small distance from the boundaries. For the weld toe notch, stresses are seen to concentrate at the middle of the weld depth.

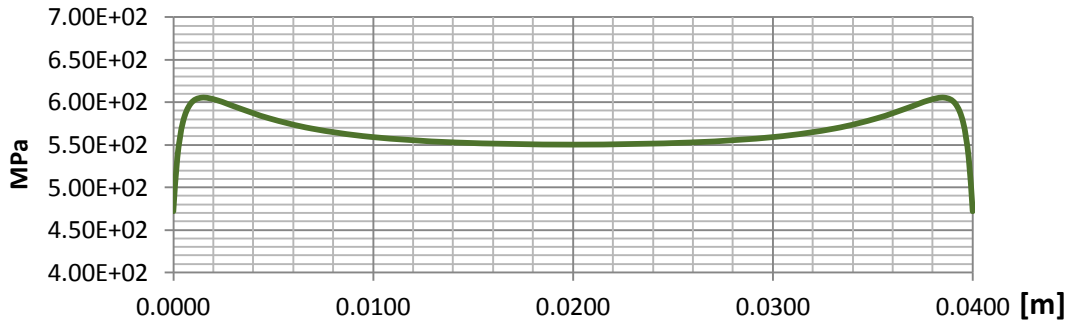

Figure 56 - Stress extracted along the depth of the weld root notch for root 3, with 4 elements along a quarter circumference.

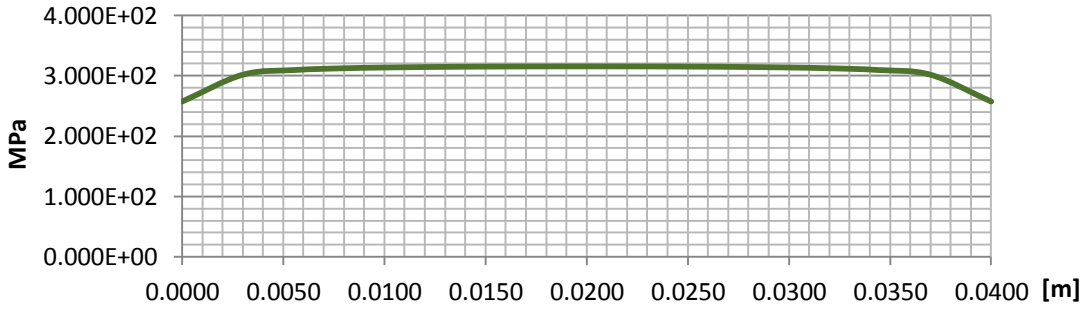

Figure 57 - Stress extracted along the depth of the weld toe notch for toe 2, with 5 elements along a quarter circumference.

The effective notch stresses obtained from the FEA are shown and compared to the target notch stress in Table 7.

Table 7 - Effective notch stress obtained in FEA.

	Maximum notch stress [Mpa]				Deviation from target value [%]			
# of elements per quarter circumference	2	4	8	10	2	4	8	12
Root1	606.52	605.44	601.76	-	-2.96	-3.13	-3.72	-
Root2	-	668.36	-	-	-	6.94	-	-
Root3	609.48	609.15	605.65	602.89	-2.48	-2.54	-3.10	-3.54
Root 3 (combined model)	-	606.84	-	-	-	-2.91	-	-
Root 3 (root partition radius, r=2.2mm)	-	608.07	-	-	-	-2.71	-	-
# of elements per quarter circumference	2	5	10	-	2	5	10	-
Toe 1	-	278.43	-	-	-	-12.17	-	-
Toe 2	296.47	315.46	315.50	-	-6.48	-0.49	-0.47	-
Toe 2 (comb. Model)	-	479.73	-	-	-	19.40	-	-

For the root 3 configuration, the initial weld root partition of 2.2mm was seen to give a slightly less conservative result than that of a 4mm radius. The increase in radii did not affect the number of elements required for the model significantly, and was thus used for further analyses.

The root 1-, root 3- and toe 2 notch configurations gave the most promising results and were hence chosen for the mesh convergence study shown in Figure 58 and Figure 59, respectively.

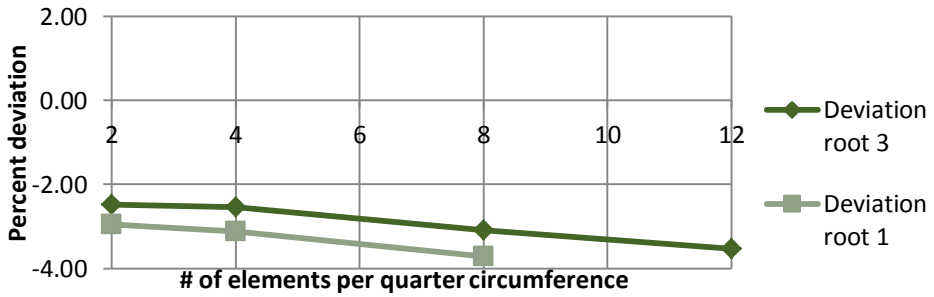

Figure 58 - Mesh convergence study for root 1, deviation from effective notch stress target value.

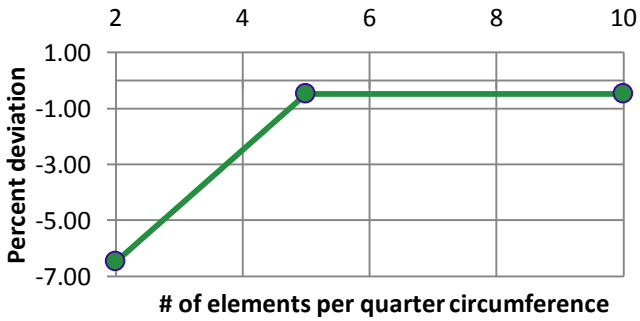

Figure 59 - Mesh convergence study for toe 2, deviation from effective notch stress target value.

It is seen that the effective notch stress for root 3 tends to converge towards a stress deviation of approximately -3.5%, corresponding to a SCF value equal to 6.03. The difference in stress deviation obtained from 2-12 elements along the quarter circumference is quite minimal, approximately 1%.

For the weld toe, 4 elements along the quarter circumference gave lower stresses at the nodes than 5 elements. It is thus noted that if stresses are seen to concentrate in between nodes, mesh should be adjusted accordingly.

The weld toe convergence study showed convergence towards a stress deviation of about -0.5%, which correspond to an SCF equal to 3.15 for 5 or more elements along the quarter circumference.

The combined model containing fictitious notches at both weld toe and root, gave a +14.6% deviation from the target value at the weld toe, which was relatively large compared to the other results. The primary objective with this model was to analyze the weld toe of the fillet welded joint, and very small stress variations were seen in the mesh convergence study for the full penetration weld toe model. A mesh convergence study for this model was therefore not performed. It is however noted that the effective notch stress for the weld toe of the fillet welded joint is on the conservative side. The effective notch stress for root 1 in the combined model is slightly more non-conservative than for the root 1 model, approximately 2.4%.

4.1.3 Undocumented observations

It is noted, that introducing a different mesh for the partition containing the weld and plate intersection area, was observed to only slightly lower the stress concentrations at the weld root. For an analysis containing elements with a worst element angle of 18 degrees in this partition, and also containing elements in the root partition with an aspect ratio of 25, the effective notch stress was found to be approximately 3 % lower than initially.

For the outer plate partitions, changing mesh size over the thickness was not observed to affect the weld root stress. Some variations were observed to appear for the weld toe, these variations were however on the conservative side, as stress concentrations were only seen to increase for decreasing mesh sizes.

4.1.4 Fatigue life

Fatigue life obtained using the effective notch stress approach and deviation of this fatigue life relative to that obtained from the nominal stress approach, is given in Table 8.

Table 8 - Assessed fatigue life using the effective notch stress approach, comparison with fatigue life obtained from nominal approach.

	Effective notch stress fatigue life [cycles to failure]				Deviation from nominal approach fatigue life [%]			
# of elements per quarter	2	4	8	10	2	4	8	10
Root 1	1.02E+05	1.03E+05	1.05E+05	-	9.51	10.10	12.13	-
Root 2	-	7.64E+04	-	-	-	-18.16	-	-
Root 3	1.01E+05	1.01E+05	1.03E+05	1.04E+05	7.92	8.10	9.99	11.50
Root 3 (comb.	-	1.02E+05	-	-	-	9.34	-	-
# of elements per quarter	2	5	10	-	2	5	10	-
Toe 1	-	1.06E+06	-	-	-	47.53	-	-
Toe 2	8.75E+05	7.26E+05	7.26E+05	-	22.22	1.45	1.41	-
Toe 2 (comb. Model)	-	2.08E+05	-	-	-	-40.71	-	-

As expected, the fatigue life deviation is greater than the stress deviation for the two approaches. This is due to the stress inserted for fatigue life in equation (2) is raised to the power of three. It is seen that root 3 and toe 2 give the smallest deviations, with root 3 somewhat overestimating the fatigue life. Assessed fatigue life at the weld toe of the fillet welded joint, which is given as the toe 2 combination model, is observed to be very conservative. The weld root fatigue life for the combination model is seen to be slightly more overestimated.

4.2 Parametric weld size study

4.2.1 Effective notch stress for varying weld size

In the same manner as the validation procedure, target values for the effective notch stress approach were obtained using equation (27). The results are shown in Table 9, where the DNV validated results have been highlighted. The values are further used for comparison with the obtained FEA results.

Table 9 - Target stress values for the notch stress approach for varying weld sizes, obtained from the nominal approach.

Weld stress calculations					Target notch stress [MPa]		
$\sigma_{m,p}$	$\sigma_{b,p}$	t [m]	a [m]	$\sigma_{n,w}$	σ_{root}	$\sigma_{toe,comb}$	$\sigma_{ful\ pen}$
100	0	0.016	0.004	200	1250.34	401.79	316.95
100	0	0.016	0.006	133.33	833.56	401.79	316.95
100	0	0.016	0.008	100	625.17	401.79	316.95
100	0	0.016	0.010	80	500.13	401.79	316.95
100	0	0.016	0.012	66.67	416.78	401.79	316.95

The obtained notch stresses extracted from the FEA are shown in Table 10, where increasing absolute deviation for both decreasing and increasing weld sizes, relative to the original 8mm weld size, is observed for both weld root and at the toe of the full-pen weld. More

specifically, the stress results are lower than predicted for smaller weld sizes and higher for larger weld sizes. This leads to an inaccuracy when using the effective notch stress approach for assessing the design life, assuming the nominal approach is more accurate. For weld sizes larger than 8mm, design life obtained using the effective notch stress approach is conservative, while for weld sizes smaller than 8mm it is non-conservative. For the weld toe of the fully penetration welded joint, the results are seen to be far more similar to the target values, compared to that of the weld root.

Table 10 - Notch stress results for varying weld sizes, compared with target values.

Weld size [m]	Extracted stress [MPa]		Deviation from target stress [%]		Design life [cycles to failure]		Deviation from target design life [%]	
a	σ_{root}	$\sigma_{toe,ful\ pen}$	root	Toe, full pen	N_{root}	$N_{toe,full\ pen}$	root	Toe, full pen
0.004	928.59	302.05	-25.71	-4.70	2.85E+04	8.27E+05	144.13	15.55
0.006	728.40	306.56	-12.62	-3.28	5.90E+04	7.92E+05	49.87	10.52
0.008	609.15	315.46	-2.56	-0.47	1.01E+05	7.26E+05	8.10	1.43
0.01	530.91	323.35	6.15	2.02	1.52E+05	6.74E+05	-16.40	-5.82
0.012	470.97	323.95	13.00	2.21	2.18E+05	6.71E+05	-30.70	-6.33

By further plotting the target- and extracted notch stress for the inverse weld size, the difference between the target values and the obtained effective notch stress can be seen in Figure 60.

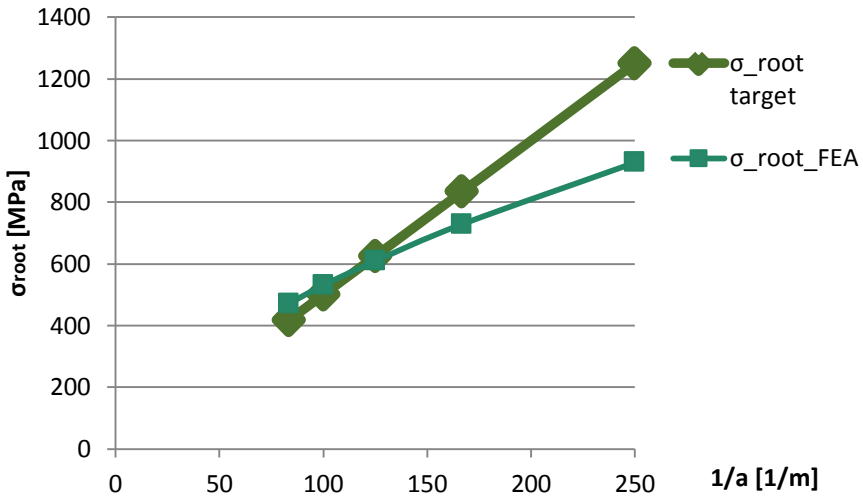

Figure 60 - Target values and obtained effective notch stress plotted for inverse weld size.

From Figure 60 it can be seen that the target values are linear for varying weld sizes, whereas the obtained effective notch stress is slightly non-linear.

4.2.2 Notch size study

Ideal notch radiuses, redeeming the discrepancies between the nominal and effective notch stress approach, were found by iteration. The final iterated results, determining ideal notch radiuses for each weld size, are shown in Table 11. By comparing Table 10 and Table 11, it is noticed that a larger notch radii results in lower effective notch stress and vice versa. The ideal radiuses are further plotted for weld sizes in Figure 61, and fitted with a linear and 2.-order polynomial.

Table 11 - Ideal notch radii iteration results.

Ideal results, Numerically est. notch size for root				
Weld size [mm]	Notch radii [mm]	Extracted ideal stress [MPa]	Taget stress [MPa]	Deviation
4	0.495	1250.0	1250.3	0.029
6	0.736	834.8	833.6	-0.148
8	0.944	625.3	625.2	-0.020
10	1.143	499.8	500.1	0.068
12	1.311	417.1	416.8	-0.080

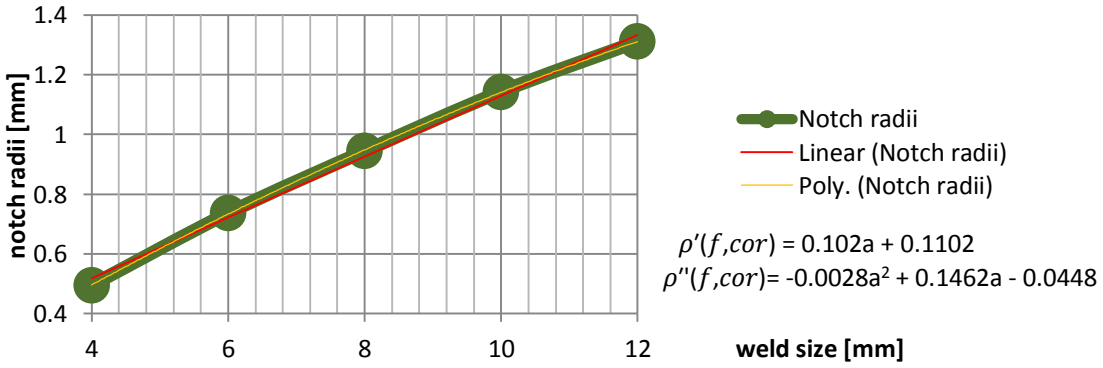

Figure 61 – Iterated ideal notch radii fitted with linear and 2. order polynomial.

As seen in Figure 61, the ideal notch radiuses have a close to linear relation with weld size. The fitted linear- and second order polynomial are given as equations for corrected fictitious notch radiuses $\rho_{f,cor}$, in equations (32) and (33), respectively.

$$\rho'_{f,cor} = 0.102a + 0.1102 \quad (32)$$

$$\rho''_{f,cor} = -0.0028a^2 + 0.1462a - 0.0448 \quad (33)$$

Verification

The precision of using a corrected notch radii was quantified by computing these radiuses, and use the computed radiuses in a new FEA. From this FEA, the corrected notch radiuses' stress results were found and compared to the former ideal stress results.

As can be seen in Table 11, the corrected notch radiuses obtained from the linear parameters were seen to differ more from the iterated ideal notch sizes obtained for weld size 4 and 12. It was thus decided to verify the corrected fictitious notch radii for the linear parameters, for these weld sizes only. The results are shown in Table 12, where notch stress obtained using the ideal notch radii for each weld size, is compared with the notch stress obtained using the corrected linear notch radii. The largest deviation using the linear approximation was found to be approximately 2%.

Table 12 - Verification of the notch size study.

	Ideal results		Verification of 'linear' relation			Verification of '2.ord. poly' relation	
Weld size [mm]	Notch radii [mm]	Extracted ideal stress [MPa]	Notch radii [mm]	Extracted stress [MPa]	Deviation from ideal stress [%]	Notch radii [mm]	Extracted stress [MPa]
4	0.495	1250.0	0.518	1224.5	2.04	0.495	
6	0.736	834.8	0.722			0.732	
8	0.944	625.3	0.926			0.946	
10	1.143	499.8	1.130			1.137	
12	1.311	417.1	1.334	414.0	0.75	1.306	

4.2.3 Notch stress correction study

The relation between the target- and obtained values are illustrated in Figure 62, where notch stress and design life has been plotted for weld size.

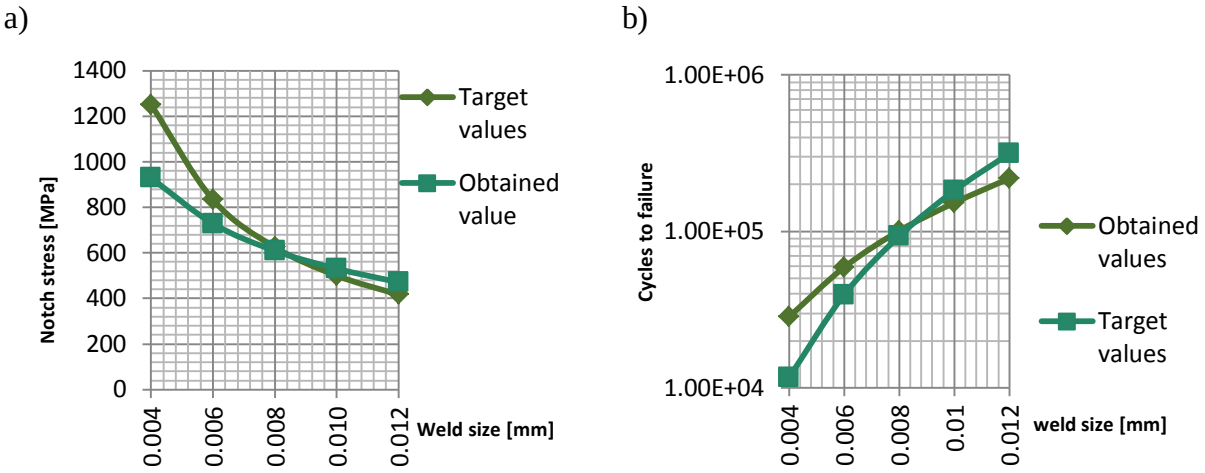

Figure 62 – Comparison of a) Target notch stress and obtained notch stress, and b) Design life obtained from the notch stress approach and target values .

By further plotting the obtained notch stress relative to the target stress for the defined weld sizes, a close to linear relation can be observed in Figure 63. As can be seen in the figure, using the linearized relation for correction, notch stress will be slightly overestimated for weld sizes of approximately 5-11mm, while underestimating for all weld sizes above 11mm and below 5mm, assuming that the trend observed is continued. This would lead to non-conservative design life for the latter. Visual inspections of the fitted second order polynomial shows very good potential of correcting the effective notch stress.

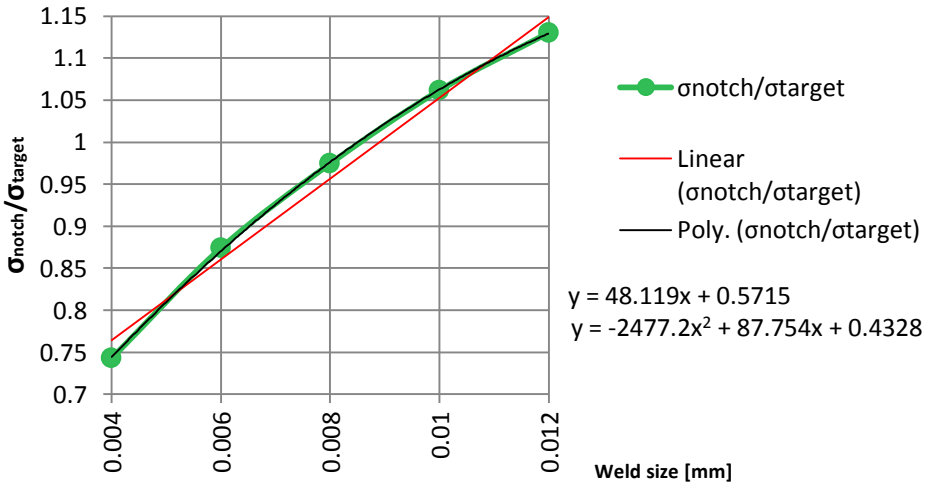

Figure 63 - Relation between notch stress, relative to target stress and weld size.

The fitted linear and 2.-order relation between notch stress and target stress for varying weld sizes, are given in equations (34) and (35), respectively. Here the equations have been solved for the target notch stress, resulting in corrected stress amplitudes which further will be addressed to as corrected notch stress ($\Delta\sigma_{cor}$).

$$\Delta\sigma'_{cor} = \frac{\Delta\sigma_{notch}}{48.119a+0.5715} \quad (34)$$

$$\Delta\sigma''_{cor} = \frac{\Delta\sigma_{notch}}{-2477.2a^2+87.754a+0.4328} \quad (35)$$

Verification

The results of the notch stress correction parameters are verified in Table 13, where it is compared to the target values. As seen from the table, the largest deviation for the linear notch stress is found for the smallest weld size, approximately 2.8%, which is an improvement of about 23%. For the 2-order correction, notch stress deviation is close to zero for all weld sizes.

Table 13 - Verification of corrected notch stress.

Weld size	Target value	Verification –Linear notch stress correction		Verification –2. order poly notch stress correction	
a [m]	$\Delta\sigma_{notch}$ [MPa]	$\Delta\sigma'_{cor}$ [MPa]	Deviation [%]	$\Delta\sigma''_{cor}$ [MPa]	Deviation [%]
0.004	1250.35	1215.47	-2.79	1247.80	-0.20
0.006	833.56	846.76	1.58	837.10	0.42
0.008	625.17	636.88	1.87	623.94	-0.20
0.01	500.14	504.33	0.84	499.62	-0.10
0.012	416.78	409.92	-1.65	417.11	0.08

By once again plotting notch stress values for the inverse of the weld size, the second order notch stress correction can be seen to coincide with the target values obtained from the nominal stress approach.

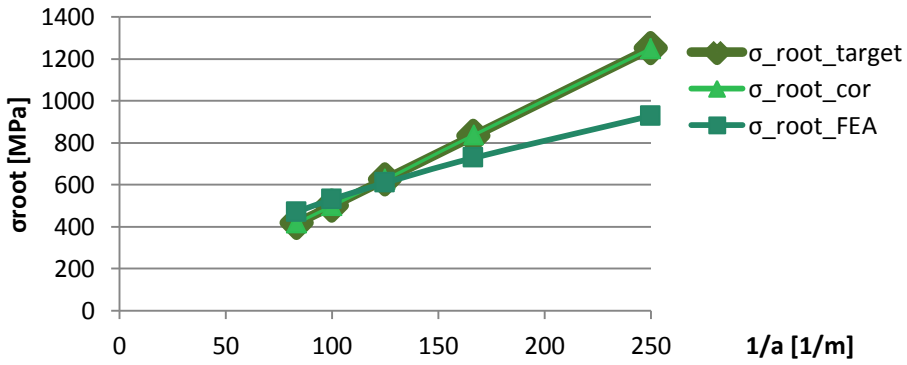

Figure 64 - Correction of the notch stress FEA results performed using equation (35).

4.2.4 Undocumented observations

Effective notch stress at the weld root was seen to be slightly affected by the plate thickness. Deviation from target notch stress values was seen to be less than 3% for plate thicknesses between 8mm and 24mm. The deviation was however seen to be increasingly conservative for larger plate thicknesses, and due to the small deviation this was not further pursued.

4.3 Fillet welded knee plate

Results from variable loading and Miner summation are further given in detail for 10 stress blocks. The complete results for effective notch stress and Miner summation of 15 stress blocks are given in appendix *H*.

4.3.1 Verification of simplifications

Brace validation model 1 and 2 is compared in Figure 65a, where maximum principal stress have been extracted along the length of the brace. For BV1, the stresses were found to be quite similar at both the centre of the flat partition and at the edge of the flat partition. Deviation between BV1 and BV2 has thus been plotted in Figure 65b, using the maximum difference between the two models. Absolute deviation from BV2 is seen to increase towards the fixed boundary conditions representing the column. Stress in BV1 is also seen to be approximately 6% lower than that of BV2, some distance from the applied load. Between 4.4 and 5m from the applied boundary conditions, which is the area corresponding to the knee plate's position; deviation was found to be less than 0.3%.

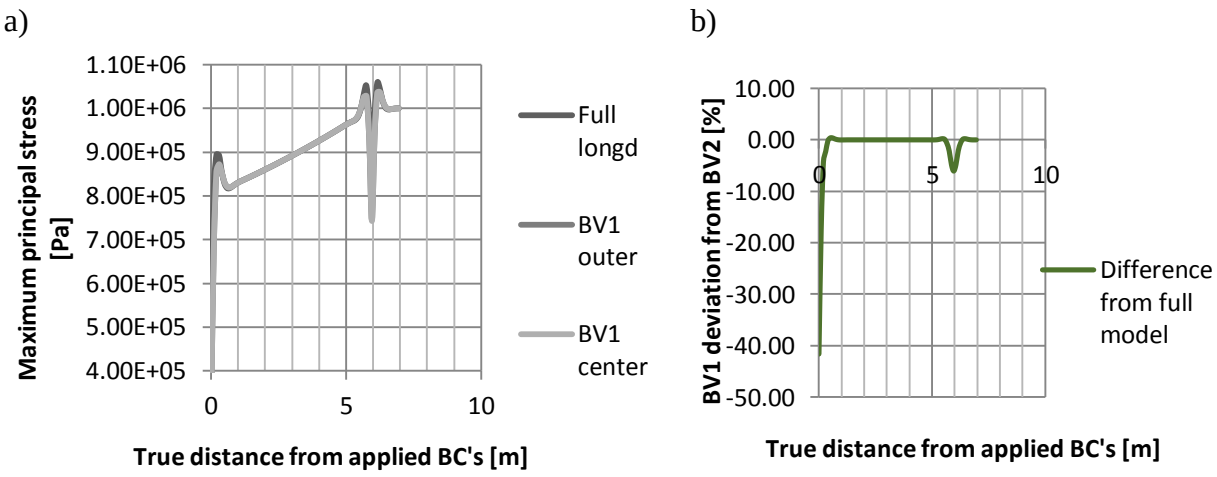

Figure 65 - Results for BV1 and BV2 compared for a) stress results and b) Stress deviation for BV1, using BV2 as target value.

The simplified knee plate ending, located opposite of the column, was visually verified. Stress was seen to diminish towards the tip of the knee plate, as shown in Figure 66.

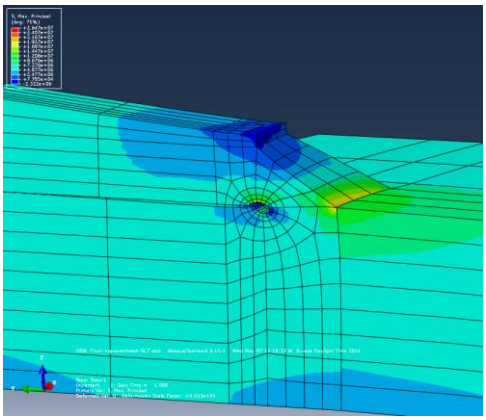

Figure 66 – Contour plot of maximum principal stress at the simplified knee plate ending.

4.3.2 Weld toe and root SCF

For the unit loaded brace model, the SCF obtained for weld toe *a* is compared to Aker Solutions' SCF in Table 14. The SCF's are given as the effective hot spot stress when subjected to a unit load of 1 MN in the axial direction. As can be seen from the table, the result from the brace model is found to be more conservative than that of Aker Solutions' results. It is however noted, that for the brace model, the weld is modelled as a fillet weld, according to the notch stress approach.

Table 14 - Stress concentrations at the weld toe and root path *a*, compared to Aker Solutions results, for a tension load of 1MN.

	Brace model	Aker Solutions' result
Weld toe SCF	9.01 MPa	7.952MPa
Weld Root SCF	26.47 MPa	-

4.3.3 Applied loading according to Miner summation

Stress results in the axial direction for 10 stress blocks, based on the stress range exceedances diagrams provided by Aker solutions, are shown in Table 15 for all four clock positions. As can be seen from the table, all stresses have been determined for the same number of cycles, as given by the n'-vector.

Table 15 - Applied loads for the analysis of 10 stress blocks.

	n'-vector	Stress range at clock positions [Pa]			
Step	Log(*n'*)	12:00	03:00	06:00	09:00
1	0.38	2.00E+08	2.09E+08	2.03E+08	2.08E+08
2	1.14	1.80E+08	1.88E+08	1.81E+08	1.86E+08
3	1.9	1.59E+08	1.66E+08	1.60E+08	1.65E+08
4	2.66	1.38E+08	1.44E+08	1.39E+08	1.43E+08
5	3.42	1.17E+08	1.22E+08	1.18E+08	1.21E+08
6	4.18	9.62E+07	1.00E+08	9.68E+07	9.98E+07
7	4.94	7.54E+07	7.86E+07	7.56E+07	7.81E+07
8	5.7	5.45E+07	5.68E+07	5.45E+07	5.64E+07
9	6.46	3.37E+07	3.50E+07	3.33E+07	3.48E+07
10	7.22	1.29E+07	1.32E+07	1.22E+07	1.31E+07

Stress ranges are seen to include a bending stress component acting over the cross section of the brace. The bending stress component is however minimal.

4.3.4 Weld toe fatigue life

As the maximum principal stress was seen to act approximately normal to the weld, the effective hot spot stress was taken as 1.12 times the read out stress, according to the effective hot spot approach method B. The resulting effective hot spot stress for the variable amplitude loading is given for 10 stress blocks in Table 16.

Table 16 – Effective hot spot stress for weld toes *a* of the knee plate model, for 10 stress blocks at 4 clock positions.

	Effective hot spot stress [Pa]			
step #	hotsp_cl12	hotsp_cl03	hotsp_cl06	hotsp_cl09
1	3.29E+08	3.29E+08	3.30E+08	3.29E+08
2	2.95E+08	2.95E+08	2.96E+08	2.95E+08
3	2.61E+08	2.61E+08	2.62E+08	2.60E+08
4	2.27E+08	2.26E+08	2.27E+08	2.26E+08
5	1.92E+08	1.92E+08	1.93E+08	1.92E+08
6	1.58E+08	1.58E+08	1.58E+08	1.58E+08
7	1.24E+08	1.24E+08	1.24E+08	1.23E+08
8	8.94E+07	8.92E+07	8.94E+07	8.91E+07
9	5.51E+07	5.49E+07	5.50E+07	5.48E+07
10	2.09E+07	2.06E+07	2.05E+07	2.06E+07

Fatigue life, corresponding to the effective hot spot stress and the D curve for air environment, is given in Table 17, where the thickness correction has been applied. The fatigue lives calculated here are further taken as the N_i values used for Miner summation, and the final calculation of expected fatigue life given in years.

Table 17 - Fatigue life calculated by the hot spot approach.

	N_i – For the weld toe [cycles to failure]			
step #	hotsp_cl12	hotsp_cl03	hotsp_cl06	hotsp_cl09
1	3.81E+04	3.81E+04	3.78E+04	3.84E+04
2	5.30E+04	5.31E+04	5.25E+04	5.34E+04
3	7.67E+04	7.69E+04	7.61E+04	7.73E+04
4	1.17E+05	1.17E+05	1.16E+05	1.18E+05
5	1.92E+05	1.92E+05	1.90E+05	1.93E+05
6	3.45E+05	3.47E+05	3.44E+05	3.49E+05
7	7.20E+05	7.23E+05	7.17E+05	7.27E+05
8	1.90E+06	1.92E+06	1.91E+06	1.93E+06
9	8.13E+06	8.22E+06	8.21E+06	8.27E+06
10	9.13E+08	9.66E+08	9.90E+08	9.75E+08

From the defined n'-vector, the number of cycles for every stress block were calculated, thus allowing for calculation of the Miner sum and resulting fatigue life. The obtained values are shown in Table 18, where n_i^1 and n_i^2 represent the number of cycles at the beginning and end of each stress block, respectively.

Table 18 - Fatigue life for each stress block, as well as the Miner sum calculations for the weld toe according to the effective hot spot approach.

	Defining stress block cycles				$D_i = \frac{n_i}{N_i}$			
step #	$\log(n_i^1)$	$\log(n_i^2)$	$\log(n_i)=\log(n_i^2 - n_i^1)$	n_i	$D_{i,cl12}$	$D_{i,cl03}$	$D_{i,cl06}$	$D_{i,cl09}$
1	0	0.76	0.68	4.75E+00	0.00	0.00	0.00	0.00
2	0.76	1.52	1.44	2.74E+01	0.00	0.00	0.00	0.00
3	1.52	2.28	2.20	1.57E+02	0.00	0.00	0.00	0.00
4	2.28	3.04	2.96	9.06E+02	0.01	0.01	0.01	0.01
5	3.04	3.8	3.72	5.21E+03	0.03	0.03	0.03	0.03
6	3.8	4.56	4.48	3.00E+04	0.09	0.09	0.09	0.09
7	4.56	5.32	5.24	1.73E+05	0.24	0.24	0.24	0.24
8	5.32	6.08	6.00	9.93E+05	0.52	0.52	0.52	0.51
9	6.08	6.84	6.76	5.72E+06	0.70	0.70	0.70	0.69
10	6.84	7.6	7.52	3.29E+07	0.04	0.03	0.03	0.03
$D = \sum_i \frac{n_i}{N_i}$					1.63	1.61	1.62	1.60
Fatigue life [years]					12.31	12.42	12.37	12.49

For comparison, Aker Solutions provided assessed fatigue life for the four clock positions, based on the effective hot spot approach. The Hot spot method B was applied also for this model, but a global model was used for FEA. Their results are compared to the results for both 10 and 15 stress blocks in Table 19. Comparing to Aker Solutions' results, it can be seen that a significant amount of bending has affected their results. It is however observed that the results obtained from the solid brace model is conservative compared to the provided fatigue life. It is also seen that increasing the number of stress blocks used for Miner summation increases the assessed fatigue life.

Table 19 - Fatigue life assessed for the brace model, and life assessed by Aker Solutions global model.

Clock position	12:00	03:00	06:00	09:00
Fatigue life obtained for 10 stress blocks [years]	12.31	12.42	12.37	12.49
Fatigue life obtained for 15 stress blocks [years]	13,64	13,78	13,73	13,86
Aker solutions fatigue life [years]	16.8	20.6	34.2	19.1

4.3.5 Weld root fatigue life

Weld root fatigue was evaluated for variable amplitude loading for the 12o'clock position, which was seen to contain the highest principal stress. As can be seen in Table 20, the results for 10 stress blocks show that the highest stress concentrations are found in path c. Corrected notch stress was calculated according to the second order notch stress correction, obtained from the parameter study. The resulting stress, also shown Table 20, is approximately 10% higher than what initially obtained in the FEA.

Table 20 – Extracted stresses from the weld root paths of the knee plate, as well as corrected notch stress.

	Maximum principal stress read at root paths at 12o'clock [Pa]				Corrected notch stress [Pa]			
Step #	path a	path b	path c	path d	path a	path b	path c	path d
1	9.68E+08	5.73E+08	1.42E+09	3.49E+08	1.11E+09	6.59E+08	1.64E+09	4.01E+08
2	8.68E+08	5.13E+08	1.27E+09	3.13E+08	9.97E+08	5.90E+08	1.46E+09	3.59E+08
3	7.67E+08	4.54E+08	1.13E+09	2.76E+08	8.81E+08	5.21E+08	1.29E+09	3.18E+08
4	6.66E+08	3.94E+08	9.79E+08	2.40E+08	7.65E+08	4.53E+08	1.12E+09	2.76E+08
5	5.65E+08	3.34E+08	8.30E+08	2.04E+08	6.50E+08	3.84E+08	9.54E+08	2.34E+08
6	4.64E+08	2.75E+08	6.82E+08	1.67E+08	5.34E+08	3.16E+08	7.84E+08	1.92E+08
7	3.64E+08	2.15E+08	5.34E+08	1.31E+08	4.18E+08	2.47E+08	6.14E+08	1.51E+08
8	2.63E+08	1.56E+08	3.86E+08	9.47E+07	3.02E+08	1.79E+08	4.44E+08	1.09E+08
9	1.62E+08	9.59E+07	2.38E+08	5.84E+07	1.86E+08	1.10E+08	2.74E+08	6.71E+07
10	6.13E+07	3.62E+07	9.00E+07	2.21E+07	7.04E+07	4.17E+07	1.03E+08	2.54E+07

Analysis stress results for the first stress block, step 1, extracted from the 12o'clock position at the side of the knee plate seen to have the highest stress concentrations, are illustrated in Figure 67. As can be seen from the figure, the highest stress concentrations occur at the weld between the knee plate and the ring stiffener close to the brace. It is noticed, that the highest stress concentration was found to be located three elements away from the elements subjected to analysis warnings.

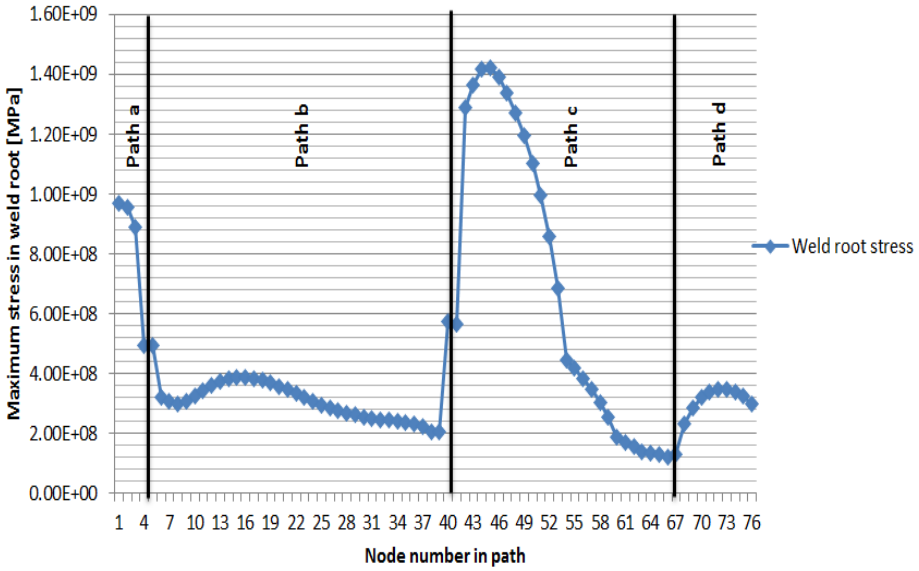

Figure 67 – Maximum principal stress in the defined weld roots for step 1 of the analysis. Where points indicated in the graph represents the nodes of stress extraction.

From the corrected notch stress results, fatigue life based on the effective notch stress SN-curve for air was calculated for all root paths. The results are given Table 21, which are further used for calculating the Miner sum, and assess the number of fatigue life years.

Table 21 - Fatigue life calculated for all root paths by the effective notch stress SN-curve for air.

	Ni Root fatigue [cycles]			
Step #	Path a	Path b	Path c	Path d
1	1.65E+04	7.99E+04	5.22E+03	3.54E+05
2	2.30E+04	1.11E+05	7.25E+03	4.92E+05
3	3.33E+04	1.61E+05	1.05E+04	7.12E+05
4	5.09E+04	2.45E+05	1.60E+04	1.09E+06
5	8.32E+04	4.02E+05	2.62E+04	1.78E+06
6	1.50E+05	7.24E+05	4.73E+04	3.21E+06
7	3.12E+05	1.51E+06	9.85E+04	6.68E+06
8	8.27E+05	3.99E+06	2.61E+05	3.06E+11
9	3.53E+06	2.95E+11	1.11E+06	1.30E+12
10	1.13E+12	5.46E+12	3.57E+11	2.40E+13

The lowest fatigue life is observed for root path c, which is consistent with the root path found to have the highest stress concentrations. Similarly path d is found to contain the lowest stress concentrations, and thus the highest fatigue life is found in path d. For miner sum calculations, fatigue life for path *a* and *c* were assessed, only.

Similarly to the hot spot approach, the number of cycles for every stress block was defined from the n'-vector. The Miner sum for the weld roots were then obtained as shown in Table 22.

Table 22 - Fatigue life for each stress block, as well as the Miner sum calculations for the weld root, according to the effective notch stress approach.

	Defining stress block cycles				$D_i = \frac{n_i}{N_i}$	
step #	$\log(n_i^1)$	$\log(n_i^2)$	$\log(n_i)=\log(n_i^2 - n_i^1)$	n_i	Di path a	Di path c
1	0	0,76	0,68	4,75E+00	0.00	0.00
2	0,76	1,52	1,44	2,74E+01	0.00	0.00
3	1,52	2,28	2,20	1,57E+02	0.00	0.01
4	2,28	3,04	2,96	9,06E+02	0.02	0.06
5	3,04	3,8	3,72	5,21E+03	0.06	0.20
6	3,8	4,56	4,48	3,00E+04	0.20	0.63
7	4,56	5,32	5,24	1,73E+05	0.55	1.75
8	5,32	6,08	6,00	9,93E+05	1.20	3.81
9	6,08	6,84	6,76	5,72E+06	1.62	5.13
10	6,84	7,6	7,52	3,29E+07	0.00	0.00
$D = \sum_i \frac{n_i}{N_i}$					3.66	11.6
Fatigue life [years]					5.46	1.72

Similarly, a miner summation for 15 stress blocks was performed. This resulted in a fatigue life of 1.70 years for root c.

4.3.6 Extrapolation of the notch stress results

As a linear relation was found for varying weld sizes, the results found for a weld size of 6mm may be extrapolated such that a desired fatigue life of the weld root is achieved.

Fatigue life based on cumulative damage was determined by extrapolated notch stress results for two weld sizes. Firstly, a weld size of 11.2mm results in a fatigue life of 14 years, which is the same fatigue life as was obtained for the weld toe in the brace model analysis. Secondly, a weld size of 13mm is given as reference, which resulted in a fatigue life of 22 years. The estimated fatigue lives are based on Miner summation of 15 stress blocks.

4.3.7 Summary of the fillet welded knee plate results

All brace analyses required a large amount of physical memory, and thus computational time was high. For the sake of further work, analyses details are listed in Table 23.

Table 23 - Analyses details.

Analysis	Brace model SCF	Brace model 10 Stress blocks	Brace model 15 Stress blocks	BV1	BV2
# Elements	241056	241056	241056	5600	4830
# Steps	1	10	15	1	1
Memory used	27Gb (max)	27Gb (max)	27Gb (max)	0.6Gb	0.6Gb
Computational time	30 min	5 hours	7 hours	30 sec	30 sec

A summary of the fatigue lives obtained, and given from Aker Solutions' global analysis, is given in Figure 68, where all results based on the brace model are given for a Miner summation of 15 stress blocks. It is noted that weld root fatigue life was found lowest for the 12o'clock position at path c, while weld toe fatigue was given for toe a at all clock positions.

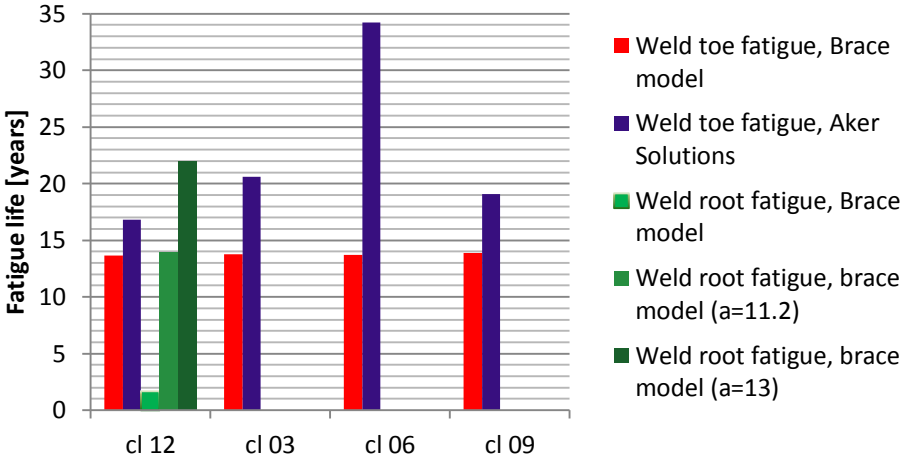

Figure 68 - Assessed fatigue life compared for weld toe and –root at all clock positions, for a miner summation of 15 stress blocks, as well as Aker Solutions fatigue results.

5 Discussion

Loading mode dependent microsupport factor

A loading mode dependent microsupport factor for the effective notch stress approach would make the procedure of assessing fatigue life more cumbersome. Taking this into account, one of the main advantages for this approach compared to the nominal stress approach is lost, as loading mode would have to be defined. It was however assumed that not accounting for the loading mode would yield more conservative results. This was however found arguable for varying weld sizes.

5.1 Validation of the effective notch stress approach

Large deviation for weld toe fatigue

The combined model intended to assess weld toe fatigue for the fillet welded joint yielded quite conservative results. However, the nominal approach used to assess the target value for this weld toe, is intended for use when weld toe fatigue is the most probable failure mode. This might be an explanation to the large deviation.

The necessity of assessing fatigue at the weld toe using the effective notch stress approach can however be argued, as this can be done in a simpler way by use of the effective hot spot approach.

Mesh convergence study

The mesh in the weld and plate intersection partition was quite fine and thus computational efforts were relatively high. It is recognised that the models used for these analyses are quite simple, and that for larger and more complex models a large amount of elements are required, and thus a large amount of physical computer memory is needed.

The mesh convergence study was performed for the welds root- and toe partitions only. During analyses, it was observed that changing the mesh in other areas had only minor effects on the weld root stress. The meshing of surrounding partitions should however be performed such that the element sizes are corresponding to the element sizes at the outer part of the root partition, in order to have a smooth mesh transition.

The outer plate mesh was seen to have little or no influence on the weld root stress concentration. However, the weld toe was to some extent affected. As the results for the toe 2 configuration was seen to converge towards a 0.5% deviation from the target value, this was not further documented. For a different plate thickness, the mesh for the outer plate partitions would have to be redefined in order to maintain a similar mesh size relative to the weld toe partition. It was however observed that higher stresses occurred for both smaller and larger

mesh sizes at the plate, and thus it can be stated that the results will be conservative regardless of the mesh size over the thickness.

5.2 Parametric weld size study

In the weld size study it was seen that the nominal approach predicts higher effective notch stress for smaller weld sizes, than what is obtained in the finite element analysis. For larger weld sizes the tendencies were opposite, yielding larger than predicted effective notch stress. Two methods were used for establishing a relation between the results. Firstly, an alternation of the notch size, and secondly, a correction of the effective notch stress for varying weld sizes.

The notch size study

From the notch size study, it was seen that by reducing the notch size for smaller weld sizes, maximum principal stress at the root of the notch increased. This was expected, as notch stress is increased for smaller notch radiuses (Radaj et al., 2013).

Altering the notch radii according to weld size was found to give promising results for describing the difference between the approaches. The relation found between an ideal notch size and weld size, was observed to be close to linear in Figure 61. However, if the tendency for the ideal notch radii shown in the figure is assumed to be continued, a better fit for the curve would be to use the second order fit. Although verifying analyses of the second order polynomial were not performed, comparing the ideal notch sizes to the linear and second order estimate shows that this is a far better approximation for the notch size.

For the notch size study, it is noticed that the method implies altering the theoretical values used for calculating the fictitious radii, given in equation (22). As the microstructural support length ρ^* is considered to be a material parameter and the real notch radius is assumed to be zero (Radaj et al. 2013), it can be argued that it is the support factor s, that is affected by the weld size. The support factor has been found to vary for different loading modes (Radaj et al. 2013). Hence, an explanation may be that as the weld size is varied, the flow of stress varies with it, and therefore the loading mode is altered.

Notch stress correction

The second method, made to redeem the difference between the effective notch stress- and the nominal approach, is the notch stress correction method. This method is applied in order to correct the effective notch stress, obtained in a FEA using a 1mm notch radius, according to the weld size chosen. Altering the notch stress SN-curve parameters alone is not suitable for correcting this, as can be shown in Figure 60, where a change of SN-curve parameter would only change the slope of the curve, while the curve would still go through the origin.

Although the procedure was found to give good results, the parameters found for this method does not explain the underlying theory causing this phenomenon.

Extrapolation of notch stress

From Figure 60 it is observed that a direct extrapolation of the obtained notch stress, according to the nominal linearity, would result in non-conservative results for large weld sizes. This is due to the non-linear effects seen in the effective notch stress approach. Prior to the extrapolation, the obtained notch stress should therefore be corrected by equation (35). The corrected value will thus correspond to the magnitude of a corresponding target notch stress, which can be assumed to be as conservative as the nominal stress approach.

General

By comparing the effective notch stress found by FEA to the target notch stress in Figure 60, it is seen that the curve obtained for the effective notch stress approach is non-linear, compared to the target notch stress which is linear for inverse weld sizes. As the target notch stress is defined from weld stress and the nominal approach, this might be interpreted in two ways. One way, is that the nominal approach is a conservative approximation, and thus the effects seen for the notch stress approach is a more accurate assessment. Or, it might be interpreted that as the weld size is varied, the loading mode is varied, and thus according to Neuber's theory, a different notch radius must be used in the FEA. In order to answer this, the actual results from fatigue testing of the cruciform joint should be compared to the results from the two approaches.

5.3 The fillet welded knee plate

Base model simplifications

The simplifications made for the brace model were verified by comparing the BV1 and BV2 models. It is however noticed that the simplified models do not include the ring stiffener. The ring stiffener was made in the same manner as the brace outer plate, by simplifying the curvature of the ring stiffener to be flat close to the knee plate. It could however be argued, that the effects of the simplification would be even smaller for the ring stiffener, as the height of the ring stiffener, which is in the radial direction, far exceeds the brace plate thickness. Thus the relative change in hight is far smaller than that of the outer brace plate.

Simplification of the tip of the knee plate, shown in Figure 41, may be considered a small alteration of the model. From stress contour plots, the stress flow may also be considered to flow past the tip, thus not affecting the solution of the FEA.

Loading and local model

The SCF's found for the brace model were seen to be slightly higher than the results obtained by Aker Solutions. Some difference is however to be expected, as different modelling techniques and type of mesh has been used. Due to the small differences between SCF's, it may be interpreted that the brace model is a good match.

Cumulative damage

The cumulative damage for the weld toe, assessed from the brace model, was seen to yield approximately the same fatigue life for all clock positions. This was in conflict with Aker Solutions' results, which suggested that some bending effect caused a far longer fatigue life of the weld toe at 6o'clock than at 12o'clock. As the loading provided by Aker Solutions only indicated minor bending contributions, and the brace model is symmetrical, it may be interpreted that the bending is not caused by the applied load or the model itself. An explanation to the significant bending not being present may be due to the fixed boundary conditions representing the column. When using the sub modelling technique, it is common to define the response at the boundaries of the local model, using the responses obtained from a global model, at the region of this boundary (Moan, 2003). The simplified boundary conditions used in the FEA do not account for loading present in the column, nor the stiffness of the column.

The fatigue life assessed from the brace model was however found to give conservative results for the weld toe, compared with Aker Solutions' results. This may indicate that the assumption of the column being stiff is a conservative simplification. It can thus be argued, that for weld root fatigue assessments based on the same model, the results will be conservative.

It is also noticed, that the lowest fatigue life assessed for the weld toe by Aker Solutions, is quite close to the lowest life obtained from the brace model. This can, to some extent, be interpreted as a sign of some precision for weld root fatigue life.

6 Conclusion

6.1 General

Three approaches for assessment of design life have been reviewed. These are the nominal stress-, the structural hot spot- and the effective notch stress approach. The approaches' applicability differs, and these differences have been listed in Table 2.

In addition to the former approaches, the fracture mechanics approach has been reviewed, which may be used as a very conservative estimate for design life.

In general, the nominal stress approach is the preferred method of weld root fatigue. This approach does however require a defined nominal stress, and a comparable well tested detail. If these requirements cannot be satisfied, the effective notch stress approach may be used, which unlike the structural hot spot stress approach, is applicable for assessments of weld root fatigue.

The effective notch stress approach is performed by introducing a fictitious notch at the weld-root or toe, in a solid FEA. The maximum stresses obtained in the notch is taken as the effective notch stress and compared to a universal SN-curve. As the approach requires a solid model for FEA and a mesh able to sufficiently represent the notch, computational time for this approach is the highest of the three approaches.

6.2 Validation of the effective notch stress approach

The validation procedure given by DNV (2012) has been executed for a cruciform fillet welded- and fully penetration welded joint. The procedure involves establishing target notch stress values, by demanding equal fatigue life for the two approaches. The joint is identical to construction details given by DNV (2012), for which fatigue life provide a 97.7% probability of survival. Design life obtained using the nominal approach for these models are therefore considered to yield realistic and conservative results.

The effective notch stress was obtained as the highest maximum principal stress in the notch, using the FEA software Abaqus. Based on interpretation of figures and descriptions found in the literature, placements of the fictitious notch has been confirmed by analyzing three fictitious notch roots and two notch toes.

Results show that a fictitious notch at the weld toe should be modeled according to the model referred to as toe 2, which for the full penetration welded cruciform joint yielded approximately 1.4% longer fatigue life than that obtained from the nominal stress approach. Similarly, the placement of the fictitious weld root should be placed according to root 3, which for the fillet welded cruciform joint was seen to converge towards a fatigue life overestimated by 11.5%.

Both at the weld root and weld toe, the mesh convergence study showed small variations for an increased number of elements along the circumference, 1% or less for 4 to 12 quadrilateral elements.

6.3 Parametric weld size study

On the basis of the validation model, weld sizes were varied and effective notch stress extracted. In the same manner as the validation procedure, target notch stress values were obtained, and compared to the extracted stress. The results were found to deviate from each other, and while the target stresses can be found to be a linear function-, the extracted effective notch stress is better described by a second order polynomial, as a function of inverse weld sizes.

Whether or not the validation procedure is intentionally chosen for one specific weld size, is considered to be unclear. In order to confirm that the notch stress approach is sufficiently conservative for varying weld sizes, the actual fatigue testing results should be reviewed. If the effective notch stress approach is found not to be in line with the fatigue results, an explanation for the deviation may be due to a varying loading mode for varying weld sizes. This has been found to affect the microsupport factor, and thus the size of the fictitious notch (Radaj et al. 2013).

A relation between the linear target stress and the obtained effective notch stress has been established. The relation is best expressed with the second order polynomial given in equation (35). Utilizing the expressed relation, a corrected notch stress is obtained which is in compliance with the nominal stress approach. This allows for extrapolation of the corrected stress found from a single FEA of one weld size.

Another relation, between weld size and fictitious notch radii, has also been established. The relation, given by equation (33), shows that the use of a smaller notch radius for smaller weld sizes, and vice versa, will result in a fatigue life corresponding to the nominal approach.

None of the above relations have been confirmed for other joints. Therefore, additional studies are recommended, in order to validate the established relations for varying weld sizes.

6.4 The fillet welded knee plate

Fatigue life at the weld root of the fillet welded knee plate, has been assessed for the provided load spectra by Miner summation. In order to verify the results, model simplifications and loading methodology have been discussed based on verifying FEA models and SCF results, and are found to be acceptable. Boundary conditions applied to the brace model has also been discussed. It is concluded that the fixed boundary conditions applied in the brace model, causes the weld toe fatigue to differ from that of Aker Solutions global model. The results, and thus the boundary conditions representing a stiff column, are however conservative, and therefore accepted for evaluation of weld root fatigue.

Weld root fatigue was found to be most critical for *path c*, as shown in Figure 67. This weld root is approximately normal to the applied loading, and thus found fit for fatigue assessment according to the effective notch stress approach. Fatigue assessments were performed

conservatively by use of the established notch stress correction. Weld root fatigue for a fillet weld of 6mm was, by FEA, found to give non-conservative results, compared to the weld toe in the same analysis. An extrapolation of the obtained results suggested the fillet weld to be welded with a minimum weld size of 11.2mm, in order to obtain a greater fatigue life at the weld root, than that of the toe. Further, a weld size of 13mm was assessed to give a fatigue life approximately 75% greater than that of the weld toe.

7 Future work

The effective notch stress approach has been found to be non-conservative for small weld sizes compared to the nominal approach. As the nominal approach is defined as a linear relation for weld size, it might be beneficial to compare results from the effective notch stress approach for small weld sizes, to actual fatigue tests.

It might also be useful to study the loading modes of the fictitious weld root notch for varying weld sizes. Results from such a study, should be compared with the parameters found for the microsupport factor *s* and loading mode. This might explain a possible need for a fictitious notch size dependent on weld size.

As the notch size and stress relations, found between the nominal- and the effective notch stress approach, only has been found for the cruciform joint, it might be useful to validate the relation for other well tested joints. This could confirm that the effective notch stress can be conservatively extrapolated to any reasonable weld size, from a single FEA.

8 References

Berge, S. (2006). *Fatigue and fracture design of marine structures* (Vol. UK-2006-93). Trondheim: Marinteknisk senter.

Bruder, T., Störzel, K., Baumgartner, J., & Hanselka, H. (2012). Evaluation of nominal and local stress based approaches for the fatigue assessment of seam welds. *International Journal of Fatigue, 34*(1), 86-102. doi: http://dx.doi.org/10.1016/j.ijfatigue.2011.06.002

BSI. (2005). Guide for assessing the significance of flaws in metallic structures. British Standards Institution. BS 7910:2005.

Crack force lines. [Picture] (2013). Retrieved from http://en.wikipedia.org/wiki/Force_lines

Djavit, D. E., & Strande, E. (2013). *Fatigue failure analysis of fillet welded joints used in offshore structures* (Master's Thesis), Chalmers University of Technology, Göteborg, Sweden. Retrieved from http://publications.lib.chalmers.se/records/fulltext/194840/194840.pdf (X-13/294)

DNV. (2012). Recommended practice DNV-RP-C203 - Fatigue Design of Offshore Steel Structures. *Det Norske Veritas, October*.

Fricke, W. (2003). Fatigue analysis of welded joints: state of development. *Marine Structures, 16*(3), 185-200. doi: http://dx.doi.org/10.1016/S0951-8339(02)00075-8

Fricke, W. (2013). IIW guideline for the assessment of weld root fatigue. *Welding in the World, 57*(6), 753-791. doi: 10.1007/s40194-013-0066-y

Fricke, W., & Doerk, O. (2006). Simplified approach to fatigue strength assessment of fillet-welded attachment ends. *International Journal of Fatigue, 28*(2), 141-150. doi: http://dx.doi.org/10.1016/j.ijfatigue.2005.04.008

Fricke, W., & Kahl, A. (2005). Comparison of different structural stress approaches for fatigue assessment of welded ship structures. *Marine Structures, 18*(7–8), 473-488. doi: http://dx.doi.org/10.1016/j.marstruc.2006.02.001

Hobbacher, A. (2009a). *Recommendations for fatigue design of welded joints and components* (Vol. 520). New York, N.Y.: The Council.

Hobbacher, A. F. (2009b). The new IIW recommendations for fatigue assessment of welded joints and components – A comprehensive code recently updated. *International Journal of Fatigue, 31*(1), 50-58. doi: http://dx.doi.org/10.1016/j.ijfatigue.2008.04.002

Hole force lines. [Picture] (2013). Retrieved from http://en.wikipedia.org/wiki/Force_lines

Leira, B. J., Syvertsen, K., Amdahl, J., & Larsen, C. M. (2011). *TMR 4170 Marine konstruksjoner, grunnkurs* (Vol. UK-08-82). Trondheim: Marinteknisk senter.

Maddox, S. J. (1991). *Fatigue strength of welded structures*. Cambridge: Abington Publ.

Moan, T. (2003). *Finite element modelling and analysis of marine structures* (Vol. UK-03-98). Trondheim: Marinteknisk senter.

Næss, A. (1985). *Fatigue handbook: offshore steel structures.* Trondheim: Tapir.

Petershagen, H. (1975). Cruciform joints and their optimisation for fatigue strength - a literature survey. *Welding in the World, 13*(516), 143-154.

Radaj, D. (1990). *Design and Analysis of Fatigue Resistant Welded Structures* (pp. 218-219): Woodhead Publishing.

Radaj, D. (1996). Review of fatigue strength assessment of nonwelded and welded structures based on local parameters. *International Journal of Fatigue, 18*(3), 153-170. doi: http://dx.doi.org/10.1016/0142-1123(95)00117-4

Radaj, D., Lazzarin, P., & Berto, F. (2013). Generalised Neuber concept of fictitious notch rounding. *International Journal of Fatigue, 51*(0), 105-115. doi: http://dx.doi.org/10.1016/j.ijfatigue.2013.01.005

Radaj, D., Sonsino, C. M., & Fricke, W. (2009). Recent developments in local concepts of fatigue assessment of welded joints. *International Journal of Fatigue, 31*(1), 2-11. doi: http://dx.doi.org/10.1016/j.ijfatigue.2008.05.019

Schijve, J. (2012). Fatigue predictions of welded joints and the effective notch stress concept. *International Journal of Fatigue, 45*(0), 31-38. doi: http://dx.doi.org/10.1016/j.ijfatigue.2012.06.016

Sonsino, C. M., Fricke, W., de Bruyne, F., Hoppe, A., Ahmadi, A., & Zhang, G. (2012). Notch stress concepts for the fatigue assessment of welded joints – Background and applications. *International Journal of Fatigue, 34*(1), 2-16. doi: http://dx.doi.org/10.1016/j.ijfatigue.2010.04.011

Weld Diagram. [Picture] (2013). Retrieved from http://www.weldersuniverse.com/code_welding.html.

Stress concentration by a hole. (2013). Retrieved from http://commons.wikimedia.org/wiki/File:Stress_concentration_by_a_hole.png.

Appendix

A. Calculation of target values for the effective notch stress

In the following, “elec” represents the number of elements seeded per quarter circumference of the fictitious notch.

Comparison of approaches for the weld root				
SN-Curves	NOMINAL APPROACH		EFFECTIVE NOTCH STRESS	
	N	Δσ	N	Δσ
N<10^7	1.00E+07	21.05	1.00E+07	131.623469
	9.33E+01	1000	2.28E+04	1000
N>10^7	4.14E+13	1	3.94E+17	1
	1.00E+07	21.05	1.00E+07	131.583066
Plotting results on SN-curves	W3-curve accounts for stress concentrations		Stress concentrations are evaluated in FEA	
	N	Δσ	N	Δσ
	1.0000E+01	100.00	1.0000E+01	625.17
	9.3325E+04	100.00	9.3325E+04	625.17
	9.3325E+04	1.00	9.3325E+04	1.00

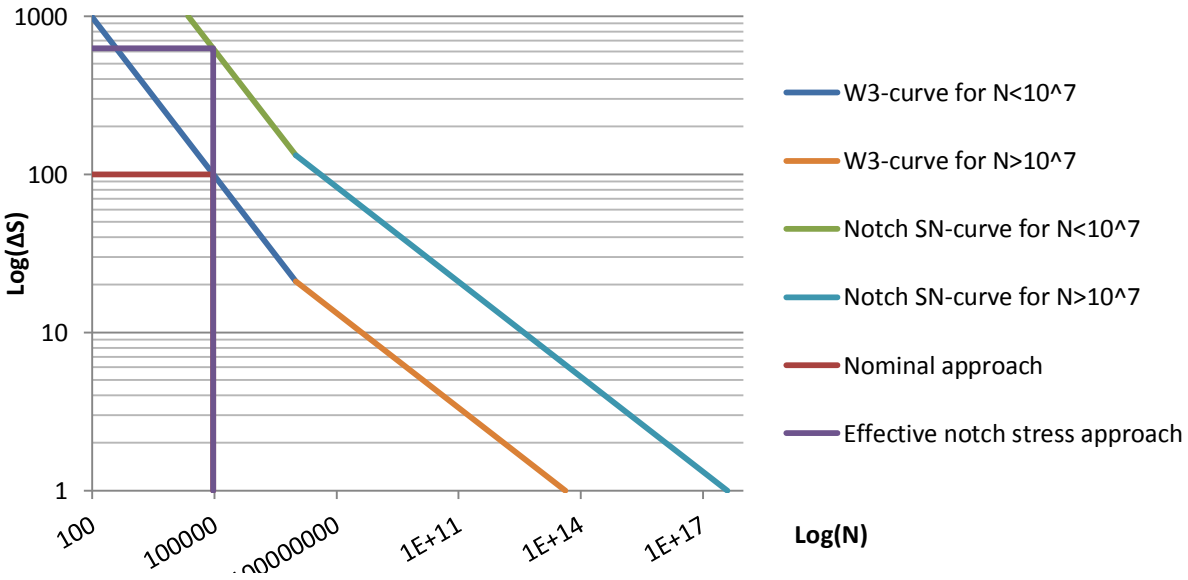

A. Calculation of target values for the effective notch stress

Comparison of approaches for the full pen weld toe				
SN-Curves	NOMINAL APPROACH		EFFECTIVE NOTCH STRESS	
	N	Δσ	N	Δσ
N<10^7	1.001E+07	41.52	1.000E+07	131.623469
	7.161E+02	1000	2.280E+04	1000
N>10^7	1.233E+15	1	3.945E+17	1
	9.993E+06	41.52	1.000E+07	131.583066
Plotting results on SN-curves	F-curve accounts for stress concentrations		Stress concentrations are found from FEA	
	N	Δσ	N	Δσ
	1.000E+01	100.00	1.000E+01	316.98
	7.161E+05	100.00	7.160E+05	316.98
	7.161E+05	1.00	7.160E+05	1.00

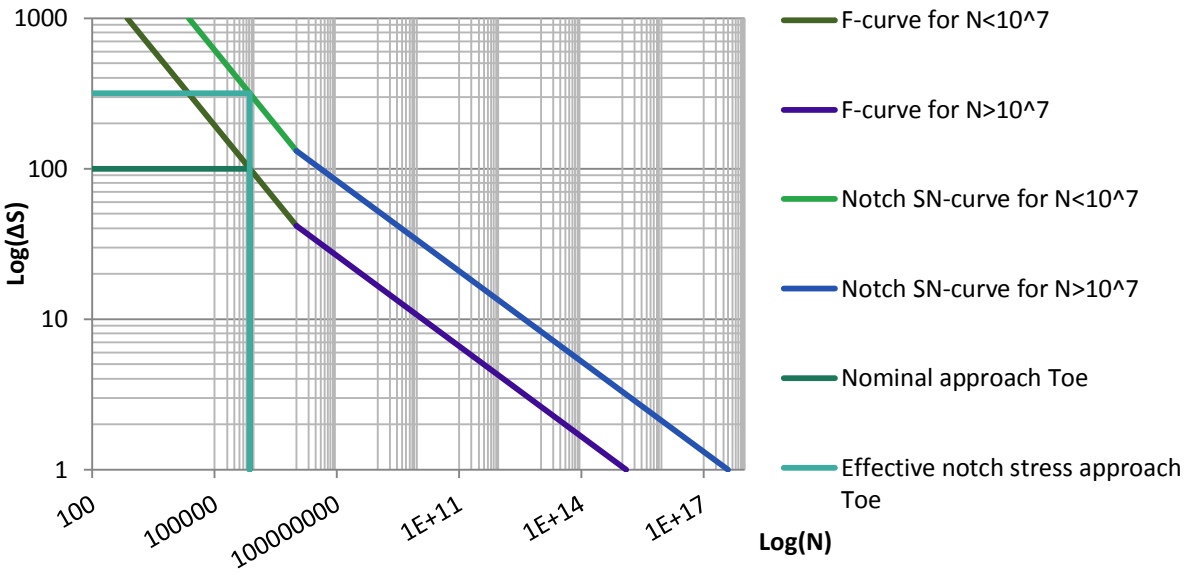

Comparison of approaches for the fillet welded weld toe				
SN-Curves	NOMINAL APPROACH		EFFECTIVE NOTCH STRESS	
	N	Δσ	N	Δσ
N<10^7	2.695E+07	23.5390179	1.001E+07	131.583066
	3.516E+02	1000	2.280E+04	1000
N>10^7	2.138E+14	1	3.945E+17	1
	2.956E+07	23.5390179	1.000E+07	131.583066
Plotting results on SN-curves	F3-curve accounts for stress concentrations		Stress concentrations are found from FEA	
	N	Δσ	N	Δσ
	1.000E+00	100.00	1.000E+01	401.78
	3.516E+05	100.00	3.516E+05	401.78
	3.516E+05	1.00	3.516E+05	1.00

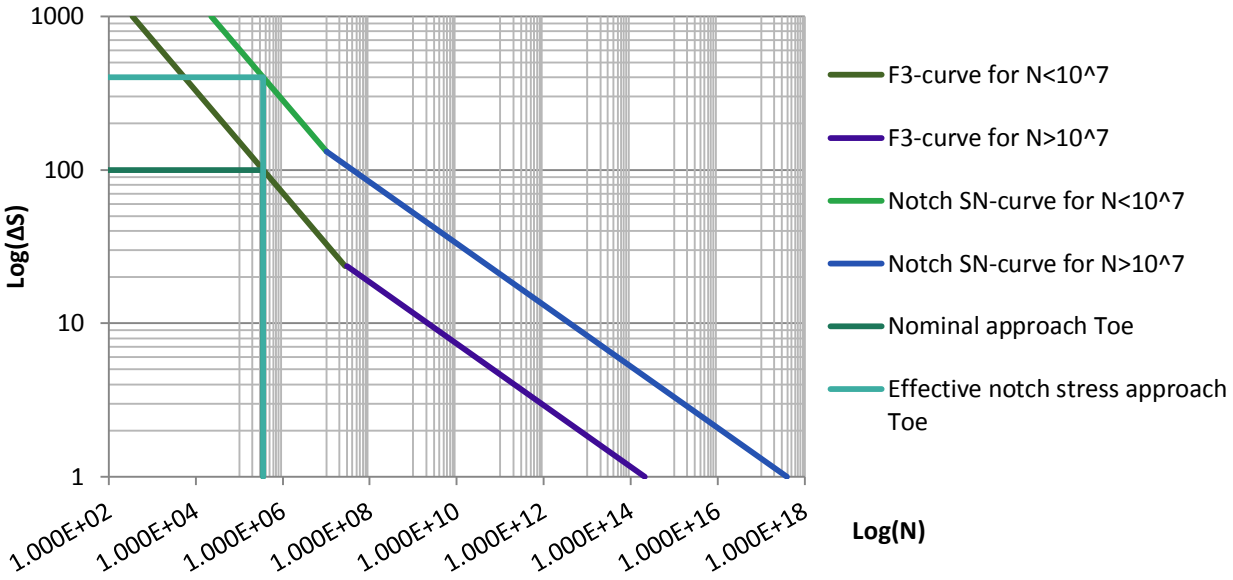

Comparison of results				
	Nominal approach		Notch stress approach	
	N	Δσ	N	Δσ
Weld root fillet	9.333E+04	100	9.340E+04	625.00
Weld toe full pen	7.161E+05	100	7.160E+05	316.98
Weld toe fillet	3.516E+05	100	3.516E+05	401.78

Weld toe using wrong design curve parameters: The F1 curve				
	Nominal approach		Notch stress approach	
	N	Δσ	N	Δσ
Weld toe fillet	5.000E+05	100.00	5.000E+05	357.28

B. Stress exceedances diagrams supplied by Aker Solutions

First sheet of data containing stresses from global model, provided by Aker Solutions. Positions correspond to nodes.

```
************************************************************
**                                                        **
**                      S T O F A T                       **
**                                                        **
**        F A T I G U E  C H E C K  R E S U L T S         **
**                          O F                           **
**                    E L E M E N T S                     **
**                                                        **
**          RUN     : PK3_1_R                             **
**          DATE/TIME: 2014-04-22 12:58:50                **
**                                                        **
************************************************************
```

PRINT OF:

- STRESS RANGES

STRESSES OF ELEMENT STRESS POINTS ARE USED

SPECTRAL MOMENTS APPLIED IN FATIGUE DAMAGE CALCULATION ARE USED

****

B. Stress exceedances diagrams supplied by Aker Solutions

Element	Positions	Exceedence_levels	Design fatigue life
497	8	61	20.00 Years

Element	Pos	Wavedir	Level	Stress_range	Exceedence
497	1	0.00	0	2.20158480E+08	0.00000000E+00
497	1	0.00	1	1.69902528E+08	6.21962428E-08
497	1	0.00	2	1.67070816E+08	1.24368995E-07
497	1	0.00	3	1.64239088E+08	2.46357956E-07
497	1	0.00	4	1.61407392E+08	4.83478289E-07
497	1	0.00	5	1.58575680E+08	9.40168491E-07
497	1	0.00	6	1.55743968E+08	1.81180746E-06
497	1	0.00	7	1.52912272E+08	3.46062325E-06
497	1	0.00	8	1.50080560E+08	6.55243730E-06
497	1	0.00	9	1.47248848E+08	1.23004884E-05
497	1	0.00	10	1.44417136E+08	2.28973349E-05
497	1	0.00	11	1.41585440E+08	4.22727935E-05
497	1	0.00	12	1.38753728E+08	7.74161454E-05
497	1	0.00	13	1.35922016E+08	1.40660515E-04
497	1	0.00	14	1.33090304E+08	2.53610138E-04
497	1	0.00	15	1.30258592E+08	4.53835004E-04
497	1	0.00	16	1.27426888E+08	8.06218595E-04
497	1	0.00	17	1.24595176E+08	1.42207649E-03
497	1	0.00	18	1.21763472E+08	2.49114120E-03
497	1	0.00	19	1.18931768E+08	4.33485769E-03
497	1	0.00	20	1.16100056E+08	7.49462657E-03
497	1	0.00	21	1.13268344E+08	1.28772762E-02
497	1	0.00	22	1.10436632E+08	2.19937060E-02
497	1	0.00	23	1.07604928E+08	3.73490639E-02
497	1	0.00	24	1.04773216E+08	6.30779937E-02
497	1	0.00	25	1.01941512E+08	1.05975434E-01
497	1	0.00	26	9.91098080E+07	1.77165762E-01
497	1	0.00	27	9.62780960E+07	2.94798046E-01
497	1	0.00	28	9.34463840E+07	4.88390386E-01
497	1	0.00	29	9.06146800E+07	8.05823505E-01
497	1	0.00	30	8.77829680E+07	1.32459962E+00
497	1	0.00	31	8.49512560E+07	2.16993570E+00
497	1	0.00	32	8.21195440E+07	3.54388332E+00
497	1	0.00	33	7.92878400E+07	5.77218485E+00
497	1	0.00	34	7.64561360E+07	9.37982750E+00
497	1	0.00	35	7.36244240E+07	1.52129068E+01
497	1	0.00	36	7.07927200E+07	2.46355057E+01
497	1	0.00	37	6.79610080E+07	3.98485107E+01
497	1	0.00	38	6.51292960E+07	6.44055481E+01
497	1	0.00	39	6.22975880E+07	1.04048248E+02
497	1	0.00	40	5.94658840E+07	1.68054016E+02
497	1	0.00	41	5.66341720E+07	2.71396332E+02

497	1	0.00	42	5.38024640E+07	4.38160645E+02
497	1	0.00	43	5.09707560E+07	7.06838379E+02
497	1	0.00	44	4.81390480E+07	1.13826404E+03
497	1	0.00	45	4.53073400E+07	1.82696814E+03
497	1	0.00	46	4.24756280E+07	2.91633423E+03
497	1	0.00	47	3.96439200E+07	4.61682959E+03
497	1	0.00	48	3.68122120E+07	7.22443848E+03
497	1	0.00	49	3.39805040E+07	1.11330000E+04
497	1	0.00	50	3.11487940E+07	1.68302227E+04
497	1	0.00	51	2.83170860E+07	2.48640410E+04
497	1	0.00	52	2.54853780E+07	3.57667461E+04
497	1	0.00	53	2.26536700E+07	4.99311211E+04
497	1	0.00	54	1.98219600E+07	6.74488359E+04
497	1	0.00	55	1.69902520E+07	8.79418203E+04
497	1	0.00	56	1.41585430E+07	1.10438695E+05
497	1	0.00	57	1.13268350E+07	1.33355062E+05
497	1	0.00	58	8.49512600E+06	1.54623781E+05
497	1	0.00	59	5.66341750E+06	1.71982094E+05
497	1	0.00	60	2.83170875E+06	1.83369234E+05
497	1	0.00	61	0.00000000E+00	1.87338516E+05
497	1	15.00	0	2.20158480E+08	0.00000000E+00
497	1	15.00	1	1.69902528E+08	5.80036108E-08
497	1	15.00	2	1.67070816E+08	1.16093169E-07
497	1	15.00	3	1.64239088E+08	2.30155464E-07
497	1	15.00	4	1.61407392E+08	4.52007839E-07
497	1	15.00	5	1.58575680E+08	8.79500817E-07
497	1	15.00	6	1.55743968E+08	1.69569705E-06
497	1	15.00	7	1.52912272E+08	3.23994186E-06
497	1	15.00	8	1.50080560E+08	6.13578868E-06
497	1	15.00	9	1.47248848E+08	1.15188859E-05

C. Script: Importing load spectra and exporting Abaqus input commands

Script used for extracting stresses from the data set provided by Aker Solutions, as well as writing Abaqus input commands.

```
clear all
clc
%-----------------------------------------------------------------
--------------------------------
% Script used for extracting stresses from the data set
provided by Aker Solutions,
% create stress range exceedance diagrams for each node and
averaging the stress at i
% number of cycles defined in th n'-vector
%
%  Input:   Data set from Aker solutions: input2.txt
%           Number of loadcases intended for the analysis
%           The name assigned to the model in Abaqus
%
%  Output:  Excel sheet containing load inputs for abaqus
%           Abaqus input commands.
%-----------------------------------------------------------------
--------------------------------

nsteps=input('How many loadcases (steps) for Abaqus?\n');
modelname=input('What is the model name? write as string\n');
logNi=linspace(0,7.6,nsteps+1)';

%-----------------------------------------------------------------
--------------------------------
% Importing data from input file
%-----------------------------------------------------------------
--------------------------------

for i=1:nsteps
    logN(i,1)=logNi(i)+(logNi(i+1)-logNi(i))/2;
end
logN
fprintf('---***Reading from input.txt***---')
fid=fopen('input2.txt','r');
count=1;
values=zeros(10,6);

fprintf('\n\n---Extracting all lines that are given a wave
direction of 9999999999---')
while 1
    skip=0;
    str=fgetl(fid);
    k=findstr(str,'9999999999');
    if str==-1
```

```
        break
    end
    if length(k)>0|k>0
            line=str2num(str);
            l=length(line);
            if l>1
                values(count,:)=line(:);
                count=count+1;
            end
    end
end
count;

fclose(fid);
fprintf('\n\n---All data have been extracted into the matrix
"values"---')

n=max(values(:,4))+1;
fprintf('\n\n---Number of steps found in data n=%0.0f---',n)

fprintf('\n\n---Averaging nodal stress- and fatigue results @
clock positions...---\n---...into matrices cl12, cl03, cl06
and cl09---\n')


logni=log10(values(:,6));
si=values(:,5);

%-----------------------------------------------------------------
--------------------------------
% Fitting the stress range exceedance diagrams for each node
with a linear
% polynomial, extracting stresses for cycles defined in the
n'-vector(logN)
% and averaging these stresses for each clock position
%-----------------------------------------------------------------
--------------------------------

%---------------------------------------
%cl12 average from node 809 and 7425,
%Exceedance stress range diagram plotted
%only as example for node 8, element 809
%---------------------------------------
cl12=zeros(nsteps,3);

I=find(values(:,1)==809);
pose=I(1);

for i=1:8
    fit1=polyfit(logni((pose+i*n-n):(pose-
1+n*i)),si((pose+i*n-n):(pose-1+n*i)),1);
```

```
    ffit1=@(x) fit1(1)*x+fit1(2);
    for j=1:nsteps
        Sr(j,1)=ffit1(logN(j));
        steps(j,1)=j;
    end
    cl12=cl12+[steps,Sr,logN];
    if i==8
        h=figure;
        hold on
        bar(logN,Sr,1,'y')
        plot(logni((pose+i*n-n):(pose-1+n*i)),si((pose+i*n-
n):(pose-1+n*i)),'r')
        plot(logN,Sr,'b')
        xlabel('stress range exceedances
[log(n'')]','FontWeight','bold')
        ylabel('S_r_,_i [Pa]','FontWeight','bold')
        legend('Fitted stress blocks','Provided stress
exceedances','Linear fit')
        saveas(h,'barplot','jpg')
        hold off
    end
end

I=find(values(:,1)==7425);
pose=I(1);

for i=1:8
    fit1=polyfit(logni((pose+i*n-n):(pose-
1+n*i)),si((pose+i*n-n):(pose-1+n*i)),1);
    ffit1=@(x) fit1(1)*x+fit1(2);
    for i=1:nsteps
        Sr(i,1)=ffit1(logN(i));
        steps(i,1)=i;
    end
    cl12=cl12+[steps,Sr,logN];
end

cl12=cl12./16;

%-----------------------------------
%cl03 average from node 7241 and 7486
%-----------------------------------
cl03=zeros(nsteps,3);

I=find(values(:,1)==7241);
pose=I(1);
for i=1:8
    fit1=polyfit(logni((pose+i*n-n):(pose-
1+n*i)),si((pose+i*n-n):(pose-1+n*i)),1);
    ffit1=@(x) fit1(1)*x+fit1(2);
    for i=1:nsteps
```

```
        Sr(i,1)=ffit1(logN(i));
        steps(i,1)=i;
    end
    cl03=cl03+[steps,Sr,logN];
end

I=find(values(:,1)==7486);
pose=I(1);
for i=1:8
    fit1=polyfit(logni((pose+i*n-n):(pose-
1+n*i)),si((pose+i*n-n):(pose-1+n*i)),1);
    ffit1=@(x) fit1(1)*x+fit1(2);
    for i=1:nsteps
        Sr(i,1)=ffit1(logN(i));
        steps(i,1)=i;
    end
    cl03=cl03+[steps,Sr,logN];
end

cl03=cl03./16;

%-----------------------------------
%cl06 average from node 546 and 7174
%-----------------------------------
cl06=zeros(nsteps,3);

I=find(values(:,1)==564);
pose=I(1);
for i=1:8
    fit1=polyfit(logni((pose+i*n-n):(pose-
1+n*i)),si((pose+i*n-n):(pose-1+n*i)),1);
    ffit1=@(x) fit1(1)*x+fit1(2);
    for i=1:nsteps
        Sr(i,1)=ffit1(logN(i));
        steps(i,1)=i;
    end
    cl06=cl06+[steps,Sr,logN];
end

I=find(values(:,1)==7174);
pose=I(1);
for i=1:8
    fit1=polyfit(logni((pose+i*n-n):(pose-
1+n*i)),si((pose+i*n-n):(pose-1+n*i)),1);
    ffit1=@(x) fit1(1)*x+fit1(2);
    for i=1:nsteps
        Sr(i,1)=ffit1(logN(i));
        steps(i,1)=i;
    end
    cl06=cl06+[steps,Sr,logN];
end
```

```
cl06=cl06./16;

%-----------------------------------
%cl09 average from node 748 and 497
%-----------------------------------
cl09=zeros(nsteps,3);

I=find(values(:,1)==748);
pose=I(1);
for i=1:8
    fit1=polyfit(logni((pose+i*n-n):(pose-
1+n*i)),si((pose+i*n-n):(pose-1+n*i)),1);
    ffit1=@(x) fit1(1)*x+fit1(2);
    for i=1:nsteps
        Sr(i,1)=ffit1(logN(i));
        steps(i,1)=i;
    end
    cl09=cl09+[steps,Sr,logN];
end

I=find(values(:,1)==497);
pose=I(1);
for i=1:8
    fit1=polyfit(logni((pose+i*n-n):(pose-
1+n*i)),si((pose+i*n-n):(pose-1+n*i)),1);
    ffit1=@(x) fit1(1)*x+fit1(2);
    for i=1:nsteps
        Sr(i,1)=ffit1(logN(i));
        steps(i,1)=i;
    end
    cl09=cl09+[steps,Sr,logN];
end

cl09=cl09./16;

%-----------------------------------------------------------------
---------------------------------
%Writing results to excel file: abainp.xls
%-----------------------------------------------------------------
---------------------------------
c={'Average stress provided from Stofat for four clock
positions'};
d={'Clock pose',' ','12:00','Clock pose',' ','03:00','Clock
pose',' ','06:00','Clock pose',' ','09:00'};
e={'Step','Sr','Log(N)','Step','Sr','Log(N)','Step','Sr','Log(
N)','Step','Sr','Log(N)','log(n_1)','log(n_2)'};
stepnum=(1:1:nsteps)';
n12=[logNi(1:nsteps),logNi(2:nsteps+1)];

xlswrite(sprintf('abainp%0.0f',nsteps),c,1,'A1')
```

```
xlswrite(sprintf('abainp%0.0f',nsteps),d,1,'A2')
xlswrite(sprintf('abainp%0.0f',nsteps),e,1,'A3')

xlswrite(sprintf('abainp%0.0f',nsteps),n12,sprintf('M4:N%0.0f'
,(nsteps+3')))

xlswrite(sprintf('abainp%0.0f',nsteps),cl12,sprintf('A4:C%0.0f
',(nsteps+3)))
xlswrite(sprintf('abainp%0.0f',nsteps),cl03,sprintf('D4:F%0.0f
',(nsteps+3)))
xlswrite(sprintf('abainp%0.0f',nsteps),cl06,sprintf('G4:I%0.0f
',(nsteps+3)))
xlswrite(sprintf('abainp%0.0f',nsteps),cl09,sprintf('J4:L%0.0f
',(nsteps+3)))



fprintf('\n---Input data for abaqus has been stored in
abainp%0.0f.xls---\n\n',nsteps)

%-----------------------------------------------------------------
---------------------------------
%Creating command inputs for Abaqus that imports Abaqus
modules, creates steps, creates load fields,
%creates loads for the steps and assigns the load fields to
the loads.
%-----------------------------------------------------------------
---------------------------------
fid = fopen(sprintf('abainp.txt%0.0f',nsteps),'w');
fprintf(fid,'---Script defining models and jobs for all %0.0f
steps---\r\n\r\n\r\n\r\n',n);


fprintf(fid,'from abaqus import *\r\nfrom abaqusConstants
import *\r\nimport part\r\nimport step\r\nimport
load\r\nimport visualization\r\nimport job\r\nimport
assembly\r\nimport section\r\n\r\n\r\n');

for i=1:nsteps
    %creating step
    if 1<i
        fprintf(fid,'mdb.models[''');
        fprintf(fid,modelname);
        fprintf(fid,'''].StaticStep(name=''Step-%0.0f'',
previous=''Step-%0.0f'')\r\n\r\n',i,i-1);
    end

    %-------------------------------------------------
    %Creating mapped analytical field for load case i
    %-------------------------------------------------
    fprintf(fid,'mdb.models[''');
```

```
    fprintf(fid,modelname);
    fprintf(fid,'''].MappedField(description='''',
fieldDataType=SCALAR,\r\n');
    fprintf(fid,'    localCsys=mdb.models[''');
    fprintf(fid,modelname);
    fprintf(fid,''''].rootAssembly.datums[182],
name=''fieldstep%0.0f'',\r\n',i) ;
    fprintf(fid,'    partLevelData=False, pointDataFormat=XYZ,
regionType=POINT, xyzPointData=((\r\n');
    fprintf(fid,'    0.0, 0.0, 1.014, %0.0f), (1.014, 0.0,
0.0, %0.0f), (0.0, 0.0, -1.014, %0.0f),
\r\n',cl12(i,2),cl03(i,2),cl06(i,2));
    fprintf(fid,'    (-1.014, 0.0, 0.0,
%0.0f)))\r\n\r\n',cl09(i,2));

    %---------------------------
    %Creating load for load case
    %---------------------------
    if 1<i
        fprintf(fid,'mdb.models[''');
        fprintf(fid,modelname) ;
        fprintf(fid,''''].Pressure(amplitude=UNSET,
createStepName=''Step-%0.0f''\r\n',i);
        fprintf(fid,', distributionType=FIELD,
field=''fieldstep%0.0f'', magnitude=-1.0, name=\r\n',i);
        fprintf(fid,'''pressure%0.0f'', region=\r\n',i);
        fprintf(fid,'mdb.models[''');
        fprintf(fid,modelname);
        fprintf(fid,''''].rootAssembly.surfaces[''Surf-
12'']\r\n\r\n');
    elseif 1==i
        fprintf(fid,'mdb.models[''');
        fprintf(fid,modelname);

fprintf(fid,''''].loads[''pressure1''].setValues(\r\n');
        fprintf(fid,'    distributionType=FIELD,
field=''fieldstep%0.0f'', magnitude=-1.0)\r\n\r\n',i);
    end

    %-----------------------------------
    %Deactivating loads not used in step
    %-----------------------------------
    if i>1
        for k=1:i-1
            fprintf(fid,'mdb.models[''');
            fprintf(fid,modelname);

fprintf(fid,''''].loads[''pressure%0.0f''].deactivate(''Step-
%0.0f'')\r\n',k,i);
        end
    end
```

```
    fprintf(fid,'\r\n\r\n\r\n');
end
fclose(fid);

%-----------------------------------------------------------------
----
%Ploting stress range exceedances diagrams for all clock
positions
%-----------------------------------------------------------------
----
fprintf('---***Input commands for Abaqus created in
abainp%0.0f.txt***--- \n\n',nsteps)
figure
hold on
plot(cl03(:,2)',cl03(:,3)')
plot(cl06(:,2)',cl06(:,3)')
plot(cl09(:,2)',cl09(:,3)')
plot(cl12(:,2)',cl12(:,3)')

for i=1:nsteps
    ntest(i,1)=log10(10^logNi(1+i)-10^logNi(i));
end
```

D. Abaqus input commands

Abaqus input commands created from the matlab script. Creates analytical fields for all stress ranges and assigns these fields to the steps needed. Only the second and third stress ranges are included below, that is *Step2* and *Step3*, all other steps are made correspondingly. The first step, *Step1* and the corresponding unit load, *pressure1*, is defined prior to inserting the input commands.

---Script defining models and jobs for all 62 steps---

```
from abaqus import *
from abaqusConstants import *
import part
import step
import load
import visualization
import job
import assembly
import section

mdb.models['Model_Finalonly'].MappedField(description='', fieldDataType=SCALAR,
    localCsys=mdb.models['Model_Finalonly'].rootAssembly.datums[290], name='fieldstep1',
    partLevelData=False, pointDataFormat=XYZ, regionType=POINT, xyzPointData=((
    0.0, 0.0, 1.014, 200389199), (1.014, 0.0, 0.0, 209357179), (0.0, 0.0, -1.014, 202535882),
    (-1.014, 0.0, 0.0, 208039966)))

mdb.models['Model_Finalonly'].loads['pressure1'].setValues(
    distributionType=FIELD, field='fieldstep1', magnitude=-1.0)
```

```
mdb.models['Model_Finalonly'].StaticStep(name='Step-2', previous='Step-1')

mdb.models['Model_Finalonly'].MappedField(description='', fieldDataType=SCALAR,
    localCsys=mdb.models['Model_Finalonly'].rootAssembly.datums[290], name='fieldstep2',
    partLevelData=False, pointDataFormat=XYZ, regionType=POINT, xyzPointData=((
    0.0, 0.0, 1.014, 179554919), (1.014, 0.0, 0.0, 187563398), (0.0, 0.0, -1.014, 181384598),
    (-1.014, 0.0, 0.0, 186383513)))

mdb.models['Model_Finalonly'].Pressure(amplitude=UNSET, createStepName='Step-2'
, distributionType=FIELD, field='fieldstep2', magnitude=-1.0, name=
'pressure2', region=
mdb.models['Model_Finalonly'].rootAssembly.surfaces['Surf-12'])

mdb.models['Model_Finalonly'].loads['pressure1'].deactivate('Step-2')



mdb.models['Model_Finalonly'].StaticStep(name='Step-3', previous='Step-2')
…
```

E. Stress output from Abaqus

Stress output from Abaqus, containing the highest and lowest stresses along each path. Complete output data are given for the first and last step only. For further scripting purposes, the row containing the lowest stresses is given the name “1111111” and the row containing the highest stresses is given the name “9999999”.

	X	Step1-1	Step1-2	Step1-3	Step1-4	Step1-5	Step1-6	Step1-7	Step1-8
1111111	0.	163.384E+06	163.155E+06	163.912E+06	162.834E+06	505.301E+06	208.344E+06	140.74E+06	140.74E+06
AT X =		0.	0.	0.	0.	9.16966E-03	499.842E-03	184.578E-03	0.
9999999	515.65E-03	299.28E+06	299.185E+06	300.21E+06	298.618E+06	985.133E+06	516.314E+06	1.44753E+09	354.948E+06
AT X =		28.0097E-03	28.0093E-03	28.0097E-03	28.0093E-03	0.	515.65E-03	45.2583E-03	8.16591E-03

...

Step15-1	Step15-2	Step15-3	Step15-4	Step15-5	Step15-6	Step15-7	Step15-8
7.38664E+06	7.25608E+06	7.20433E+06	7.24194E+06	22.8214E+06	9.40417E+06	6.33136E+06	6.33136E+06
0.	0.	0.	0.	9.16966E-03	499.842E-03	184.578E-03	0.
13.5185E+06	13.3104E+06	13.1975E+06	13.2857E+06	44.4975E+06	23.3148E+06	65.2798E+06	16.0677E+06
28.0097E-03	28.0093E-03	28.0097E-03	28.0093E-03	0.	515.65E-03	45.2583E-03	8.16591E-03

The paths above are recognized as the following

Stepx-1 $S_{r,i=x}$, Hot spot toe a @ 12o’clock
Stepx-2 $S_{r,i=x}$, Hot spot toe a @ 03o’clock
Stepx-3 $S_{r,i=x}$, Hot spot toe a @ 06o’clock
Stepx-4 $S_{r,i=x}$, Hot spot toe a @ 09o’clock
Stepx-5 $S_{r,i=x}$, Root path a @ 12o’clock
Stepx-6 $S_{r,i=x}$, Root path b @ 12o’clock
Stepx-7 $S_{r,i=x}$, Root path c @ 12o’clock
Stepx-8 $S_{r,i=x}$, Root path d @ 12o’clock

F. Script sorting stress results from Abaqus

Script sorting all maximum stresses from the Abaqus output file, according to stress range, that is step number.

```
clear all
clc

%-------------------------------------------------------
% This script is made for sorting all maximum stresses
% from the Abaqus XY data report file.
% Stresses are sorted according to stress range, that is
% step number, and which path they are taken from
%
%  Input:    String containing output file's name.
%            Number of loadcases used in the analysis.
%
%  Output    Excel sheet containing stresses obtained from
%            Abaqus
%-------------------------------------------------------


fprintf('---***Opening ''abaout.rpy'', which is a Abaqus
Column min/max output data file***---\n\n\n')
fprintf('---Prior to reading file, the following words in
abaout.txt is to be replaced---\n')
fprintf('---"MAXIMUM" to be replaced with 9999999\n\n')

abaout=input('What is the name of the output file? \nInsert as
string including file extension.\n');
fid=fopen(abaout,'r');
nsteps=input('How many loadcases (steps) is used in
Abaqus?\n\n');

%-----------------------------
%The following paths are used:
%-----------------------------
stepx1='hotsp_cl12';
stepx2='hotsp_cl03';
stepx3='hotsp_cl06';
stepx4='hotsp_cl09';
stepx5='path a';
stepx6='path b';
stepx7='path c';
stepx8='path d';

fprintf('---Extracting all lines that are given a wave
direction of 9999999---\n\n')
while 1
    skip=0;
    str=fgetl(fid);
    %j=findstr(str,'1111111');
```

```
    k=findstr(str,'9999999');
    %if j>1
    %    minmax(1,:)=str2num(str);
    %end
    if k>1
        minmax(2,:)=str2num(str);
    end
    if str<0
        break
    end
end
fclose(fid);


minmax=minmax(1:2,3:length(minmax'));

%-----------------------------------------
%Sorting data according to points of stress
%extraction paths, including only maximum stress values
%-----------------------------------------
npaths=length(minmax')/nsteps;
for i=1:nsteps
    allstep(i,1:npaths)=minmax(2,npaths*(i-1)+1:i*npaths);
end

%-----------------------------------------------
%Writing results & hot spot stress to abaout.xls
%-----------------------------------------------
c={'Maximum stress read from hot spot and root paths'};
d={'step
#',stepx1,stepx2,stepx3,stepx4,stepx5,stepx6,stepx7,stepx8};
stepnum=(1:1:nsteps)';
excelout=sprintf('abaout%0.0f',nsteps);

xlswrite(excelout,c,1,'F1')
xlswrite(excelout,d,1,'A2')
xlswrite(excelout,stepnum,1,sprintf('A3:A%0.0f',length(allstep
')+2))
xlswrite(excelout,allstep,sprintf('B3:I%0.0f',length(allstep')
+2))

fprintf('\n-------****************************************-------
--\n---***** All Abaqus results have been sorted *****---\n---
*** Results have been written to abaout.xls ***---\n------
****************************************------\n\n\n')
```

G. Extracted stresses from validation model FEA

combined root1elec4 & toe2elec5			
Distance z [m]	Max princ root [Mpa]	Distance z [m]	Max princ toe [Mpa]
0.0000	4.747E+08	0.0000	3.443E+08
0.0004	5.696E+08	0.0004	3.979E+08
0.0009	6.029E+08	0.0009	4.202E+08
0.0014	6.102E+08	0.0014	4.315E+08
0.0020	6.083E+08	0.0020	4.395E+08
0.0027	6.026E+08	0.0027	4.457E+08
0.0036	5.954E+08	0.0036	4.508E+08
0.0045	5.877E+08	0.0045	4.551E+08
0.0056	5.804E+08	0.0056	4.588E+08
0.0069	5.737E+08	0.0069	4.619E+08
0.0084	5.680E+08	0.0084	4.646E+08
0.0101	5.633E+08	0.0101	4.669E+08
0.0120	5.597E+08	0.0120	4.686E+08
0.0143	5.570E+08	0.0143	4.698E+08
0.0170	5.554E+08	0.0170	4.706E+08
0.0200	5.548E+08	0.0400	3.441E+08
0.0230	5.554E+08		Max stress included (Manually veryfied)
0.0257	5.570E+08		
0.0280	5.597E+08		
0.0299	5.633E+08		
0.0316	5.680E+08		
0.0331	5.737E+08		
0.0344	5.804E+08		
0.0355	5.877E+08		
0.0364	5.954E+08		
0.0373	6.026E+08		
0.0380	6.083E+08		
0.0386	6.102E+08		
0.0391	6.029E+08		
0.0396	5.696E+08		
0.0400	4.747E+08		
Max stress [Mpa]	610.215		470.574
Diff Target-obtained [Mpa]	-14.785		68.794
Difference [%]	-2.366		17.122
Number of elements	50907.000		50907.000

G. Extracted stresses from validation model FEA

root3elec4		root2elec4		BADCIRC root1elec4	
Distance z [m]	Max princ [Mpa]	Distance z [m]	ax princ root [Mpa]	Distance z [m]	Max princ root [Mpa]
0.0000	4.753E+08	0.0000	5.22E+08	0.0000	4.81E+08
0.0002	5.384E+08	0.0002	5.90E+08	0.0002	5.45E+08
0.0005	5.802E+08	0.0005	6.36E+08	0.0005	5.87E+08
0.0009	6.022E+08	0.0009	6.60E+08	0.0009	6.09E+08
0.0014	6.091E+08	0.0014	6.68E+08	0.0014	6.17E+08
0.0022	6.061E+08	0.0022	6.65E+08	0.0022	6.13E+08
0.0033	5.971E+08	0.0033	6.56E+08	0.0033	6.04E+08
0.0048	5.855E+08	0.0048	6.43E+08	0.0048	5.91E+08
0.0069	5.740E+08	0.0069	6.31E+08	0.0069	5.79E+08
0.0099	5.648E+08	0.0099	6.21E+08	0.0099	5.68E+08
0.0141	5.589E+08	0.0141	6.15E+08	0.0141	5.61E+08
0.0200	5.566E+08	0.0200	6.13E+08	0.0200	5.58E+08
0.0259	5.589E+08	0.0259	6.15E+08	0.0259	5.61E+08
0.0301	5.648E+08	0.0301	6.21E+08	0.0301	5.68E+08
0.0331	5.740E+08	0.0331	6.31E+08	0.0331	5.79E+08
0.0352	5.855E+08	0.0352	6.43E+08	0.0352	5.91E+08
0.0367	5.971E+08	0.0367	6.56E+08	0.0367	6.04E+08
0.0378	6.061E+08	0.0378	6.65E+08	0.0378	6.13E+08
0.0386	6.091E+08	0.0386	6.68E+08	0.0386	6.17E+08
0.0391	6.022E+08	0.0391	6.60E+08	0.0391	6.09E+08
0.0395	5.802E+08	0.0395	6.36E+08	0.0395	5.87E+08
0.0398	5.384E+08	0.0398	5.90E+08	0.0398	5.45E+08
0.0400	4.753E+08	0.0400	5.22E+08	0.0400	4.81E+08
Max stress [Mpa]	609.15		668.36		616.55
Diff Target-obtained [Mpa]	-15.85		43.36		-8.46
Difference [%]	-2.54		6.94		-1.35
Number of elements	21228.00		11108.00		35610.00

root1elec2		root1elec4		root1elec8	
Distance z [m]	Max princ root [Mpa]	Distance z [m]	Max princ root [Mpa]	Distance z [m]	Max princ root [Mpa]
0.0000	4.98E+08	0.0000	4.86E+08	0.0000	4.75E+08
0.0002	5.60E+08	0.0002	5.51E+08	0.0002	5.44E+08
0.0005	5.99E+08	0.0005	5.94E+08	0.0005	5.89E+08
0.0009	6.21E+08	0.0009	6.17E+08	0.0009	6.13E+08
0.0014	6.29E+08	0.0014	6.24E+08	0.0014	6.20E+08
0.0022	6.25E+08	0.0022	6.20E+08	0.0022	6.17E+08
0.0033	6.16E+08	0.0033	6.11E+08	0.0033	6.07E+08
0.0048	6.03E+08	0.0048	5.98E+08	0.0048	5.94E+08
0.0069	5.91E+08	0.0069	5.85E+08	0.0069	5.82E+08
0.0099	5.80E+08	0.0099	5.74E+08	0.0099	5.71E+08
0.0141	5.73E+08	0.0141	5.67E+08	0.0141	5.64E+08
0.0200	5.71E+08	0.0200	5.65E+08	0.0200	5.61E+08
0.0259	5.73E+08	0.0259	5.67E+08	0.0259	5.64E+08
0.0301	5.80E+08	0.0301	5.74E+08	0.0301	5.71E+08
0.0331	5.91E+08	0.0331	5.85E+08	0.0331	5.82E+08
0.0352	6.03E+08	0.0352	5.98E+08	0.0352	5.94E+08
0.0367	6.16E+08	0.0367	6.11E+08	0.0367	6.07E+08
0.0378	6.25E+08	0.0378	6.20E+08	0.0378	6.17E+08
0.0386	6.28E+08	0.0386	6.24E+08	0.0386	6.20E+08
0.0391	6.21E+08	0.0391	6.17E+08	0.0391	6.13E+08
0.0395	5.99E+08	0.0395	5.94E+08	0.0395	5.89E+08
0.0398	5.60E+08	0.0398	5.51E+08	0.0398	5.44E+08
0.0400	4.98E+08	0.0400	4.86E+08	0.0400	4.75E+08
Max stress [Mpa]	628.50		623.72		620.00
Diff Target-obtained [Mpa]	3.50		-1.28		-5.00
Difference [%]	0.56		-0.21		-0.80
Number of elements	32280.00		33570.00		41070.00

G. Extracted stresses from validation model FEA

toe1elec4	
Distance z [m]	max princ toe
0.0000	2.392E+08
0.0027	2.769E+08
0.0054	2.783E+08
0.0078	2.784E+08
0.0102	2.781E+08
0.0125	2.776E+08
0.0146	2.771E+08
0.0167	2.768E+08
0.0186	2.766E+08
0.0205	2.765E+08
0.0222	2.766E+08
0.0239	2.768E+08
0.0255	2.771E+08
0.0271	2.774E+08
0.0285	2.777E+08
0.0299	2.780E+08
0.0313	2.782E+08
0.0325	2.781E+08
0.0337	2.778E+08
0.0349	2.771E+08
0.0360	2.758E+08
0.0371	2.736E+08
0.0381	2.698E+08
0.0391	2.642E+08
0.0400	2.264E+08
Max stress [Mpa]	278.434
Diff Target-obtained [Mpa]	-38.566
Difference [%]	-12.166
Number of elements	21228.000

toe2elec2		toe2elec5		toe2elec10	
distance z	max princ toe	distance z	max princ toe	distance z	max princ toe
0.0000	2.511E+08	0.0000	2.572E+08	0.0000	Manually extracted
0.0030	2.921E+08	0.0030	3.017E+08	0.0030	
0.0056	2.953E+08	0.0056	3.095E+08	0.0056	
0.0079	2.965E+08	0.0079	3.122E+08	0.0079	
0.0098	2.963E+08	0.0098	3.135E+08	0.0098	
0.0115	2.960E+08	0.0115	3.142E+08	0.0115	
0.0130	2.956E+08	0.0130	3.147E+08	0.0130	
0.0143	2.953E+08	0.0143	3.150E+08	0.0143	
0.0154	2.951E+08	0.0154	3.152E+08	0.0154	
0.0164	2.950E+08	0.0164	3.153E+08	0.0164	
0.0172	2.949E+08	0.0172	3.154E+08	0.0172	
0.0179	2.948E+08	0.0179	3.154E+08	0.0179	
0.0186	2.948E+08	0.0186	3.154E+08	0.0186	
0.0191	2.947E+08	0.0191	3.155E+08	0.0191	
0.0196	2.947E+08	0.0196	3.155E+08	0.0196	
0.0200	2.947E+08	0.0200	3.155E+08	0.0200	
0.0204	2.947E+08	0.0204	3.155E+08	0.0204	
0.0209	2.947E+08	0.0209	3.155E+08	0.0209	
0.0214	2.948E+08	0.0214	3.154E+08	0.0214	
0.0221	2.948E+08	0.0221	3.154E+08	0.0221	
0.0228	2.949E+08	0.0228	3.154E+08	0.0228	
0.0236	2.950E+08	0.0236	3.153E+08	0.0236	
0.0246	2.951E+08	0.0246	3.152E+08	0.0246	
0.0257	2.953E+08	0.0257	3.150E+08	0.0257	
0.0270	2.956E+08	0.0270	3.147E+08	0.0270	
0.0285	2.960E+08	0.0285	3.143E+08	0.0285	
0.0302	2.963E+08	0.0302	3.135E+08	0.0302	
0.0321	2.965E+08	0.0321	3.122E+08	0.0321	
0.0344	2.953E+08	0.0344	3.095E+08	0.0344	
0.0370	2.921E+08	0.0370	3.017E+08	0.0370	
0.0400	2.511E+08	0.0400	2.573E+08	0.0400	
Max stress [Mpa]	296.47		315.46		315.50
Diff Target-obtained [Mpa]	-20.53		-1.54		-1.50
Difference [%]	-6.476656151		-0.485488959		-0.47318612
Number of elements	11108		11108		11108

H. Miner summation for 15 stress blocks

Weld toe

	Maximum stress read from hot spot				Effective hot spot stress			
step #	hotsp_cl12	hotsp_cl03	hotsp_cl06	hotsp_cl09	hotsp_cl12	hotsp_cl03	hotsp_cl06	hotsp_cl09
1	2.99E+08	2.99E+08	3.00E+08	2.99E+08	3.35E+08	3.35E+08	3.36E+08	3.34E+08
2	2.79E+08	2.79E+08	2.80E+08	2.78E+08	3.12E+08	3.12E+08	3.13E+08	3.12E+08
3	2.58E+08	2.58E+08	2.59E+08	2.58E+08	2.89E+08	2.89E+08	2.90E+08	2.89E+08
4	2.38E+08	2.38E+08	2.39E+08	2.37E+08	2.67E+08	2.66E+08	2.67E+08	2.66E+08
5	2.18E+08	2.18E+08	2.18E+08	2.17E+08	2.44E+08	2.44E+08	2.44E+08	2.43E+08
6	1.97E+08	1.97E+08	1.98E+08	1.97E+08	2.21E+08	2.21E+08	2.21E+08	2.20E+08
7	1.77E+08	1.77E+08	1.77E+08	1.76E+08	1.98E+08	1.98E+08	1.98E+08	1.97E+08
8	1.56E+08	1.56E+08	1.57E+08	1.56E+08	1.75E+08	1.75E+08	1.76E+08	1.75E+08
9	1.36E+08	1.36E+08	1.36E+08	1.36E+08	1.52E+08	1.52E+08	1.53E+08	1.52E+08
10	1.16E+08	1.15E+08	1.16E+08	1.15E+08	1.29E+08	1.29E+08	1.30E+08	1.29E+08
11	9.52E+07	9.50E+07	9.52E+07	9.48E+07	1.07E+08	1.06E+08	1.07E+08	1.06E+08
12	7.48E+07	7.46E+07	7.47E+07	7.44E+07	8.37E+07	8.35E+07	8.37E+07	8.34E+07
13	5.43E+07	5.41E+07	5.42E+07	5.40E+07	6.09E+07	6.06E+07	6.07E+07	6.05E+07
14	3.39E+07	3.37E+07	3.37E+07	3.37E+07	3.80E+07	3.78E+07	3.77E+07	3.77E+07
15	1.35E+07	1.33E+07	1.32E+07	1.33E+07	1.51E+07	1.49E+07	1.48E+07	1.49E+07

Ni (found from Effective HS stress and D curve)				Defining stress block cycles			ni [Cycles]	Miner sum			
hotsp_cl12	hotsp_cl03	hotsp_cl06	hotsp_cl09	log(n1)	log(n2)	log(n2-n1)	All positions	Di cl12	Di cl03	Di cl06	Di cl09
3.62E+04	3.62E+04	3.59E+04	3.64E+04	0.00	0.51	0.34	2.21E+00	0.00	0.00	0.00	0.00
4.47E+04	4.48E+04	4.43E+04	4.50E+04	0.51	1.01	0.85	7.10E+00	0.00	0.00	0.00	0.00
5.62E+04	5.63E+04	5.57E+04	5.66E+04	1.01	1.52	1.36	2.28E+01	0.00	0.00	0.00	0.00
7.19E+04	7.20E+04	7.13E+04	7.24E+04	1.52	2.03	1.86	7.32E+01	0.00	0.00	0.00	0.00
9.41E+04	9.43E+04	9.34E+04	9.48E+04	2.03	2.53	2.37	2.35E+02	0.00	0.00	0.00	0.00
1.26E+05	1.27E+05	1.26E+05	1.27E+05	2.53	3.04	2.88	7.55E+02	0.01	0.01	0.01	0.01
1.76E+05	1.76E+05	1.74E+05	1.77E+05	3.04	3.55	3.38	2.42E+03	0.01	0.01	0.01	0.01
2.54E+05	2.54E+05	2.52E+05	2.56E+05	3.55	4.05	3.89	7.79E+03	0.03	0.03	0.03	0.03
3.86E+05	3.87E+05	3.84E+05	3.89E+05	4.05	4.56	4.40	2.50E+04	0.06	0.06	0.07	0.06
6.28E+05	6.31E+05	6.26E+05	6.35E+05	4.56	5.07	4.90	8.03E+04	0.13	0.13	0.13	0.13
1.13E+06	1.13E+06	1.12E+06	1.14E+06	5.07	5.57	5.41	2.58E+05	0.23	0.23	0.23	0.23
2.32E+06	2.34E+06	2.33E+06	2.35E+06	5.57	6.08	5.92	8.28E+05	0.36	0.35	0.36	0.35
6.05E+06	6.11E+06	6.09E+06	6.14E+06	6.08	6.59	6.42	2.66E+06	0.44	0.44	0.44	0.43
4.55E+07	4.68E+07	4.71E+07	4.73E+07	6.59	7.09	6.93	8.54E+06	0.19	0.18	0.18	0.18
4.53E+09	4.89E+09	5.11E+09	4.94E+09	7.09	7.60	7.44	2.74E+07	0.01	0.01	0.01	0.01
						D		1.47	1.45	1.46	1.44
						Fatigue life [years]		13.64	13.785	13.73	13.87

Weld root 12o'clock

	Max princ. stress - root [Pa]		Corrected notch stress [Pa]	
step #	Path a	Path c	Path a	Path c
1	9.85E+08	1.45E+09	1.13E+09	1.66E+09
2	9.18E+08	1.35E+09	1.05E+09	1.55E+09
3	8.51E+08	1.25E+09	9.78E+08	1.44E+09
4	7.84E+08	1.15E+09	9.01E+08	1.32E+09
5	7.16E+08	1.05E+09	8.23E+08	1.21E+09
6	6.49E+08	9.54E+08	7.46E+08	1.10E+09
7	5.82E+08	8.55E+08	6.69E+08	9.83E+08
8	5.15E+08	7.56E+08	5.92E+08	8.69E+08
9	4.48E+08	6.58E+08	5.14E+08	7.56E+08
10	3.80E+08	5.59E+08	4.37E+08	6.42E+08
11	3.13E+08	4.60E+08	3.60E+08	5.29E+08
12	2.46E+08	3.61E+08	2.83E+08	4.15E+08
13	1.79E+08	2.63E+08	2.06E+08	3.02E+08
14	1.12E+08	1.64E+08	1.28E+08	1.88E+08
15	4.45E+07	6.53E+07	5.11E+07	7.50E+07

Ni Root fatigue [cycles]		Defining stress block cycles			n_i [Cycles]	Miner sum	
Path a	Path c	log(n1)	log(n2)	log(n2-n1)	All positions	Di path a	Di path c
1.57E+04	4.95E+03	0.00	0.51	0.34	2.21E+00	0.00	0.00
1.94E+04	6.12E+03	0.51	1.01	0.85	7.10E+00	0.00	0.00
2.44E+04	7.69E+03	1.01	1.52	1.36	2.28E+01	0.00	0.00
3.12E+04	9.84E+03	1.52	2.03	1.86	7.32E+01	0.00	0.01
4.09E+04	1.29E+04	2.03	2.53	2.37	2.35E+02	0.01	0.02
5.49E+04	1.73E+04	2.53	3.04	2.88	7.55E+02	0.01	0.04
7.62E+04	2.40E+04	3.04	3.55	3.38	2.42E+03	0.03	0.10
1.10E+05	3.47E+04	3.55	4.05	3.89	7.79E+03	0.07	0.22
1.68E+05	5.28E+04	4.05	4.56	4.40	2.50E+04	0.15	0.47
2.73E+05	8.60E+04	4.56	5.07	4.90	8.03E+04	0.29	0.93
4.89E+05	1.54E+05	5.07	5.57	5.41	2.58E+05	0.53	1.67
1.01E+06	3.18E+05	5.57	6.08	5.92	8.28E+05	0.82	2.60
2.63E+06	8.28E+05	6.08	6.59	6.42	2.66E+06	1.01	3.21
1.87E+11	3.41E+06	6.59	7.09	6.93	8.54E+06	0.00	2.51
2.95E+12	9.34E+11	7.09	7.60	7.44	2.74E+07	0.00	0.00
				D		2.93	11.80
				Fatigue life [years]		6.82	1.70

I. Drawings for the fillet welded knee plate

Inspection position 2 being the knee plate weld toe.

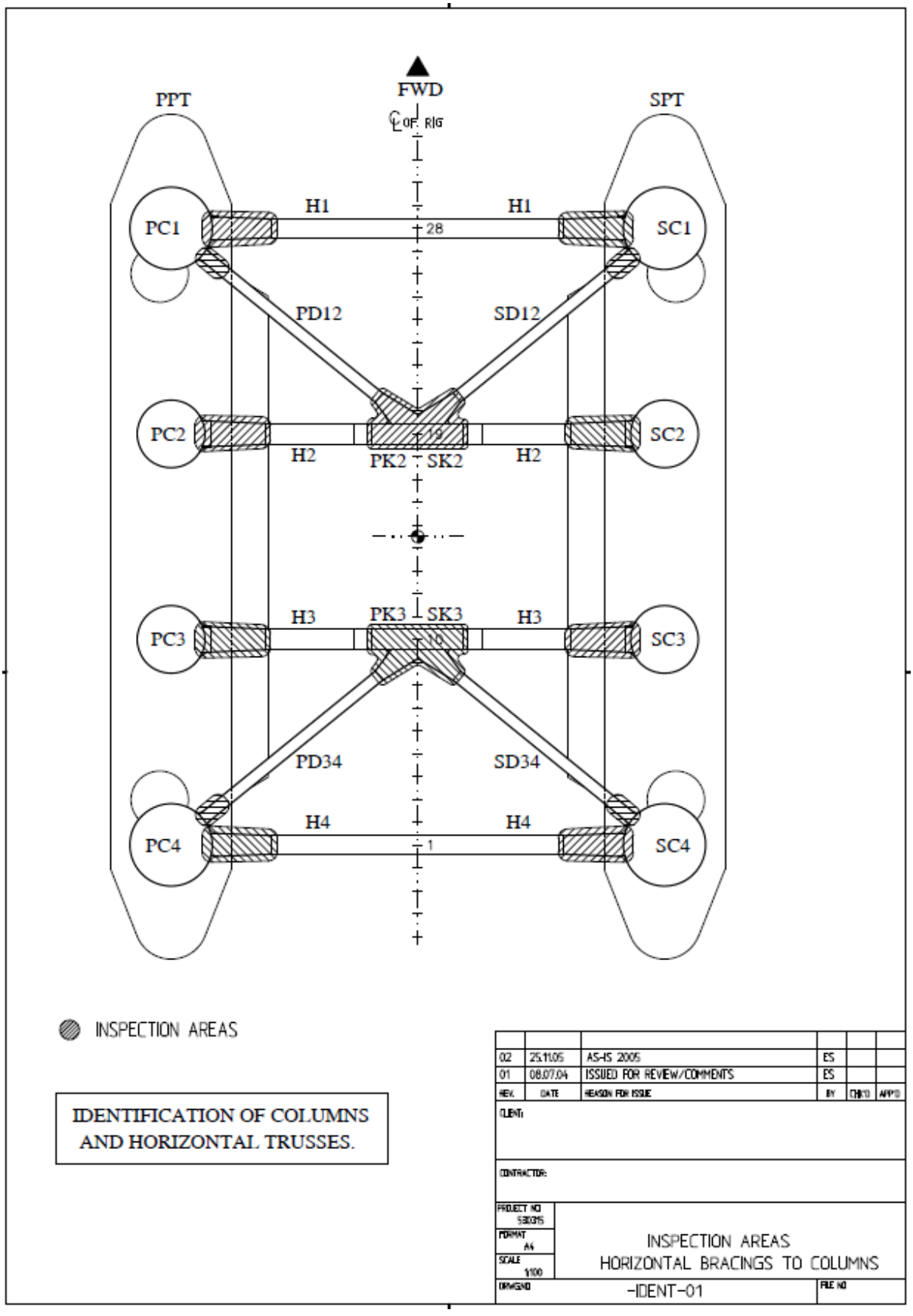

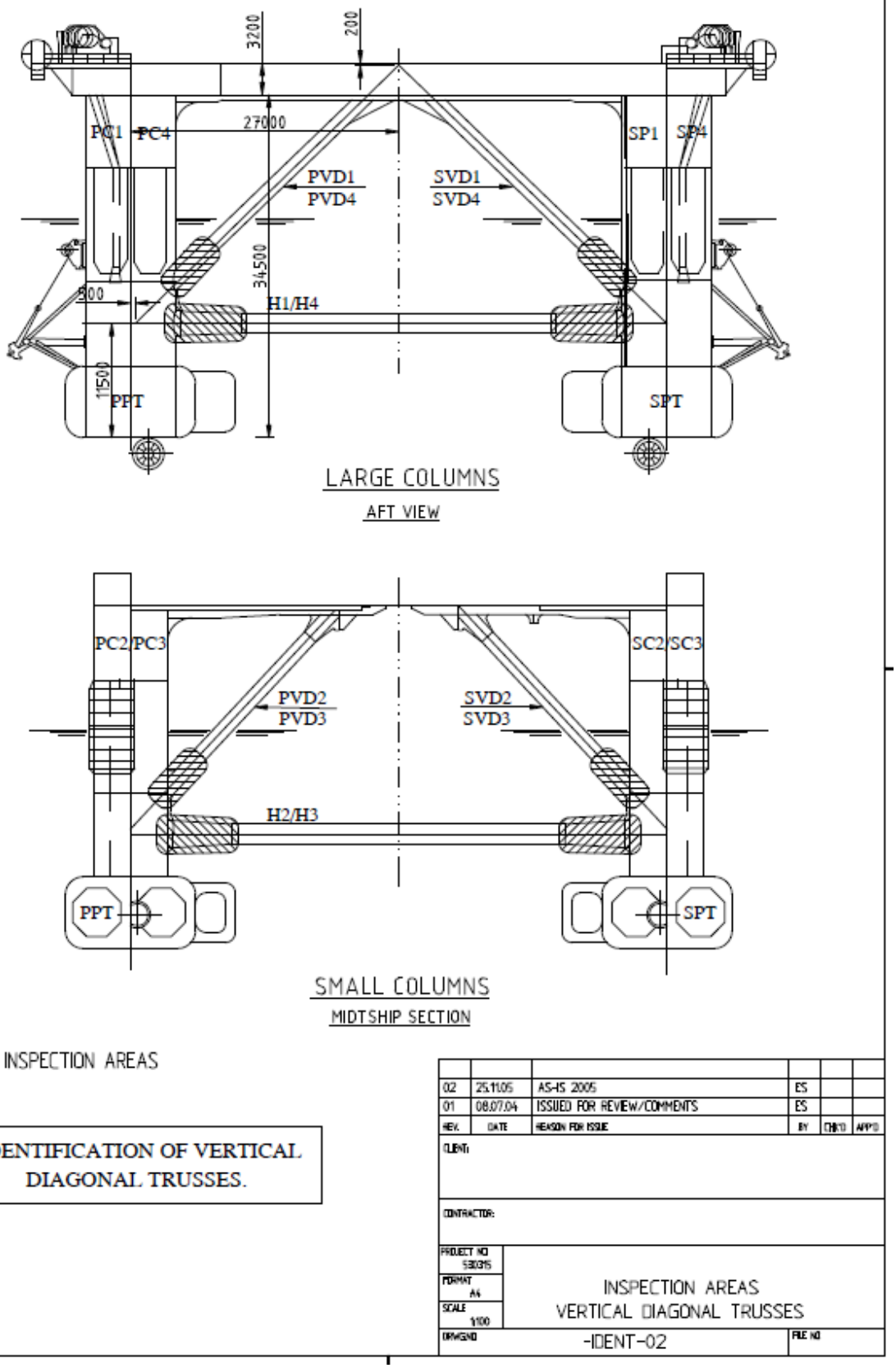
3200
200
27000
PC1
PC4
SP1
SP4
PVD1
PVD4
SVD1
SVD4
34500
H1/H4
1500
PPT
SPT
LARGE COLUMNS
AFT VIEW
PC2/PC3
SC2/SC3
PVD2
PVD3
SVD2
SVD3
H2/H3
PPT
SPT
SMALL COLUMNS
MIDTSHIP SECTION
INSPECTION AREAS
IDENTIFICATION OF VERTICAL DIAGONAL TRUSSES.
02 25.11.05 AS-IS 2005 ES
01 08.07.04 ISSUED FOR REVIEW/COMMENTS ES
REV. DATE REASON FOR ISSUE BY CHK'D APP'D
CLIENT:
CONTRACTOR:
PROJECT NO 530315
FORMAT A4
SCALE 1:100
INSPECTION AREAS
VERTICAL DIAGONAL TRUSSES
DRWGNO -IDENT-02
FILE NO

I. Drawings for the fillet welded knee plate

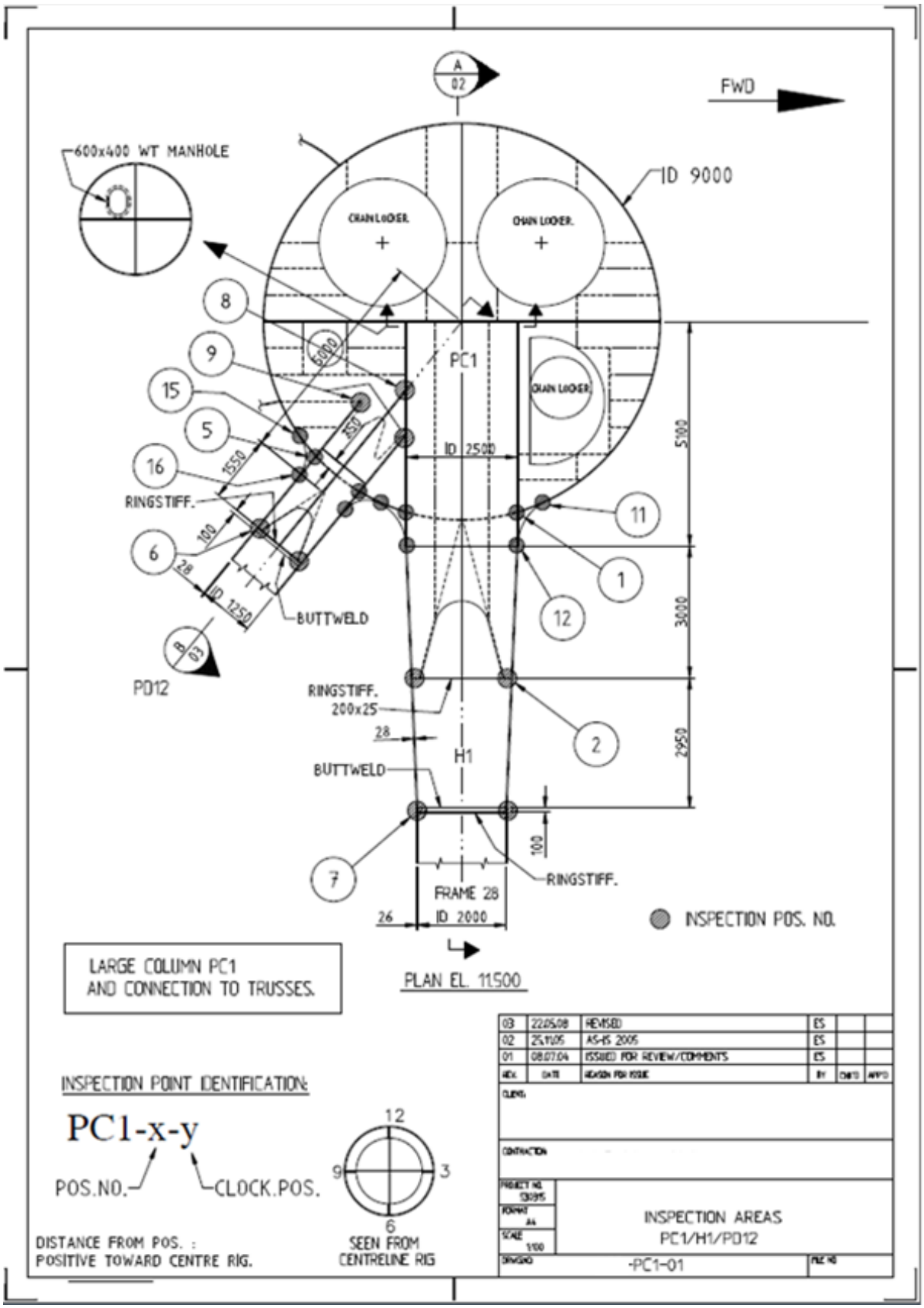

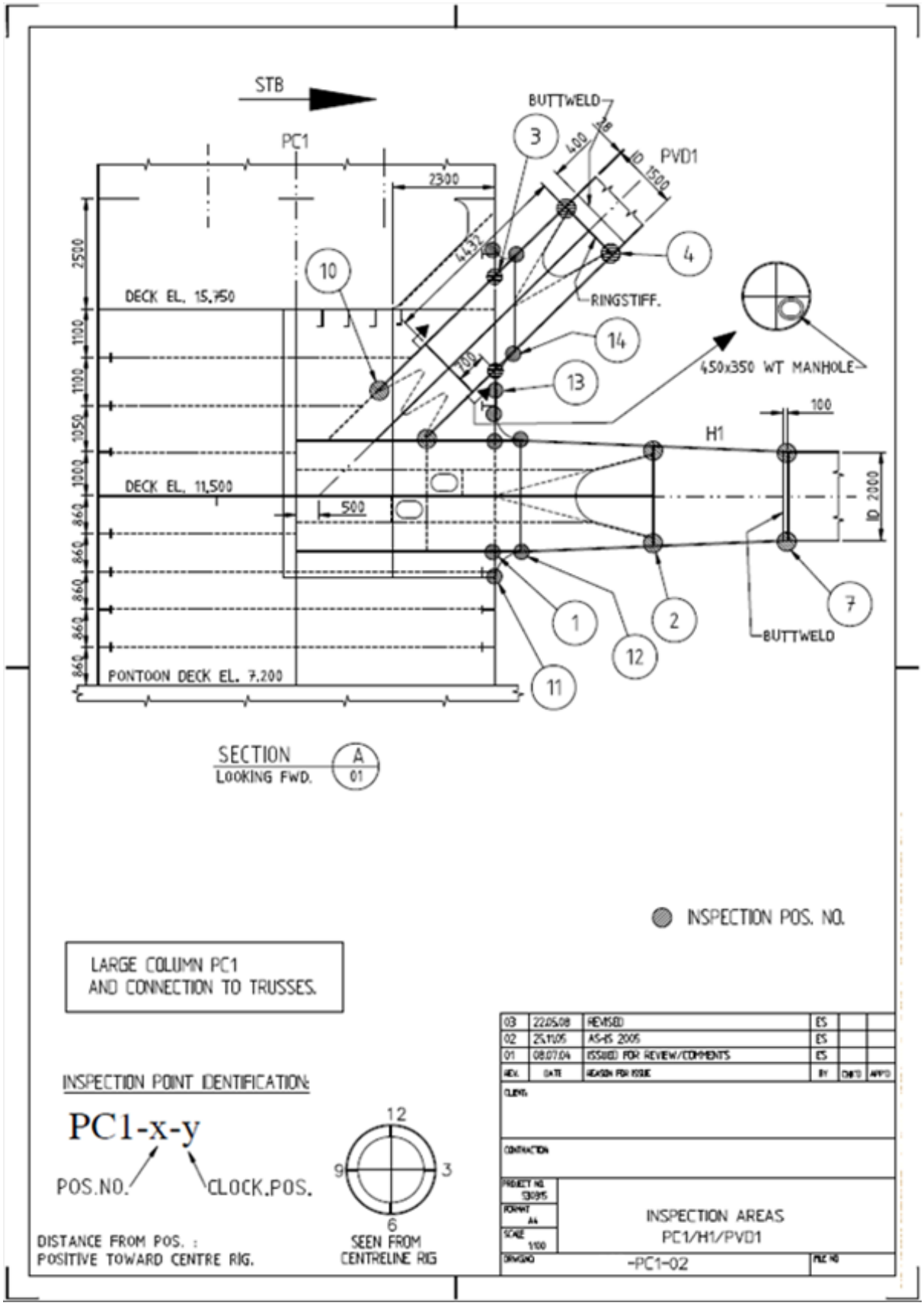
STB
PC1
BUTTWELD
3
400
PVD1
ID 1500
2300
2500
4
10
DECK EL. 15.750
RINGSTIFF.
14
13
450x350 WT MANHOLE
1100
1100
1050
1300
H1
100
DECK EL. 11,500
500
ID 2000
860
860
860
860
860
1
2
12
7
BUTTWELD
PONTOON DECK EL. 7.200
11
SECTION A
LOOKING FWD. 01
INSPECTION POS. NO.
LARGE COLUMN PC1
AND CONNECTION TO TRUSSES.
INSPECTION POINT IDENTIFICATION:
PC1-x-y
POS.NO.
CLOCK.POS.
12
9
3
6
SEEN FROM
CENTRELINE RIG
DISTANCE FROM POS. :
POSITIVE TOWARD CENTRE RIG.
03 22.05.08 REVISED ES
02 25.11.05 AS-IS 2005 ES
01 08.07.04 ISSUED FOR REVIEW/COMMENTS ES
CLIENT:
CONTRACTOR:
PROJECT NO. 53095
FORMAT A4
SCALE 1:100
INSPECTION AREAS
PC1/H1/PVD1
DRAWING -PC1-02

I. Drawings for the fillet welded knee plate

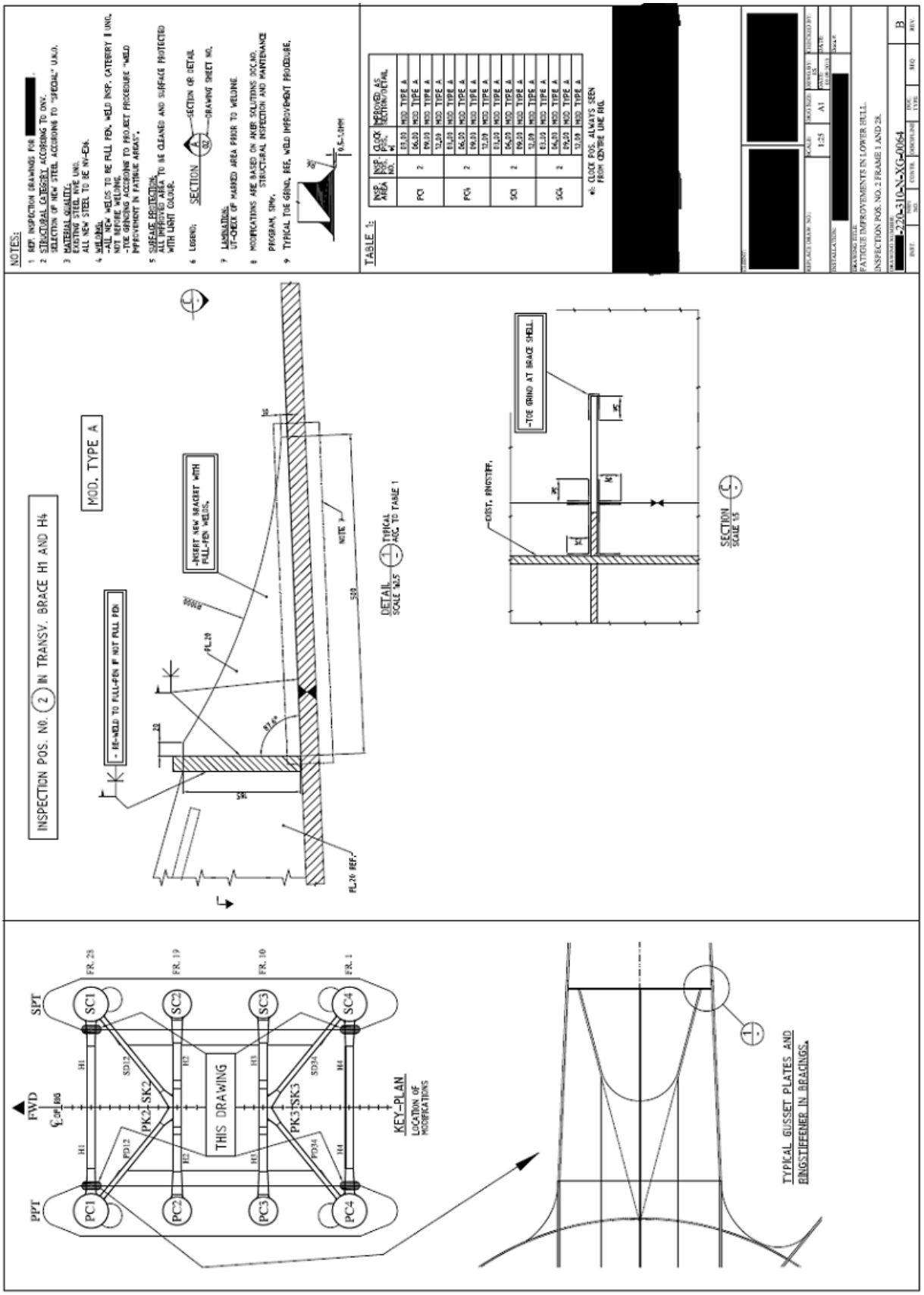

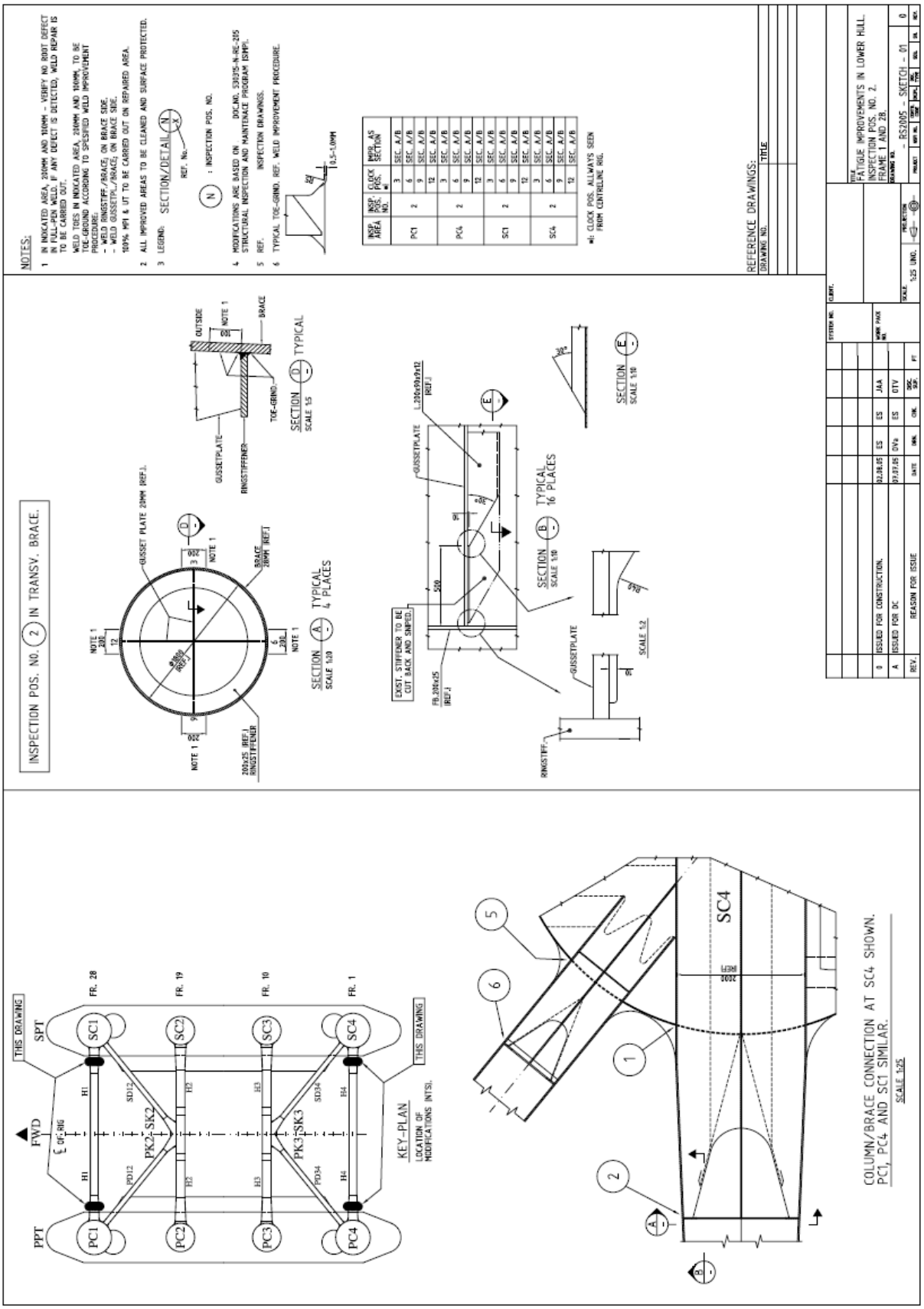
NOTES:
INSPECTION POS. NO. (2) IN TRANSV. BRACE.
SECTION/DETAIL
REFERENCE DRAWINGS:
FATIGUE IMPROVEMENTS IN LOWER HULL.
INSPECTION POS. NO. 2.
FRAME 1 AND 28.
- RS2005 - SKETCH - 01
SECTION (A) TYPICAL 4 PLACES
SECTION (B) TYPICAL 16 PLACES
SECTION (D) TYPICAL
SECTION (E)
KEY-PLAN
LOCATION OF MODIFICATIONS INTSL.
COLUMN/BRACE CONNECTION AT SC4 SHOWN.
PC1, PC4 AND SC1 SIMILAR.
SCALE 1:25
PPT
SPT
FWD
THIS DRAWING
PC1
PC2
PC3
PC4
SC1
SC2
SC3
SC4
FR. 28
FR. 19
FR. 10
FR. 1
PK2-SK2
PK3-SK3
SC4

I. Drawings for the fillet welded knee plate

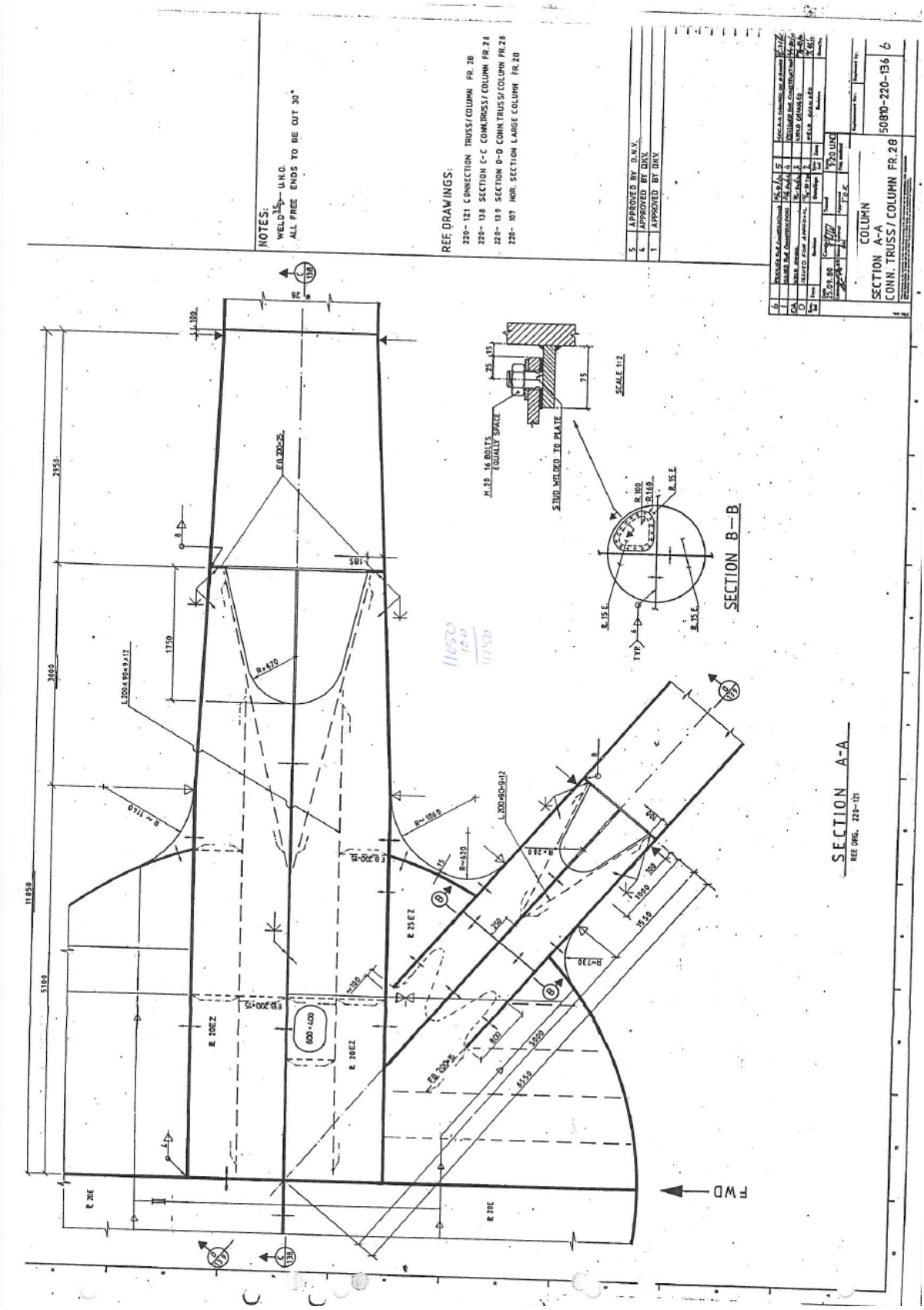

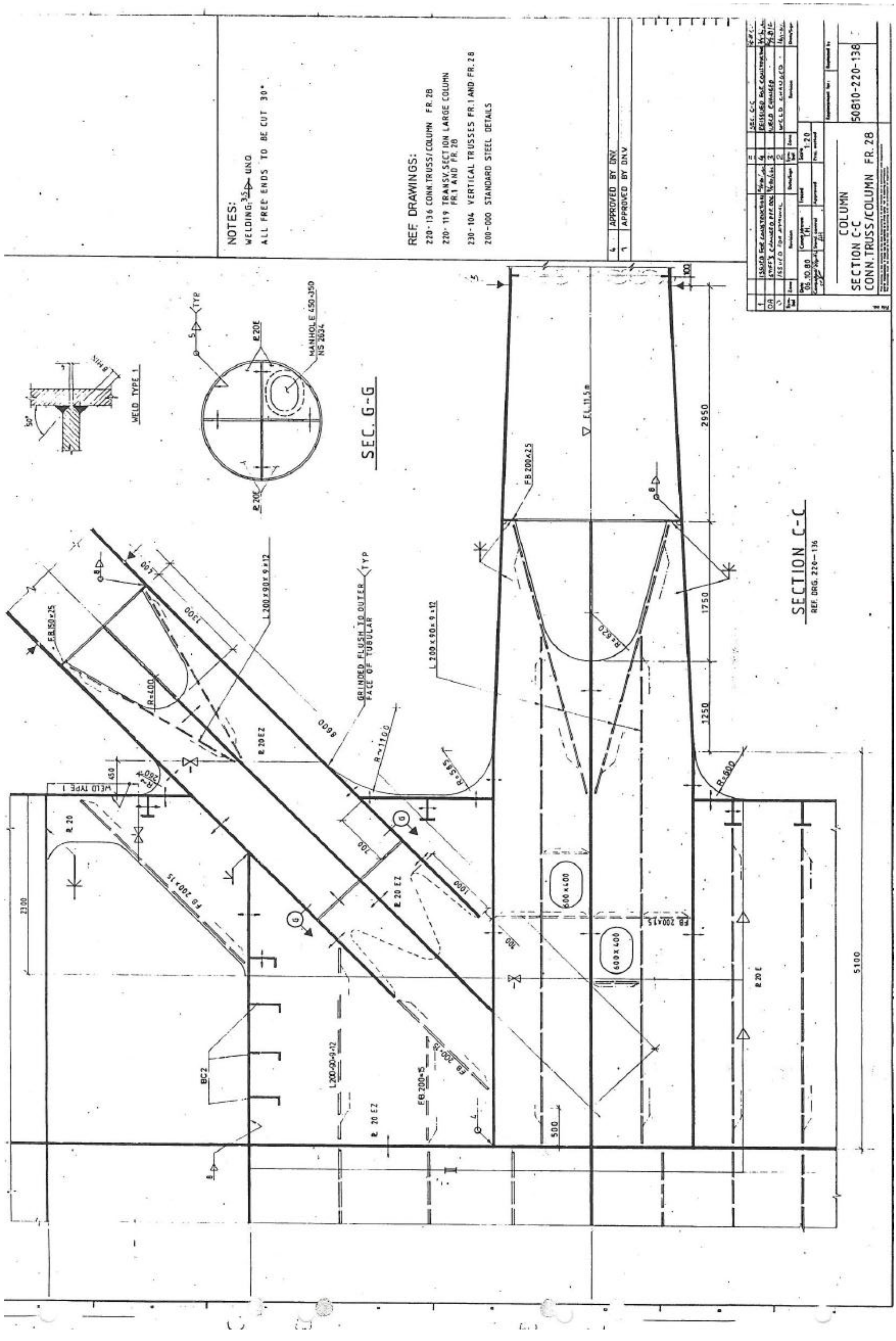
NOTES:
ALL FREE ENDS TO BE CUT 30°
REF. DRAWINGS:
APPROVED BY DNV
SEC. G-G
SECTION C-C
WELD TYPE 1
COLUMN
SECTION C-C
CONN. TRUSS/COLUMN FR. 28
50810-220-138